



LEWIS ACIDIC ZN(II) SCHIFF BASE COMPLEXES IN HOMOGENEOUS CATALYSIS

Daniele Anselmo

Dipòsit Legal: T. 1564-2013

ADVERTIMENT. L'accés als continguts d'aquesta tesi doctoral i la seva utilització ha de respectar els drets de la persona autora. Pot ser utilitzada per a consulta o estudi personal, així com en activitats o materials d'investigació i docència en els termes establerts a l'art. 32 del Text Refós de la Llei de Propietat Intel·lectual (RDL 1/1996). Per altres utilitzacions es requereix l'autorització prèvia i expressa de la persona autora. En qualsevol cas, en la utilització dels seus continguts caldrà indicar de forma clara el nom i cognoms de la persona autora i el títol de la tesi doctoral. No s'autoritza la seva reproducció o altres formes d'explotació efectuades amb finalitats de lucre ni la seva comunicació pública des d'un lloc aliè al servei TDX. Tampoc s'autoritza la presentació del seu contingut en una finestra o marc aliè a TDX (framing). Aquesta reserva de drets afecta tant als continguts de la tesi com als seus resums i índexs.

ADVERTENCIA. El acceso a los contenidos de esta tesis doctoral y su utilización debe respetar los derechos de la persona autora. Puede ser utilizada para consulta o estudio personal, así como en actividades o materiales de investigación y docencia en los términos establecidos en el art. 32 del Texto Refundido de la Ley de Propiedad Intelectual (RDL 1/1996). Para otros usos se requiere la autorización previa y expresa de la persona autora. En cualquier caso, en la utilización de sus contenidos se deberá indicar de forma clara el nombre y apellidos de la persona autora y el título de la tesis doctoral. No se autoriza su reproducción u otras formas de explotación efectuadas con fines lucrativos ni su comunicación pública desde un sitio ajeno al servicio TDR. Tampoco se autoriza la presentación de su contenido en una ventana o marco ajeno a TDR (framing). Esta reserva de derechos afecta tanto al contenido de la tesis como a sus resúmenes e índices.

WARNING. Access to the contents of this doctoral thesis and its use must respect the rights of the author. It can be used for reference or private study, as well as research and learning activities or materials in the terms established by the 32nd article of the Spanish Consolidated Copyright Act (RDL 1/1996). Express and previous authorization of the author is required for any other uses. In any case, when using its content, full name of the author and title of the thesis must be clearly indicated. Reproduction or other forms of for profit use or public communication from outside TDX service is not allowed. Presentation of its content in a window or frame external to TDX (framing) is not authorized either. These rights affect both the content of the thesis and its abstracts and indexes.

UNIVERSITAT ROVIRA I VIRGILI

LEWIS ACIDIC ZN(II) SCHIFF BASE COMPLEXES IN HOMOGENEOUS CATALYSIS

Daniele Anselmo

Dipòsit Legal: T. 1564-2013

UNIVERSITAT ROVIRA I VIRGILI

LEWIS ACIDIC ZN(II) SCHIFF BASE COMPLEXES IN HOMOGENEOUS CATALYSIS

Daniele Anselmo

Dipòsit Legal: T. 1564-2013

Daniele Anselmo

Lewis Acidic Zn(II) Schiff Base Complexes in Homogeneous Catalysis

Doctoral Thesis

Supervised by Prof. Arjan W. Kleij

Institut Català d'Investigació Química



UNIVERSITAT ROVIRA I VIRGILI

Tarragona

2013

UNIVERSITAT ROVIRA I VIRGILI

LEWIS ACIDIC ZN(II) SCHIFF BASE COMPLEXES IN HOMOGENEOUS CATALYSIS

Daniele Anselmo

Dipòsit Legal: T. 1564-2013



Av. Països Catalans 16
43004 Tarragona
Tel: +34 977 920 812
Email: akleij@iciq.es



UNIVERSITAT
ROVIRA I VIRGILI

DEPARTAMENT DE QUÍMICA FÍSICA
I INORGÀNICA

Campus Sescelades
Marcel·lí Domingo, s/n
43007 Tarragona
Tel. +34 977 55 81 37
Fax +34 977 55 95 63
www.quimica.urv.es

I STATE that the present study, entitled “Lewis Acidic Zn(II) Schiff Base Complexes in Homogeneous Catalysis”, presented by Daniele Anselmo for the award of the degree of Doctor, has been carried out under my supervision at the Institut Català d’Investigació Química.

Tarragona, February 19th, 2013

Doctoral Thesis Supervisor

Prof. Arjan W. Kleij

UNIVERSITAT ROVIRA I VIRGILI

LEWIS ACIDIC ZN(II) SCHIFF BASE COMPLEXES IN HOMOGENEOUS CATALYSIS

Daniele Anselmo

Dipòsit Legal: T. 1564-2013

Funding Agencies:



UNIVERSITAT ROVIRA I VIRGILI

LEWIS ACIDIC ZN(II) SCHIFF BASE COMPLEXES IN HOMOGENEOUS CATALYSIS

Daniele Anselmo

Dipòsit Legal: T. 1564-2013

*Sweet are the uses of adversity,
Which, like the toad, ugly and venomous,
Wears yet a precious jewel in his head;
And this our life, exempt from public haunt,
Finds tongues in trees, books in the running brooks,
Sermons in stones, and good in every thing.*

William Shakespeare, As You Like It, Act II, sc.1

UNIVERSITAT ROVIRA I VIRGILI

LEWIS ACIDIC ZN(II) SCHIFF BASE COMPLEXES IN HOMOGENEOUS CATALYSIS

Daniele Anselmo

Dipòsit Legal: T. 1564-2013

Table of Contents

Chapter 1: General Introduction

1.1	Schiff bases.....	1
1.2	Salen ligands and their metal complexes.....	1
1.3	Salphen ligands and their metal complexes.....	3
1.4	Synthesis of salphen ligands and complexes.....	4
1.5	Catalysis with salphen based complexes.....	6
1.6	Aim and outline.....	9
1.7	Notes and references.....	10

Chapter 2: Isolation and Characterization of a New Type of μ -hydroxo-bis-Zn(salphen) Assembly

2.1	Introduction.....	13
2.2	Synthesis and characterization of the assemblies.....	14
2.3	Phosphoester cleavage catalysis.....	21
2.4	Conclusions.....	27
2.5	Experimental section.....	27
2.6	Notes and references.....	34

Chapter 3: Mild Formation of Cyclic Carbonates using Zn(II) Complexes based on N_2S_2 -Chelating Ligands

3.1	Introduction.....	38
3.2	Results and discussion.....	39
3.3	Conclusions.....	45
3.4	Experimental section.....	46
3.5	Notes and references.....	49

Chapter 4: Zn-Mediated Synthesis of 3-Substituted Indoles using a Three-Component Reaction Approach

4.1	Introduction.....	53
4.2	Results and discussion.....	55
4.3	Conclusions.....	63
4.4	Experimental section.....	63
4.5	Notes and references.....	68

Chapter 5: Supramolecular Bulky Phosphines Comprising of 1,3,5-triaza-7-phosphaadamantane and Zn(salphen)s: Structural Features and Application in Hydrosilylation Catalysis

5.1	Introduction.....	72
5.2	Results and discussion.....	73
5.3	Conclusions.....	85
5.4	Experimental section.....	86
5.5	Notes and references.....	94

Chapter 6: Merging Catalysis and Supramolecular Aggregation Features of Triptycene based Zn(salphen)s

6.1	Introduction.....	97
6.2	Results and discussion.....	99
6.3	Conclusions.....	107
6.4	Experimental section.....	107
6.5	Notes and references.....	117

Summary.....121

Acknowledgements.....127

Curriculum Vitae.....129

List of Publications.....131

Chapter I

General Introduction

1.1 Schiff bases

The condensation between an aldehyde and an amine leading to an imine was first described by Hugo Schiff in 1864.^[1] These ligands (Figure 1), which are also known as Schiff bases, are considered “privileged” ligands^[2], as their properties may be easily altered by the condensation between aldehydes and amines ligands; as such Schiff base ligands are able to coordinate metals in a highly versatile way and combined with O-donors to provide multidentate ligand systems.

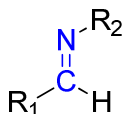


Figure 1. Schematic drawing of a Schiff base.

The ability of Schiff base ligands to coordinate metals and to stabilize them in various oxidation states makes their metal complexes ideal candidates for a large variety of useful catalytic transformations. Stereogenic centers or other elements of chirality (i.e., planar, axial) can be introduced in the synthetic design and the chiral information can also be transmitted by these complexes through a catalytic process to produce enantio-enriched products.

1.2 Salen ligands and their metal complexes

When two equivalents of a salicylaldehyde are combined with a diamine, a particular N_2O_2 -chelating Schiff base is produced known as “salen” ligand (Figure 2). With four equatorial donor sites and two potential axial coordination sites for ancillary ligands, salens are very much like porphyrins but more easily prepared. Although the term “salen” was originally used to describe the tetradentate Schiff base derived from ethylenediamine, nowadays the term “salen” is used in the literature to describe this general class of N_2O_2 -chelating bis-Schiff base ligands.

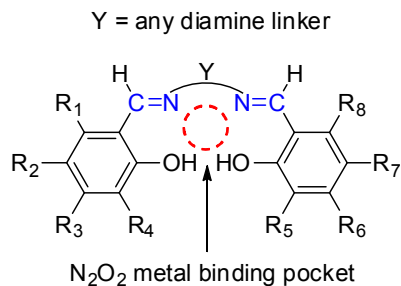


Figure 2. Schematic drawing of the “salen” ligand showing the N_2O_2 metal binding pocket and possible substitutions in both the bridging and aromatic side groups.

Their synthesis is very straightforward, and usually after a double condensation reaction between one equivalent of a diamine and two equivalents of a (substituted) salicylaldehyde the ligand is obtained in high yield by simple filtration. The resulting tetradentate ligand can chelate a wide variety of metal ions in its N_2O_2 binding pocket. Further fine-tuning of the ligand is achieved through variation of the substituents on the salicylidene rings (R_1 - R_8), for instance by introducing electron-withdrawing or -donating groups, or functionalities that allow for immobilization or hybridization. Also a number of synthetic routes have been described for the preparation of non-symmetrical ligands,^[3] increasing the amount of structures available to reach the desired functions.

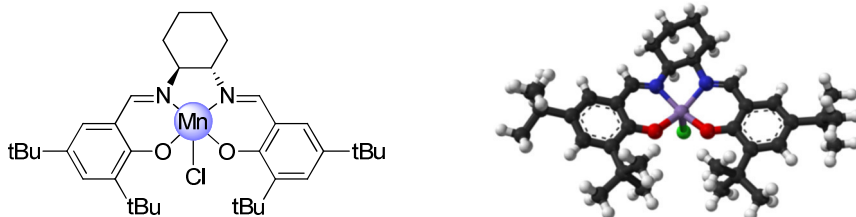


Figure 3. Schematic drawing (left) and molecular structure (right) of the Jacobsen's catalyst.

N,N' -bis(salicylidene)ethylenediamine (salen) ligands and their complexes are well-studied substances within the field of homogeneous catalysis.^[4] The most widely utilized salen-based catalyst system is undoubtedly the manganese(III) complex of the salen ligand bearing a chiral cyclo-hexyl bridging fragment known as Jacobsen's epoxidation catalyst (Figure 3). The Jacobsen catalyst is renowned for its ability to transform prochiral alkenes into chiral epoxides.^[5a] Metal-derived (chiral) salen complexes are versatile and they have proven to be effective catalysts for

many asymmetric conversions including (ep)oxidations,^[6] epoxide ring-opening reactions^[7] and stereo-selective polymerizations.^[8] Analogous multinuclear metallosalens have also received a great deal of attention since in a number of cases interesting cooperative effects have been observed that improve the overall kinetics and process selectivity.^[9] Non-chiral salen complexes have received much less attention since their application potential in (homogeneous) catalysis has been considered limited.

1.3 Salphen ligands and their metal complexes

When in a salen-type ligand the ethylene diamine linker is substituted by a phenylenediamine a new type of ligand with a higher rigidity is obtained. This phenylene-based ligand is denoted as salphen or salophen [*N,N'*-bis(salicylidene)phenylenediamine] and its metal complexes are fully conjugated and highly planar. These salphen and related structures have been neglected for a long time despite the fact that they provide particular advantages over their salen analogues; they represent π -conjugated ligand systems with tunable photophysical properties, and are more cost-effective than the corresponding (chiral) salen ligands. For these reasons, such salphen systems have excellent potential as building blocks in material science amongst other applications.^[10] It should also be noted that the rigid geometry around the metal center is dictated by the salphen ligand and can be used to manipulate properties such as the Lewis acid character of the metal; therefore it may be effectively used to increase the reactivity of the resulting complex. Furthermore the solubility of their complexes and the electron density on the metal center can be fine-tuned by the introduction of appropriate substituents on the side groups or on the phenylenediamine linker of the ligand. All these features make metallosalphen excellent candidates for their use in homogeneous catalysis.

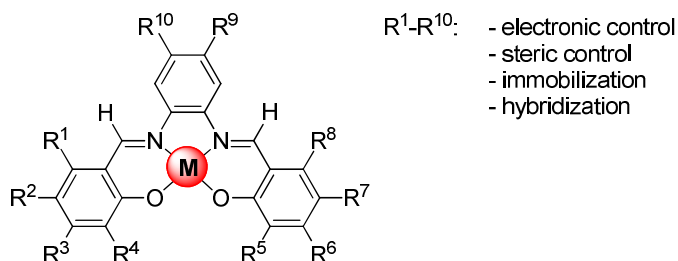
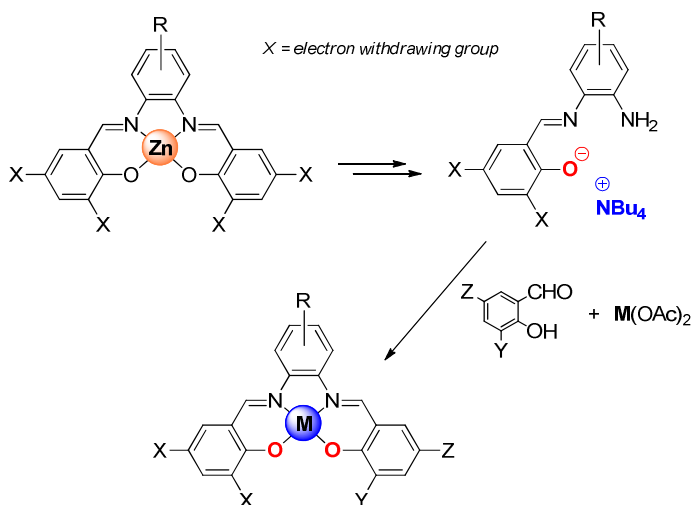


Figure 4. Schematic drawing of a metallosalphen complex with various possible substitutions.

1.4 Synthesis of salphen ligands and complexes

Salphen ligands are easily synthesized by simple combination of two equivalents of a (substituted) salicylaldehyde and one equivalent of 1,2-phenylenediamine. A large library of derivatives can be created by using substituted aldehydes and *ortho*-phenylenediamines. Their metal complexes can be generally synthesized by simple reaction with a metal acetate salt or other metal precursor. More recently, the interest has shifted towards the synthesis of non-symmetrical salphen ligands^[3] which offer further amplified opportunities of tuning of the steric and electronic properties.



Scheme 1. Synthesis of non-symmetrical salphen ligands and metal complexes.

These non-symmetrical salphen ligands can be obtained starting from mono-imine precursors bearing electron-donating groups which are easily synthesized^[11] or from mono-imines bearing electron withdrawing groups which, on the contrary, are synthetically highly challenging^[12]. Our group has recently developed a simple metal-templated procedure (Scheme 1) for the synthesis of non-symmetrical salphen scaffolds with several substitution patterns.^[13] This new methodology is based on the selective hydrolysis of a Zn(salphen) imine bond provoked by addition of an OH nucleophile. The nucleophilic addition of the hydroxide anion is likely facilitated by the presence of the highly Lewis acidic Zn center that increases the reactivity of the imine bond. The reported protocol is advantageous in terms of reaction conditions, isolation, and gives access to mono-imine salts that are not easily synthesized via other methods.

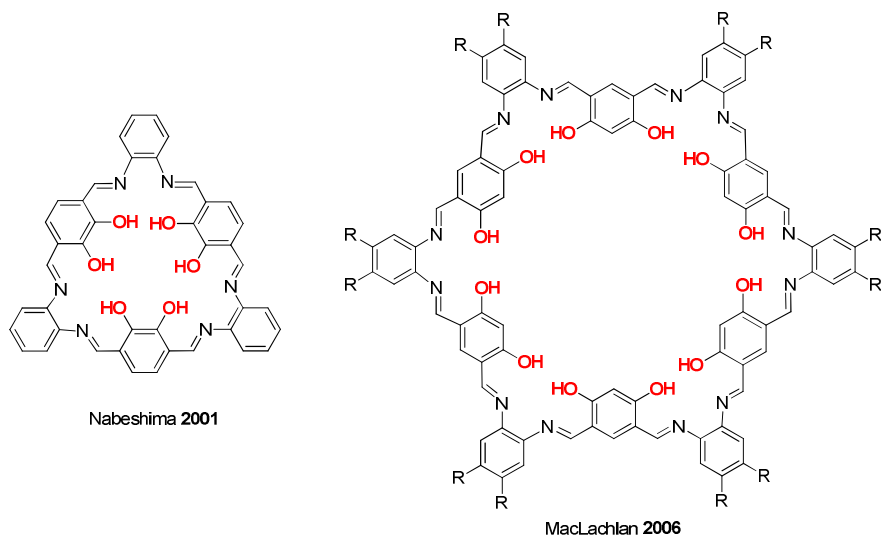


Figure 5. Macrocyclic systems comprising multi-salphen ligands scaffolds.

The ease of access of these mono-imines can lead to the synthesis of new non-symmetric chiral mono- or bis-salphen ligands and complexes. The same approach was later extended to bis-salphen derivatives leading to the formal desymmetrization of the coordination environment of the salphen unit in bis-salphen scaffolds.^[14] It is also possible to synthesize larger molecules based on the salphen scaffold. In 2001 Nabeshima and co-workers presented a tri-salphen macrocycle synthesized from the condensation of 2,3-dihydroxybenzene-1,4-dicarbaldehyde with 1,2-phenylenediamine (Figure 5) in a good yield after prolonged stirring.^[15,16] MacLachlan and coworkers also reported on the formation of various types of tri-, tetra- and hexa-salphen macrocyclic architectures (Figure 5).^[17-19]

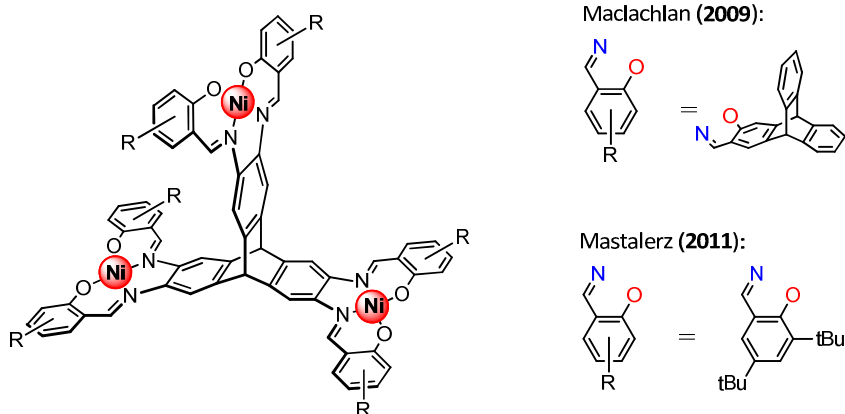


Figure 6. Schematic drawing of triptycene based Ni(salphen) complexes.

Furthermore the groups of Mastalerz and MacLachan have also made use of triptycene scaffolds to synthesize enlarged metallosalphen functionalized derivatives with D_{3h} symmetry (Figure 6) which results after self-assembly into porous materials with unusual properties.^[20]

1.5 Catalysis with salphen-based complexes

Many groups have reported on the use of metallosalphen complexes in catalysis for a diverse range of chemical transformations. Significant differences between the activities of salen catalysts and their salphen analogues in various catalytic reactions have been observed. Here some examples of chemical reactions catalyzed by metal-salphen complexes will be discussed. As mentioned before, manganese centered Schiff base complexes have a long tradition in homogeneous catalysis and are specifically useful for a number of (ep)oxidation reactions; undoubtedly the development of other applications has been inspired by the seminal work of Jacobsen and Katsuki.^[5b] Amongst these, Mikami and co-workers have studied the oxidation of diphenyl sulfide mediated by Mn(III)salen and Mn(III)salphen using sodium periodate as terminal oxidant.^[21] The salphen complex yielded a 4:1 mixture of sulfoxide and sulfone in 100% yield under mild condition. On the contrary, the analogous salen complex only led to low yields (18%) with a 2:1 ratio between sulfoxide and sulfone. Cr(III)salphen complexes were applied by Wu and co-workers^[22] as highly selective catalysts for the oxidation of benzyl alcohol to benzaldehyde using hydrogen peroxide as oxidant. The catalytic activity of the sodium salts of Cr(III)salphen complexes has been compared with the same complexes intercalated on a Mg–Al layered double hydroxide (LDH). Whereas the homogeneous catalytic system yielded a mixture of benzaldehyde (77%), benzoic acid and benzyl benzoate, the LDH supported catalyst yielded only benzaldehyde. Furthermore the salphen catalyst activity was compared with its salen analogue, proving the former to give much better catalytic performance. The selective oxidation of alkanes using *m*-CPBA as terminal oxidant was achieved using di-Fe(III) μ -oxo bridged salphen complexes as catalysts. This conversion, however, has found to be possible only when the salphen ligand contains bulky groups on the phenolate moiety.^[23] Vanadium(V) salphen complexes were found to be effective in the catalysis of the epoxidation of alkenes and sulfoxidation of thioethers by Conte and co-workers.^[24] Polymerization reactions catalyzed by metallosalphen complexes have also been reported by several groups. Amongst them Darensbourg and co-workers reported on the ring-opening polymerization of trimethylene carbonate catalyzed by Al(III) and Sn(IV) salphen complexes (Figure 7). The catalytic activity of

the Al(III)salphen complex was compared to that of its salen analogue showing the former to give higher turnover numbers.^[25]

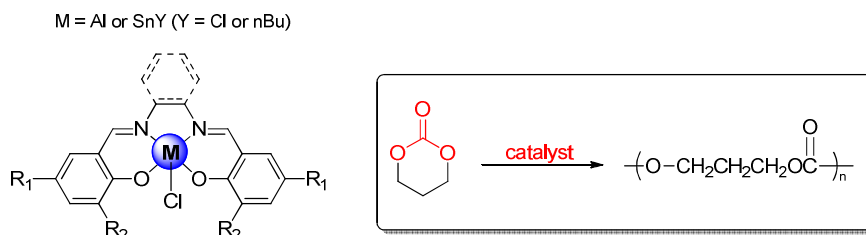


Figure 7. *M(salen) and M(salphen) derivatives employed by Darensbourg and co-workers in the ring-opening polymerization of trimethylene carbonate.*

The catalysis of the carbonylation of aniline to *N,N'*-diphenyl urea was achieved by Li and co-workers using Co(II) salphen complexes.^[26] They showed that the salphen complex is more effective than its salen analogue possibly due to the fact that conjugation of the salphen reduces the possibility of decomposition of the complexes to Co(III) oxide, which is a known to be a deactivation route.

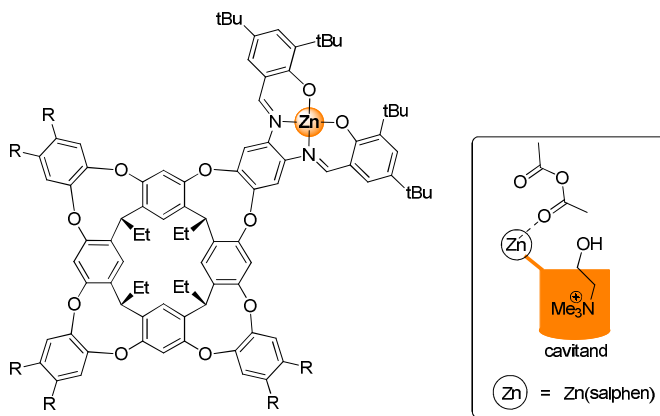


Figure 8. *A biomimetic cavitand structure proposed by Rebek and co-workers active in the acetylation of choline (left) and the proposed cooperative catalysis mode (right).*

Rebek and co-workers prepared a sophisticated biomimetic salphen based catalyst for the acetylation of choline. They used a resorcinarene-supported Zn(II) salphen complex (Figure 8) in which the bridging phenyl group of the salphen structure is an integrated part of the resorcinarene support.^[27] The Lewis acidity of the Zn(II) ion is used to bind the acetic anhydride while the choline forms a host-guest complex. The close proximity between the reagents thus achieved provides a more efficient catalytic process which was indeed observed by comparing

the reaction rates of the unsupported Zn(II) salen, the cavitand only and the Zn(II)salen/cavitand ensemble.

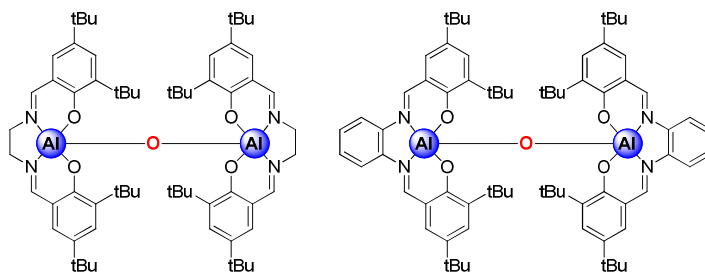


Figure 9. Structures of dinuclear, O-bridged Al(III)salen (left) and Al(III)salphen (right) catalysts presented by North and co-workers.

Metallosalphenens have also been applied as catalysts for the cycloaddition of CO_2 to terminal epoxides. North and co-workers reported on the use of di-Al(III) μ -oxo bridged salen and salphen complexes (Figure 9) in the catalyzed conversion of CO_2 and epoxides into cyclic carbonates.^[28] Using NBu_4Br as co-catalyst they were able to obtain good conversions (up to 64%) in the synthesis of styrene carbonate under highly mild conditions ($T = 25^\circ$, $p(\text{CO}_2) = 1$ bar) although in this case the salen complex showed to be more active (52% conversion) than its salphen analogue (33% conversion). Within the same catalytic context, our group recently communicated on the use of Zn(II)salphen complexes under particular mild conditions.^[29] We demonstrated that the superior activity of the Zn(II)salphen complexes over Zn(salen) complexes (Figure 10) containing ligands having chiral bridging fragments is due to the much higher Lewis acidity of the salphen complexes.^[30]

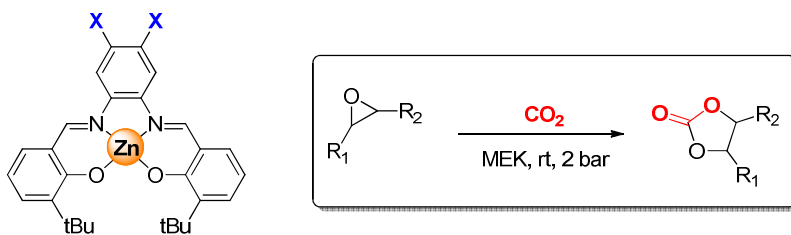


Figure 10. Zn(II)salphen catalysts for organic carbonate formation under mild reaction conditions reported by Kleij and co-workers.

Although initially reasonably mild conditions were employed for the cycloaddition of CO_2 to epoxides ($T = 45^\circ$, $p(\text{CO}_2) = 10$ bar, DCM), a significant improvement of the reaction conditions

within the context of sustainability was later reported and it was also shown that various cyclic carbonate structures can be accessed under virtually ambient and “green” conditions ($T = 25^\circ \text{C}$, $p(\text{CO}_2) = 2 \text{ bar}$) using methylethyl ketone (MEK) as solvent.^[31]

1.6 Aim and Outline

Salphen metal complexes are easily prepared and have the advantage of a rigid geometry around the metal center that can be used to manipulate the Lewis acid character of the metal which can be effectively used to increase the reactivity of a metal-substrate complex. Furthermore the steric properties of salphen complexes can be fine-tuned with the presence of different groups in the aldehyde or diamine precursors. When a Zn(II) cation is coordinated by a salphen ligand it is forced in a highly planar geometry that increases its Lewis acidity and makes it available for axial coordination, a feature that is useful in catalysis in the context of substrate activation and stabilization of reactive intermediates. Despite this advantageous feature and the fact that zinc is a cheap, abundant and relatively non-toxic metal, Zn(II)salphen complexes have received so far little attention in the field of catalysis.

The main aim of the work described in this thesis is: (i) to develop and study the properties of new Zn(II) Schiff base complexes and (ii) to further explore their potential in homogeneous catalysis applications. The focus will be mainly on Zn(II) salphen complexes because of their ease of accessibility and their unveiled potential in catalysis. Apart from salphen ligands also another type of N_2S_2 -chelating Schiff base ligand will be presented and its potential in catalysis will be explored and compared with a Zn(salphen) based system. **Chapter 2** describes a new series of complexes comprising a binuclear, OH-bridging Zn_2 assembly based on a salphen scaffold. The stability properties of the assemblies under polar and non-polar conditions have been investigated and the assembled species was applied as a potential catalyst for the phosphoester cleavage reaction that involved paraoxon. A more detailed spectroscopic study was also undertaken to find a rationale for the observed reactivity pattern. **Chapter 3** introduces a series of Zn(II) complexes based on a versatile N_2S_2 -chelating ligand abbreviated as btsc [btsc = bis(thiosemicarbazonato)] derived from simple and accessible building blocks. These Zn(btsc) complexes proved to be effective catalysts for the cycloaddition of CO_2 to various terminal epoxides under relatively mild reaction conditions. A comparison between the N_2O_2 -chelating and N_2S_2 -chelating systems has been made. **Chapter 4** focuses on the synthesis of 3-substituted indoles through a multi-component reaction (MCR) approach using aldehydes, indole and

malononitrile as reagents. The reaction has been catalyzed by Lewis acidic Zn(salphen) complexes and various process parameters have been screened (solvent, catalyst type, addition method, reagent stoichiometry) to optimize the yield of the targeted 3-CR product. Some mechanistic considerations are also put forward and discussed in relation to the state-of-the-art.

Chapter 5 describes the use of the commercially available, bifunctional phosphine 1,3,5-triaza-7-phosphaadamantane (abbreviated as PN₃) in conjunction with a series of Zn(salphen) complexes that leads to sterically encumbered phosphine ligands as a result of (reversible) coordinative Zn–N interactions. It will be demonstrated that the supramolecular formation of these bulky phosphines with little synthetic effort may be a useful alternative for (often synthetically laborious) covalent, bulky phosphines in hydrosilylation catalysis providing similar reactivity profiles. Finally, **Chapter 6** introduces a series of trinuclear, triptycene based metallo-salphen complexes (M = Zn, Ni). The Zn(II) complexes show strong self-aggregation under apolar conditions which can be reversed by the addition of a competitive ligand or increasing the polarity of the medium. Their application in organic carbonate formation has revealed that reversible supramolecular aggregation can be made an efficient recycling strategy in homogeneous catalysis by simple switching the polarity of the medium allowing for separation and respective isolation of both the binary catalyst couple as well as the product.

1.7 Notes and References

- [1] H. Schiff, *Ann. Suppl.*, 1864, **B**, 343.
- [2] T. P. Yoon and E. N. Jacobsen, *Science*, 2003, **299**, 1691.
- [3] A. W. Kleij, *Eur. J. Inorg. Chem.*, 2009, 193.
- [4] For reviews see: a) E. N. Jacobsen in *Comprehensive Organometallic Chemistry II*, Vol. 12 (Hrsg.: E. W. Abel, F. G. A. Stone, E. Willinson), Pergamon, New York, 1995, S. 1097 – 1135; b) T. Katsuki, *Coord. Chem. Rev.*, 1995, **140**, 189; c) L. Canali and D. C. Sherrington, *Chem. Soc. Rev.*, 1999, **28**, 85; d) D. A. Atwood and M. J. Harvey, *Chem. Rev.*, 2001, **101**, 37; e) T. Katsuki, *Synlett*, 2003, 281; f) P. G. Cozzi, *Chem. Soc. Rev.*, 2004, **33**, 410; h) T. Katsuki, *Chem. Soc. Rev.*, 2004, **33**, 437; i) J. F. Farlow and E. N. Jacobsen, *Top. Organomet. Chem.*, 2004, **7**, 123; j) E. M. McGarrigle and D. G. Gilheany, *Chem. Rev.*, 2005, **105**, 1563.
- [5] a) W. Zhang, J. L. Loebach, S. R. Wilson and E. N. Jacobsen, *J. Am. Chem. Soc.*, 1990, **112**, 2801. b) R. Irie, K. Noda, Y. Ito, N. Matsumoto and T. Katsuki, *Tetrahedron Lett.*, 1990, **31**, 7345.

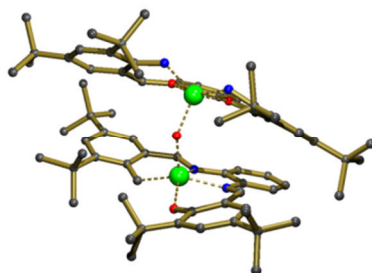
- [6] E. N. Jacobsen, *Acc. Chem. Res.*, 2000, **33**, 421. For a recent example: Y. Sawada, K. Matsumoto and T. Katsuki, *Angew. Chem., Int. Ed.*, 2007, **46**, 4559.
- [7] J. M. Ready and E. N. Jacobsen, *J. Am. Chem. Soc.*, 2001, **123**, 2687.
- [8] W. Hirahata, R. M. Thomas, E. B. Lobkovsky and G. W. Coates, *J. Am. Chem. Soc.*, 2008, **130**, 17658.
- [9] For a recent review on cooperative effects in salen chemistry: R. M. Haak, S. J. Wezenberg and A. W. Kleij, *Chem. Commun.*, 2010, **46**, 2713.
- [10] S. J. Wezenberg and A. W. Kleij, *Angew. Chem., Int. Ed.*, 2008, **47**, 2354.
- [11] For an early example refer to: M.-A. Muñoz-Hernández, T. S. Keizer, S. Parkin, B. Patrick and D.A. Atwood, *Organometallics*, 2000, **19**, 4416.
- [12] A. W. Kleij, D. M. Tooke, M. Kuil, M. Lutz, A. L. Spek and J. N. H. Reek, *Chem.–Eur. J.*, 2005, **11**, 4743.
- [13] E. C. Escudero-Adán, M. Martínez Belmonte, J. Benet-Buchholz and A. W. Kleij, *Org. Lett.*, 2010, **12**, 459.
- [14] E. C. Escudero-Adán, M. Martínez Belmonte, E. Martín, G. Salassa, J. Benet-Buchholz and A. W. Kleij, *J. Org. Chem.*, 2011, **76**, 5404.
- [15] S. Akine, T. Taniguchi and T. Nabeshima, *Tetrahedron Lett.*, 2001, **42**, 8861.
- [16] The Nabeshima group has also reported extensively on oxime-based “salen” type ligands, see for a recent account: S. Akine and T. Nabeshima, *Dalton Trans.*, 2009, 10395.
- [17] J. Jiang and M. J. MacLachlan, *Org. Lett.*, 2010, **12**, 1020.
- [18] P. D. Frischmann, J. Jiang, J. K.-H. Hui, J. J. Grzybowski and M. J. MacLachlan, *Org. Lett.*, 2008, **10**, 1255.
- [19] J. K.-H. Hui and M. J. MacLachlan, *Chem. Commun.*, 2006, 2480.
- [20] (a) J. H. Chong, S. J. Ardakani, K. J. Smith and M. J. MacLachlan, *Chem.–Eur. J.*, 2009, **15**, 11824; (b) M. Mastalerz, H.-J. S. Hauswald and R. Stoll, *Chem. Commun.*, 2012, **48**, 130; (c) M. Mastalerz and I. M. Oppel, *Eur. J. Org. Chem.*, 2011, 5971; See also: (d) J. H. Chong and M. J. MacLachlan, *J. Org. Chem.*, 2007, **72**, 8693; (e) M. Mastalerz and I. M. Oppel, *Angew. Chem. Int. Ed.*, 2012, **51**, 5252; (f) M. W. Schneider, H.-J. Siegfried Hauswald, R. Stoll and M. Mastalerz, *Chem. Commun.*, 2012, **48**, 9861.
- [21] V. Mirkhani, S. Tangestaninejad, M. Moghadam, I. P. Mohammadpoor-Baltork and H. Kargar, *J. Mol. Catal. A: Chem.*, 2005, **242**, 251.
- [22] G. Wu, X. Wang, J. Li, N. Zhao, W. Wei and Y. Sun, *Catal. Today*, 2008, **131**, 402.

- [23] R. Mayilmurugan, H. Stoeckli-Evans, E. Suresh and M. Palaniandavar, *Dalton Trans.*, 2009, 5101.
- [24] V. Conte, F. Fabbianesi, B. Floris, P. Galloni, D. Sordi, I. W. C. E. Arends, M. Bonchio, D. Rehder and D. Bogdal, *Pure Appl. Chem.*, 2009, **81**, 1265.
- [25] D. J. Darensbourg, P. Ganguly and D. Billodeaux, *Macromolecules*, 2005, **38**, 5406.
- [26] L.-J. Chen, J. Bao, F.-M. Mei and G.-X. Li, *Catal. Commun.*, 2008, **9**, 658.
- [27] F. H. Zelder and J. Rebek Jr., *Chem. Commun.*, 2006, 753.
- [28] J. Melendez, M. North and R. Pasquale, *Eur. J. Inorg. Chem.*, 2007, 3323.
- [29] A. Decortes, M. Martínez Belmonte, J. Benet-Buchholz and A. W. Kleij, *Chem. Commun.*, 2010, **46**, 4580.
- [30] For an early discussion on the Lewis acidity of Zn(salphen)s see: A. W. Kleij, D. M. Tooke, M. Kuil, M. Lutz, A. L. Spek and J. N. H. Reek, *Chem.–Eur. J.*, 2005, **11**, 4743.
- [31] A. Decortes and A. W. Kleij, *ChemCatChem*, 2011, **3**, 831.

Chapter II

Isolation and Characterization of a New Type of μ -hydroxo-bis-Zn(salphen) Assembly

A series of assemblies comprising hydroxo-bridged dinuclear Zn(salphen) structures has been prepared and fully characterized in solution and by X-ray crystallography. The solution stability of these assembled species was evaluated in polar and non-polar media, in the presence of excess of building blocks and competing ligands. The catalytic potential of this type of complex was investigated in phosphoester cleavage reactions.



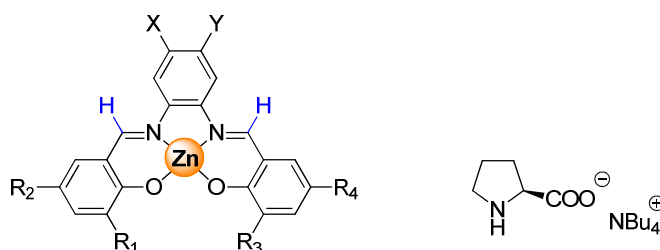
2.1 Introduction

Metallosalens are privileged catalyst systems useful for important asymmetric conversions.^[1] These complexes are also becoming increasingly important as molecular building blocks in material science^[2] as evidenced by their incorporation into a wide variety of structures and devices such as sensors,^[3] multimetallic systems useful for cooperative catalysis operations^[4] and molecular templates for (in)organic synthesis.^[5] Metallosalen building blocks provide a number of attractive features for use as components of larger ensembles such as easy accessibility, low cost manufacturing and facile introduction of various functional fragments including chiral modules^[6] and photoactive units.^[7] In this context, we have been using Zn-centered salen complexes as versatile synthons in supramolecular synthesis.^[8] The *salphen* (*salphen* = *N,N'*-bis(salicylidene)-1,2-phenylenediamine) sub-family of derivatives has proven to be extremely useful since the high Lewis acidic behavior of the metal ion allows the binding of various N- and O-donor ligands in the axial position of the complex.^[9] Even more recently, we communicated that Zn(*salphen*) complexes are also able to bind various anions which allows, in the case of acetate, anion-mediated synthesis of multinuclear assemblies.^[10] The acetate binding at the Zn ion in these *salphen* complexes proved to be very strong (K_s up to $3.1 \times 10^6 \text{ M}^{-1}$) and

we set out to construct other types of assemblies that comprise more functional anionic donor systems. In the course of these studies we decided to investigate the binding of various amino acid salts to Zn(salphen) complexes. Our initial intention focused on the reversible binding of proline derivatives since interaction with a sterically demanding Zn(salphen) complex through Zn–carboxylate bonds may provide a new entry to proline-based catalysts useful for various (asymmetric) organocatalytic transformations.^[11] Unexpectedly, the results from these initial studies revealed the formation and isolation of a remarkable assembled structure with an anionic μ_2 -OH bridging fragment. This unexpected product could also be independently prepared via a direct route (*vide infra*). The molecular features and stability of this binuclear species (and others) and the catalytic features of this type of complex^[12] were examined and are here reported.

2.2 Synthesis and characterization of the assemblies

Initially, we combined complex **1** (Scheme 1) with 1 equiv of tetrabutylammonium prolinato (NBu_4Pro)^[13] in acetone- d_6 to study the formation of the complex **1**· NBu_4Pro . As previously reported for other anionic donors, the binding of the prolinato to **1** is accompanied by a typical upfield shift for the imine-H of **1** ($\Delta\delta = -0.20$ ppm)¹⁰ and thus supports the assembly formation in solution.



1. $R_1 = R_3 = \text{tBu}$, $R_2 = R_4 = \text{H}$; $X = Y = \text{H}$
2. $R_1 = R_2 = R_3 = R_4 = \text{tBu}$; $X = Y = \text{H}$
3. $R_1 = R_2 = R_3 = \text{tBu}$, $R_4 = \text{H}$; $X = Y = \text{H}$
4. $R_1 = R_3 = \text{tBu}$, $R_2 = R_4 = \text{Br}$; $X = Y = \text{H}$
5. $R_1 = R_3 = \text{H}$; $R_2 = R_4 = \text{tBu}$; $X = Y = \text{H}$
6. $R_1 = R_2 = R_3 = R_4 = \text{tBu}$; $X = Y = \text{Cl}$
7. $R_1 = R_2 = R_4 = \text{tBu}$; $R_3 = \text{H}$; $X = Y = \text{H}$
8. $R_1 = R_3 = \text{tBu}$; $R_2 = R_4 = \text{H}$; $X = \text{NO}_2$, $Y = \text{H}$

Scheme 1. Schematic structures of Zn(salphen) complexes **1-8** and NBu_4 -prolinato.

Crystals were grown from a solution in $\text{CH}_2\text{Cl}_2/\text{Et}_2\text{O}$ and analyzed by X-ray diffraction (see Fig. 1).^[14] Crystallographic details and relevant bond distances and angles are given in Tables 2 and 3 (see experimental section). To our surprise, the structure did not comprise the proline anion but instead a μ_2 -bridging OH anion interacting with both Zn(salphen) units through a Zn–O–Zn motif.

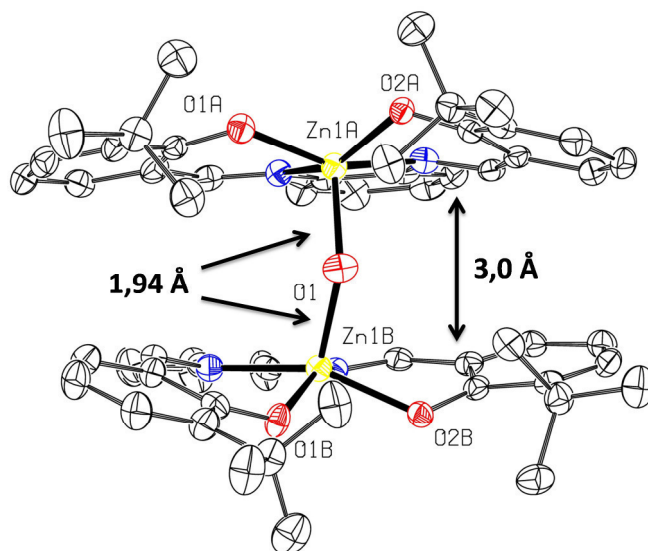


Figure 1. X-ray molecular structure determined for $(\mathbf{1})_2 \cdot \text{NBu}_4\text{OH}$ showing only one of the independent molecules of the unit cell and a partial numbering scheme. Co-crystallized solvent molecules, NBu_4 cation and hydrogens atoms are omitted for clarity.

The isolation of this structure can be rationalized by an *in situ* acid-base reaction between the proline anion and adventitious water to afford the OH anion, which then recombines with 2 equiv of Zn(salphen) complex **1** and preferentially crystallizes from the medium. In this assembled structure, the Zn ions are displaced from the N_2O_2 coordination plane defined by the salphen **1** as a result from the coordinative interaction with the OH anion. The Zn(2)–O(1) and Zn(1)–O(1) distances are 1.9470 and 1.9448 Å, respectively, which are significantly shorter than the Zn–O distances (1.97–2.00 Å) within each salphen complex. Both Zn(salphen) modules are in close proximity and the closest distance between them is around 3.0 Å. Such a small distance between both salphen ligands should give rise to anisotropic effects if the assembly is retained in solution. Crystals of $(\mathbf{1})_2 \cdot \text{NBu}_4\text{OH}$ were dissolved in acetone- d_6 and the NMR spectrum was compared to that of parent complex **1** (Fig. 2). Remarkably, the imine resonance of the assembly is located at 7.93 ppm, which is 1.13 ppm upfield compared to the imine-H of (free) **1**. The tBu

peak of assembly $(1)_2 \cdot \text{NBu}_4\text{OH}$ is displaced -0.24 ppm as compared to non-assembled **1**. The large upfield displacements found for $(1)_2 \cdot \text{NBu}_4\text{OH}$ is strong evidence for the stability of the assembly in solution, and no free **1** was noted in acetone- d_6 . Furthermore, a singlet peak was additionally observed at 1.50 ppm (assigned to the OH anion) with correct relative intensity. The ^1H NOESY spectrum of the sample (Fig. 3) showed a NOE contact between this peak and the tBu resonance of the salphen ligand, a result that is also in line with an intact assembly.

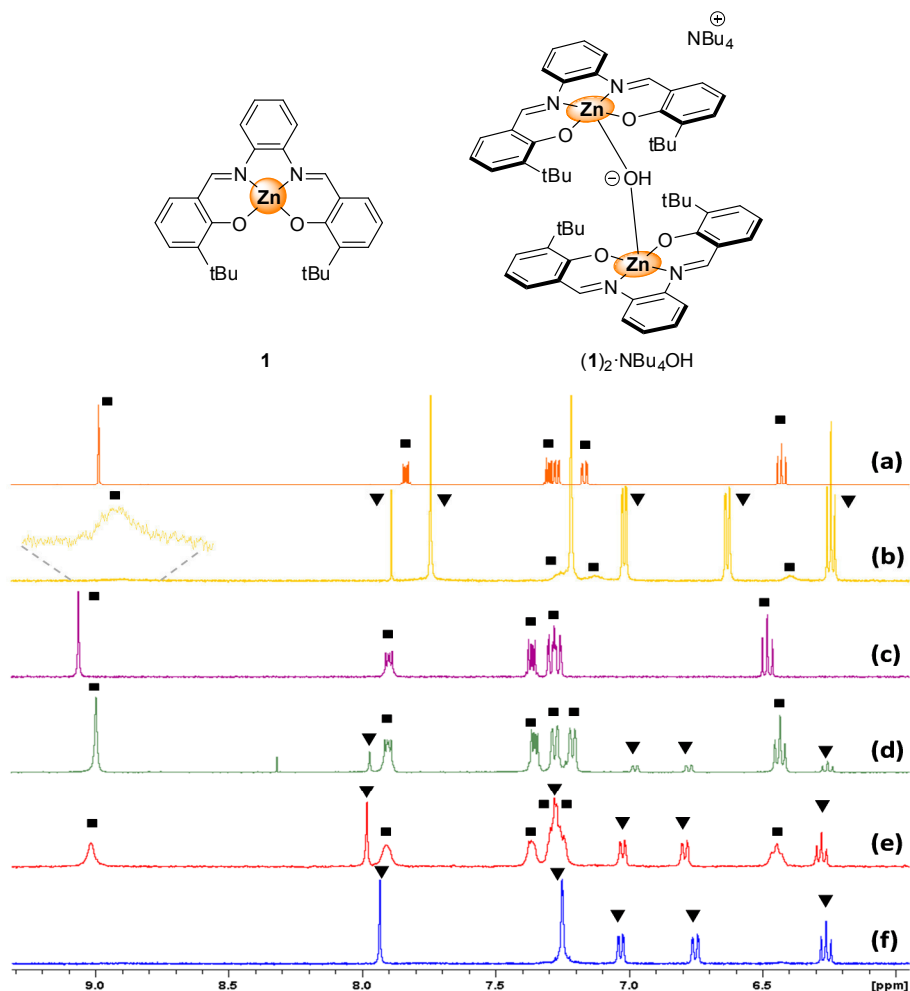


Figure 2. NMR comparison (aromatic region) between **1** (■) and assembly $(1)_2 \cdot \text{NBu}_4\text{OH}$ (▼) under various conditions: (a) complex **1** in 100% d_8 -THF; (b) assembly $(1)_2 \cdot \text{NBu}_4\text{OH}$ in 100% d_8 -THF; (c) complex **1** in 100% acetone- d_6 ; (d) assembly $(1)_2 \cdot \text{NBu}_4\text{OH}$ in 100% DMSO- d_6 ; (e) assembly $(1)_2 \cdot \text{NBu}_4\text{OH}$ in 80:20 v/v acetone- d_6 /DMSO- d_6 ; (f) assembly $(1)_2 \cdot \text{NBu}_4\text{OH}$ in 100% acetone- d_6 .

The stability of the $(\mathbf{1})_2\cdot\text{NBu}_4\text{OH}$ assembly was then probed under increasingly polar conditions (Fig. 2). Upon increasing the polarity of the medium (i.e., addition of $\text{DMSO-}d_6$) another species was identified by ^1H NMR and assigned to the free complex **1**. Remarkably, in the presence of 20 % (v/v) $\text{DMSO-}d_6$ part of the assembly (26% by signal integration) remained intact while in pure $\text{DMSO-}d_6$ the amount of intact assembly is reduced to 7%. In d_8 -THF the assembly proved to be rather stable and only 10% (by signal integration) of free complex **1** could be observed. Thus, these data support the view that the assembly has reasonable stability features in highly polar media and is able to (partially) survive competitive conditions. Additionally, the stability of another sandwich structure, i.e. $(\mathbf{2})_2\cdot\text{NBu}_4\text{OH}$ (Scheme 1, vide infra), was assessed in the presence of excess of **2** to examine the potential dynamic interchange between bonded and non-bonded **2**. In the presence of 3 equiv of 'free' **2**, two distinct sharp patterns were noted ascribed to $(\mathbf{2})_2\cdot\text{NBu}_4\text{OH}$ and **2** with no sign of dynamic inter-conversion between 'free' and assembled **2** (Fig. 4). This latter experiment sustains stability in the presence of excess of this building block. On the contrary, when similar competition experiments were conducted with excess NBu_4OH , the assembly clearly breaks up and mononuclear complexes (likely **2-OH**) are formed.

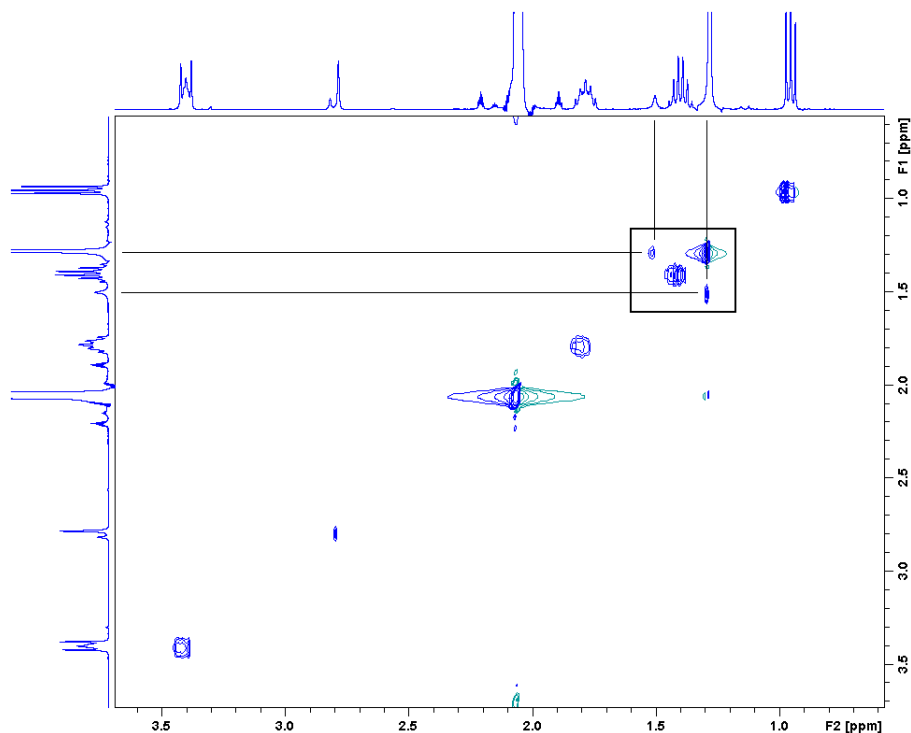


Figure 3. NOESY analysis of assembly $(\mathbf{1})_2\cdot\text{NBu}_4\text{OH}$ in $\text{acetone-}d_6$ (aliphatic region).

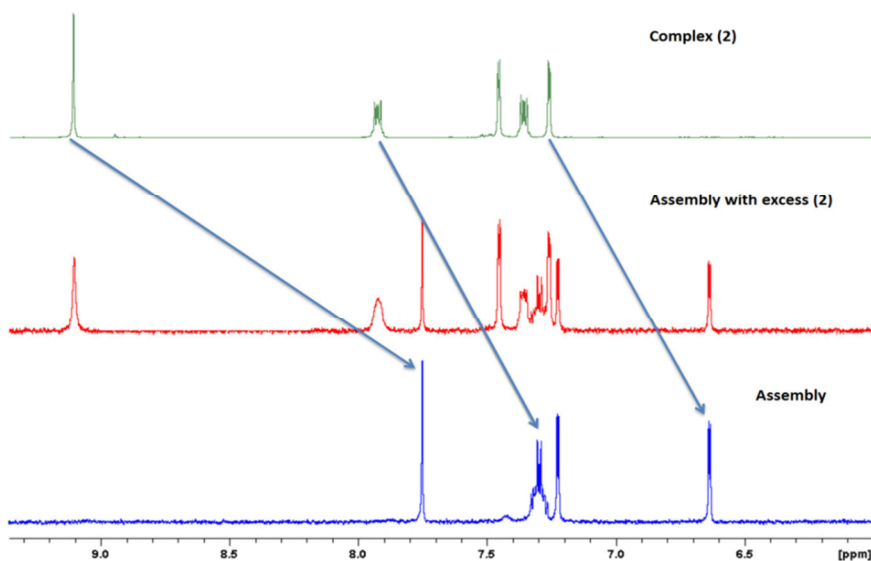
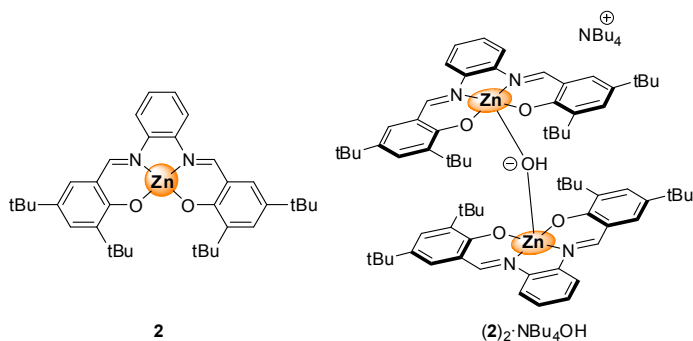


Figure 4. ^1H NMR comparison with assembly $(2)_2 \cdot \text{NBu}_4\text{OH}$ (acetone- d_6): in green complex **(2)**; in red assembly $(2)_2 \cdot \text{NBu}_4\text{OH}$ with 3 equiv of free **(2)**; in blue pure assembly $(2)_2 \cdot \text{NBu}_4\text{OH}$.

The stability of assembly $(2)_2 \cdot \text{NBu}_4\text{OH}$ was also probed under non polar conditions by monitoring the disruption of the assembly upon the addition of competitive pyridine using UV-Vis. spectroscopy. Upon addition of pyridine, the absorption maximum at $\lambda = 424$ nm increased and a typical red-shift at $\lambda = 428$ nm occurred (Fig. 5A). As can be seen from Fig. 5B approximately 300.000 equivalents are needed to fully break the assembled species. As reported previously by us for binuclear Zn(salphen) structures^[22] this is strong evidence for a high stability of these

assemblies under non-polar conditions. Attempts to realize competitive titrations under more polar conditions (i.e., in acetone or THF) resulted in non-reproducible data.

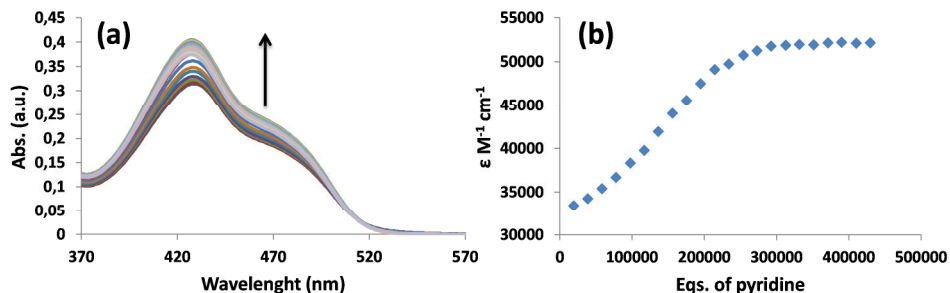


Figure 5: (a) Spectral changes of complex $(\mathbf{2})_2 \cdot \text{NBu}_4\text{OH}$ upon the addition of pyridine carried out in toluene at $[(\mathbf{2})_2 \cdot \text{NBu}_4\text{OH}] = 9.54 \times 10^{-6} \text{ M}$, and (b) the corresponding titration curve at $\lambda = 428 \text{ nm}$.

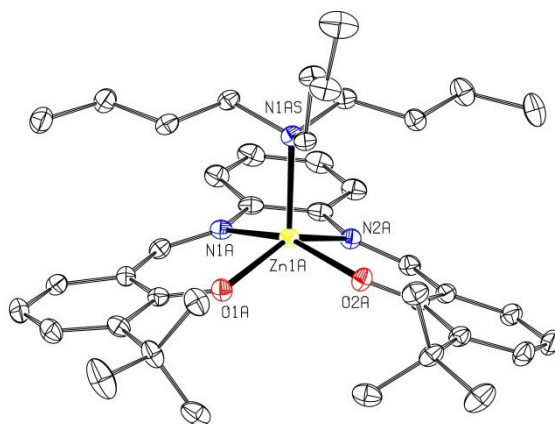
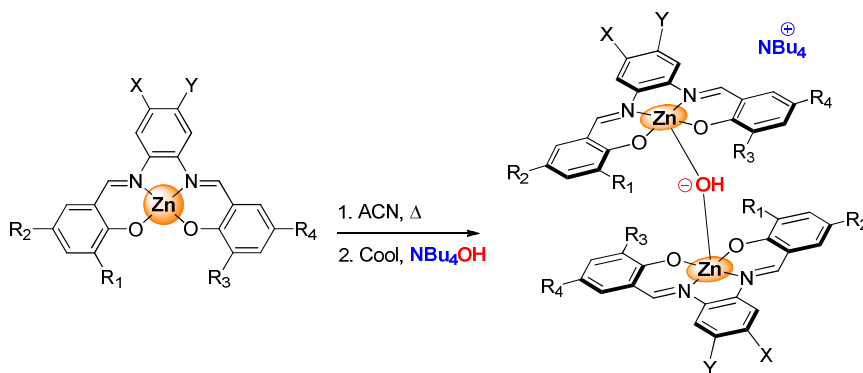


Figure 6. X-ray molecular structure determined for $\mathbf{1} \cdot \text{NBu}_3$ with a partial numbering scheme. Hydrogen atoms are omitted for clarity and only one of the independent molecules found in the unit cell is shown. The Zn ion is highlighted in yellow. Crystallographic details and relevant bond distances and angles are given in Tables 2 and 3 (see experimental section).

We attempted to prepare $(\mathbf{1})_2 \cdot \text{NBu}_4\text{OH}$ independently by combination of $\mathbf{1}$ with NBu_4OH in hot CH_3CN . Cooling of the mixture afforded crystalline material that was analyzed both by ^1H NMR and X-ray analysis (see Fig. 6, Tables 2 and 3). Unexpectedly, this procedure yielded a structure that comprises a tributyl amine coordinated to $\mathbf{1}$ (i.e., $\mathbf{1} \cdot \text{NBu}_3$). The presence of tributyl amine can be explained by a Hoffman type elimination reaction in the cation NBu_4^+ leading to undesired $\mathbf{1} \cdot \text{NBu}_3$ complex formation.^[16] To avoid the problem of Hoffman elimination of the

thermally labile NBu_4OH , the assembly $(\mathbf{1})_2\cdot\text{NBu}_4\text{OH}$ was then prepared by an adjusted method that involves dissolution of **1** in CH_3CN , cooling the solution to ambient temperature followed by addition of NBu_4OH .

Table 1. Synthesis of assembled structures of type $(\mathbf{x})_2\cdot\text{NBu}_4\text{OH}$ ($\mathbf{x} = \mathbf{1-8}$) using $\text{Zn}(\text{salphen})$ complexes **1-8**.



R_1	R_2	R_3	R_4	X	Y	Yield (%) ^a
tBu	H	tBu	H	H	H	92
tBu	tBu	tBu	tBu	H	H	60
tBu	tBu	tBu	H	H	H	47
tBu	Br	tBu	Br	H	H	83
H	tBu	H	tBu	H	H	67
tBu	tBu	tBu	tBu	Cl	Cl	63
tBu	tBu	H	tBu	H	H	^b
tBu	H	tBu	H	NO_2	H	16

^a Isolated yield; ^b Only the starting $\text{Zn}(\text{salphen})$ complex **7** was recovered.

This procedure proved to be a reliable and fast way to produce crystalline material of $(\mathbf{1})_2\cdot\text{NBu}_4\text{OH}$, and the assembly was isolated in high yield (92%). In order to amplify the scope of these compounds also other $\text{Zn}(\text{salphen})$ complexes (**2-8**, Scheme 1) were probed and combined in a similar fashion with NBu_4OH to afford the corresponding dinuclear assemblies (Table 1). In

the case of **7**, we found that the synthetic approach affords exclusively crystalline **7** and this is ascribed to competing self-dimerization of the Zn(salphen) species.^[8] Another aspect worth mentioning is that isolation of the non-symmetric assemblies (**3**)₂·NBu₄OH and (**8**)₂·NBu₄OH proved to more difficult as these systems show poorer crystallization properties and, as a result, significantly lower isolated yields were obtained in these cases. The NMR characteristics of these assemblies are complicated by the fact that all fragments are magnetically inequivalent. For instance, in the case of (**8**)₂·NBu₄OH this leads to the observation of four distinct imine and tBu resonances, and overlapping signals for the other groups. Mass spectrometric analysis (MALDI-TOF-MS or ESI-MS/MeOH, both in the negative mode) additionally confirmed the formation and stability of the assembled species. For (**1**)₂·NBu₄OH two characteristic isotopic patterns were found at $m/z = 1001.3$ and 1015.2 . The former was assigned to the ion $[M-NBu_4]^+$ (calcd 1001) while the latter is a result of the exchange of the OH for methoxy anion in the assembly ($[M-NBu_4OH+OMe]^-$, calcd 1015) and probably originates from the solvent used (MeOH) for the ESI experiment. When MALDI-TOF-MS was used no exchange of the OH anion was noted and only the fragment ion $[M-NBu_4]^+$ was observed. The assemblies based on complexes **2-8** showed similar mass features.

2.3 Phosphoester cleavage catalysis

As the assemblies are reasonably stable under polar conditions and are structurally related to various multinuclear Zn-enzymes,^[12] we examined the catalytic potential of (**2**)₂·NBu₄OH in the phosphoester hydrolysis of paraoxon (i.e., diethyl 4-nitrophenyl phosphate) using a modified reported procedure.^[17] The phosphoester cleavage reaction was initially followed by UV-Vis spectroscopy (Fig. 7). The UV-Vis data was recorded during 2.5 hours and showed increasing intensity in the region where the *p*-nitro-phenolate (formed upon hydrolysis of paraoxon) shows an absorbance maximum ($\lambda \sim 400$ nm). However, in this region also the Zn(salphen) chromophores show their maximal absorbance and thus this complicates conversion analysis. It should be noted that in the absence of the assembly (**2**)₂·NBu₄OH no conversion was noted (i.e., no changes in the UV-Vis spectrum were observed). As may be expected in this buffered system, in the presence of catalytic amounts of NaOH (up to 20 mol%) or NBu₄OH, no increase around 400 nm in the UV-Vis spectra was noted during 3 h which points to no or very low conversion. However, we found that similar but somewhat smaller UV-Vis absorption changes are noted when only complex **2** is dissolved under comparable conditions. Both in the cases of assembly (**2**)₂·NBu₄OH and complex **2**, it seems that a plateau level is reached after approximately 2.5–3 h.

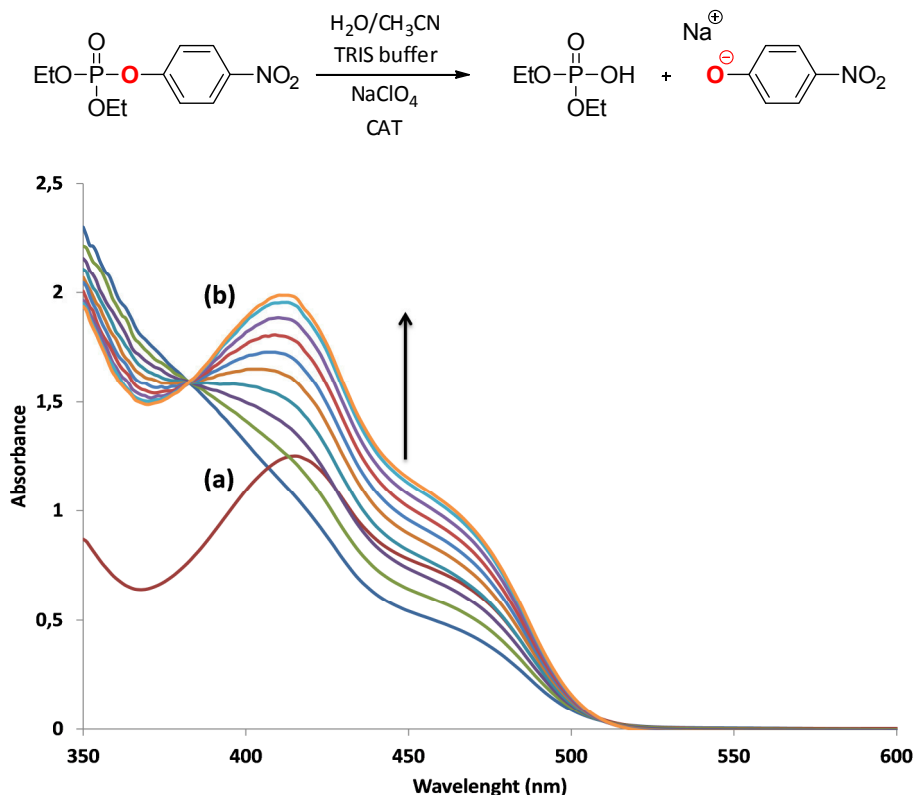


Figure 7. UV-vis spectra recorded (flow from **a** \rightarrow **b**) of the reaction of paraoxon in the presence of $(\mathbf{2})_2\text{-NBu}_4\text{OH}$. Conditions used: TRIS buffer (0.006 M), NaClO_4 (0.06 M), $(\mathbf{2})_2\text{-NBu}_4\text{OH}$ (8×10^{-5} M, 13 mol %), paraoxon (6.3×10^{-4} M), medium $\text{CH}_3\text{CN}/\text{H}_2\text{O}$ 80:20 v/v.

We then studied the influence of the buffer (TRIS = tris(hydroxymethyl)aminomethane). When the assembly $(\mathbf{2})_2\text{-NBu}_4\text{OH}$ was dissolved in the absence of the buffer, no changes were noted in the UV-Vis spectrum. Addition of TRIS buffer provoked steady increase of the absorption around $\lambda = 412$ nm with a concomitant small red shift. This indicates that the buffer itself may interact with the Zn(salphen) complex. In order to be able to examine the paraoxon conversion level in a reliable fashion $^{31}\text{P}\{^1\text{H}\}$ NMR was carried out (Fig. 8) for the catalytic mixture at $t = 2.5$ h. The volatiles were cautiously removed *in vacuo*, the residue dissolved in a mixture of $\text{CD}_3\text{CN}/\text{D}_2\text{O}$ 80:20 v/v and the $^{31}\text{P}\{^1\text{H}\}$ NMR spectrum recorded (Fig. 8C). The result was compared with a paraoxon reference sample (Fig. 8A), and another sample obtained after treatment of paraoxon with an excess of NaOH in MeOH (Fig. 8B).

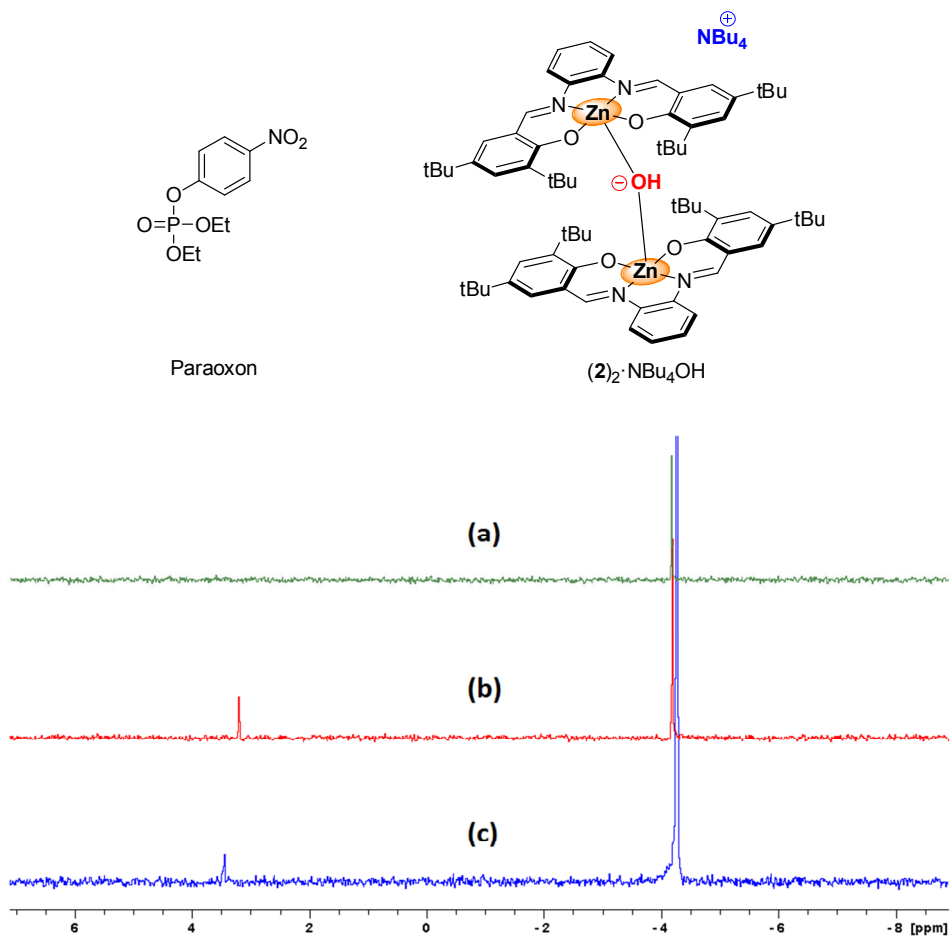


Figure 8. Recorded $^{31}\text{P}\{^1\text{H}\}$ NMR spectra of: (a) paraoxon; (b) paraoxon treated with excess NaOH to visualize the hydrolysis product (here it serves as a reference); (c) worked up reaction mixture containing $(2)_2 \cdot \text{NBu}_4\text{OH}$. All samples measured in 80:20 v/v $\text{CD}_3\text{CN}/\text{D}_2\text{O}$ at ambient conditions.

Clearly, formation of *p*-nitro-phenolate (Fig. 8C) is evident but the total conversion is very low. We also repeated the catalysis reaction at higher pH (8) but this gave a similar paraoxon conversion level. Then, the reaction was repeated but with much higher loading of the dinuclear assembly (18 mol%). In this case, the ^{31}P NMR spectrum recorded showed significantly higher conversion (Fig. 9B) and the presence of a second hydrolysis product. To further sustain the relationship between the presence of $(2)_2 \cdot \text{NBu}_4\text{OH}$ and paraoxon conversion, another batch of this dinuclear complex (18 mol%) was then added to this latter NMR sample and the ^{31}P NMR spectrum was again recorded (Fig. 9A) and showed an increased paraoxon conversion level. This

indicates that the bis-Zn(salphen) assembly plays a role in the observed paraoxon hydrolysis, but principally acts as a reagent rather than a catalyst.

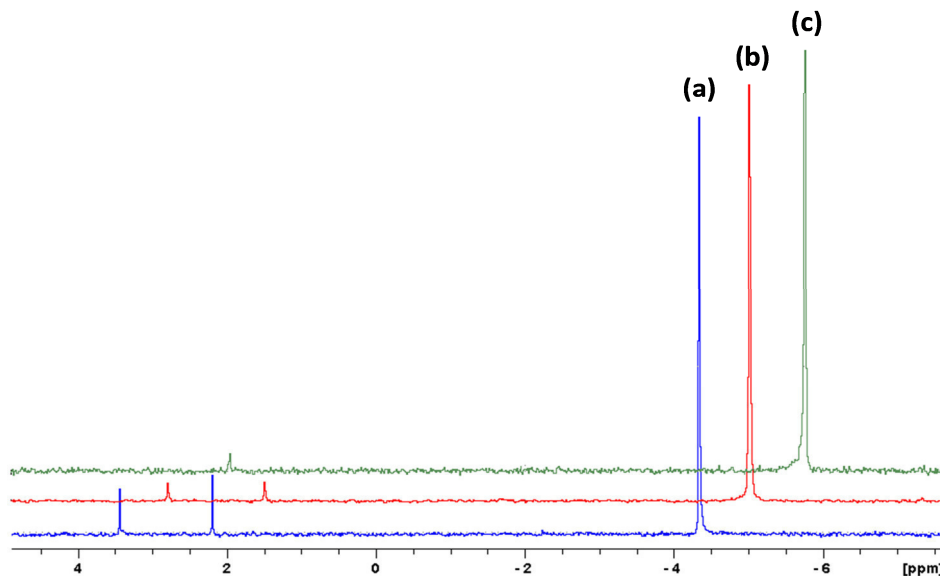


Figure 9. $^{31}\text{P}\{^1\text{H}\}$ NMR spectra recorded in $\text{CD}_3\text{CN}/\text{D}_2\text{O}$ (8:2 v/v) for (c, green) the reaction carried out with 12 mol% $(\mathbf{2})_2\cdot\text{NBu}_4\text{OH}$; (b, red) the reaction carried out with 18 mol% $(\mathbf{2})_2\cdot\text{NBu}_4\text{OH}$; (a, blue) after addition of another 18 mol% $(\mathbf{2})_2\cdot\text{NBu}_4\text{OH}$ to the sample under (b). The horizontal displacement of traces (a) and (b) are for reasons of clarity.

We assume that the assembly $(\mathbf{2})_2\cdot\text{NBu}_4\text{OH}$ is not retained under the catalytic conditions, and loses one Zn(salphen) unit to initially expose the Zn-OH fragment to the substrate. We performed a number of control experiments to investigate the species that are involved under the catalytic conditions. First of all, examination of a (dilute) NMR solution of assembly $(\mathbf{2})_2\cdot\text{NBu}_4\text{OH}$ recorded in $\text{CD}_3\text{CN}/\text{D}_2\text{O}$ (8:2 v/v) showed the presence of free $\mathbf{2}$ (by comparison with an authentic sample) and no assembled species could be detected. Second, comparison of the UV-Vis traces of $(\mathbf{2})_2\cdot\text{NBu}_4\text{OH}$ (under catalytic conditions) and salphen ligand *N,N'*-bis(3,5-di-*tert*-butylsalicylidene)-1,2-phenyldiamine confirmed that no demetalation of complex $\mathbf{2}$ takes place during the reaction. Other results that point at the de-assembled state of $(\mathbf{2})_2\cdot\text{NBu}_4\text{OH}$ under the catalytic conditions is the fact that both complex $\mathbf{2}$ as well as assembly $(\mathbf{2})_2\cdot\text{NBu}_4\text{OH}$ give rise to similar UV-Vis spectra. The instability of $(\mathbf{2})_2\cdot\text{NBu}_4\text{OH}$ in the presence of (excess) of OH anion (see Fig. 11) is further testament of a de-assembly process. It should also be noted that once the mononuclear complex $\mathbf{2}$ is formed it remains stable under the catalysis conditions as

supported by comparison of the the UV-Vis traces of the reaction mixture ($\lambda_{\max} = 412$ nm) and an authentic sample of the salphen ligand [**2** – Zn + 2H] that shows a markedly different λ_{\max} at 335 nm under comparable conditions.

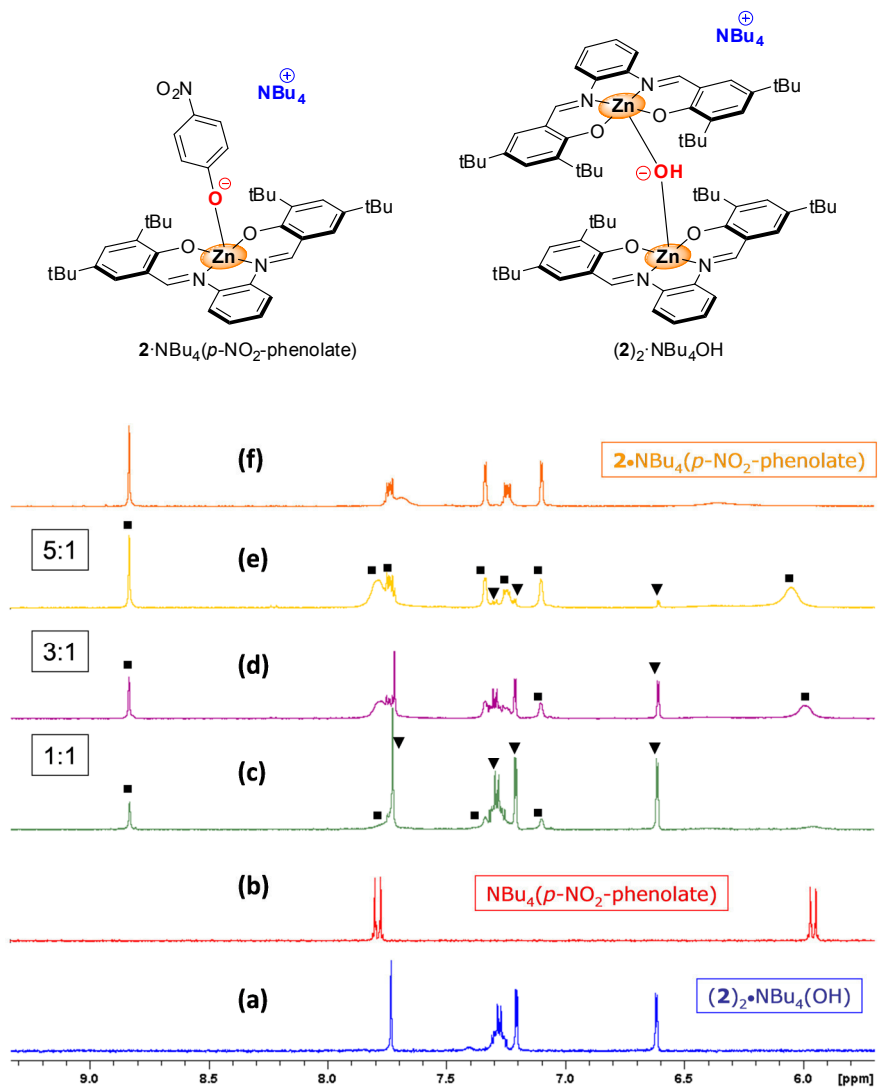


Figure 10. NMR comparison (aromatic region) between $(2)_2 \cdot \text{NBu}_4\text{OH}$ (\blacktriangledown) and assembly $2 \cdot \text{NBu}_4(\text{p-nitrophenolate})$ (\blacksquare): (a) assembly $(2)_2 \cdot \text{NBu}_4\text{OH}$; (b) $\text{NBu}_4(\text{p-nitrophenolate})$; (c) 1:1 mixture of $\text{NBu}_4(\text{p-nitrophenolate})$ and $(2)_2 \cdot \text{NBu}_4\text{OH}$; (d) 3:1 mixture of $\text{NBu}_4(\text{p-nitrophenolate})$ and $(2)_2 \cdot \text{NBu}_4\text{OH}$; (e) 5:1 mixture of $\text{NBu}_4(\text{p-nitrophenolate})$ and $(2)_2 \cdot \text{NBu}_4\text{OH}$; (f) 1:1 mixture of complex **2** and $\text{NBu}_4(\text{p-nitrophenolate})$. All experiments were done in acetone- d_6 .

Since a competing anion is produced during the reaction (i.e., *p*-nitro-phenolate) this may interfere with the re-formation of a Zn(salphen)-OH species needed for catalytic turnover and thus product inhibition occurs. To test this hypothesis we carried out the catalytic reaction (conditions: see legend Fig. 7) with 13 mol% of NBu_4 -*p*-nitro-phenolate^[18] as additive and monitored the UV-Vis changes after addition of paraoxon. Although an increase in the absorption band located around 400 nm was observed, the magnitude of this change proved to be significantly smaller as compared to the original catalysis experiment (Fig. 7) and inhibition seems apparent. We also examined the potential of *p*-nitro-phenolate to act as a competitive anion for complexation to **2** using NMR spectroscopy. Various mixtures of NBu_4 (*p*-nitro-phenolate) and $(\mathbf{2})_2\cdot\text{NBu}_4\text{OH}$ (Fig. 10, spectra c-d-e) were prepared and compared with the assemblies $(\mathbf{2})_2\cdot\text{NBu}_4\text{OH}$ (Fig. 10, spectrum a) and *in situ* prepared $\mathbf{2}\cdot\text{NBu}_4$ (*p*-nitro-phenolate) (Fig. 10, spectrum f).

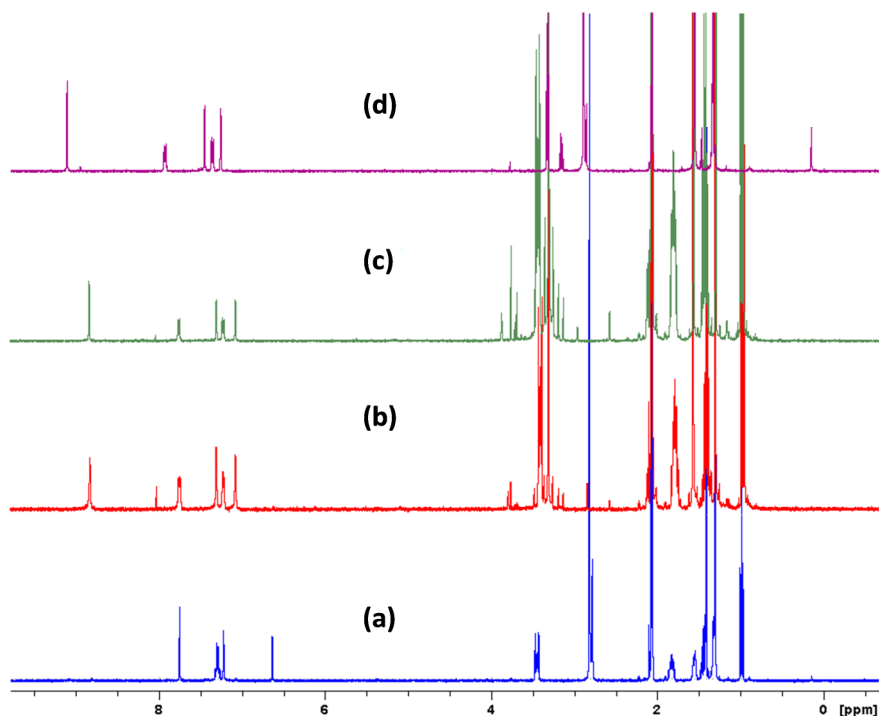


Figure 11. Influence of addition of NBu_4OH to assembly $(\mathbf{2})_2\cdot\text{NBu}_4\text{OH}$; all spectra recorded in acetone- d_6 . The small upfield shift found for the imine protons of **2** after addition of 1 or 5 equiv of NBu_4OH is ascribed to the species $\mathbf{2}\cdot\text{OH}^-$ (i.e., a mononuclear complex). (a) = pure assembly $(\mathbf{2})_2\cdot\text{NBu}_4\text{OH}$; (b) = assembly + 1 equiv of NBu_4OH ; (c) = assembly + 5 equiv of NBu_4OH ; (d) = complex **2**.

For completion also the NMR trace of the salt $\text{NBu}_4(p\text{-nitro-phenolate})$ has been provided (Fig. 10, spectrum b). The addition of $\text{NBu}_4(p\text{-nitro-phenolate})$ gives rise to the formation of a new species, viz. $2\cdot\text{NBu}_4(p\text{-nitro-phenolate})$ and increasing amounts (spectra c \rightarrow e, 1:1 to 5:1) result in a larger predominance of this assembly. The presence of two distinct NMR patterns for assemblies $(2)_2\cdot\text{NBu}_4\text{OH}$ and $2\cdot\text{NBu}_4(p\text{-nitro-phenolate})$ under these conditions points at a slow exchange process. From the much smaller upfield shift found for the imine-H ($\Delta\delta = -0.26$ ppm) of the assembly $2\cdot\text{NBu}_4(p\text{-nitro-phenolate})$ it is clear that the $p\text{-nitro-phenolate}$ anion is not able to form dinuclear assemblies with complex **2** (Fig. 11). When 1 equiv of competing $p\text{-nitro-phenolate}$ anion is added (Fig. 10, spectrum c) the ratio between both assemblies determined by signal integration was 1:1. Hence, the NMR data help to confirm that strongly interacting ligands such as $p\text{-nitro-phenolate}$ are indeed able to compete with the OH anion for complexation to **2** and can provoke formation of (catalytically inactive) mononuclear structures.

2.4 Conclusions

In conclusion, a new series of complexes comprising a binuclear, OH-bridging Zn_2 assembly based on a salphen scaffold has been presented. These structures are easily prepared in high yield and have been fully characterized by solution and solid state techniques. The stability properties of the assemblies under polar and non-polar conditions has been investigated and the assembled species $(2)_2\cdot\text{NBu}_4\text{OH}$ was applied as a potential catalyst for the phosphoester cleavage reaction that involved paraoxon. The low conversion rate is connected with an irreversible reaction that takes place between the assembly $(2)_2\cdot\text{NBu}_4\text{OH}$ and the hydrolysis product $p\text{-nitro-phenolate}$ derived from paraoxon. The fact that no further conversion takes place points at the formation of other type of mononuclear Zn(salphen) complexes under these conditions that can compete with the reformation of a hydrolysis active species. This has been illustrated by the ability of the $p\text{-nitro-phenolate}$ anion to compete with the OH anion for coordination to the Zn(salphen) complex and product inhibition is observed.

2.5 Experimental section

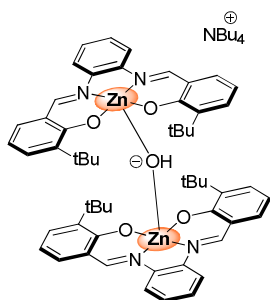
General remarks

NMR measurements were carried out on a Bruker 400 MHz spectrometer at ambient temperature, and chemical shifts are given in ppm with respect to the residual solvent peak or TMS as internal standard. Elemental analyses were performed by the Unidad de Análisis Elemental, Universidad de Santiago de Compostela (Spain). Mass spectrometric and X-ray

diffraction studies were performed by the Research Support Unit of the ICIQ. Complexes **1-7**^[19] were prepared according to previously reported procedures.

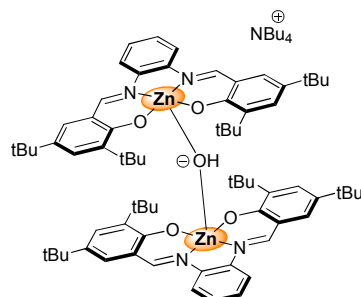
General synthetic procedure for the sandwich complexes

The respective Zn(salphen) complex was dissolved in hot acetonitrile and the orange solution was allowed to cool to room temperature. Then the appropriate amount of NBu₄OH (1 M solution in MeOH) was added and the mixture was left unstirred. In due course crystalline material was collected by filtration and dried prior to analysis. In the case of (**3**)₂·NBu₄OH and (**4**)₂·NBu₄OH the reaction mixture was cooled to -25° to force crystallization of the product. The isolated yields for the sandwich structures based on **1-3** are based on the NBu₄OH reagent, and for **4** and **5** on the respective Zn(salphen) complex.

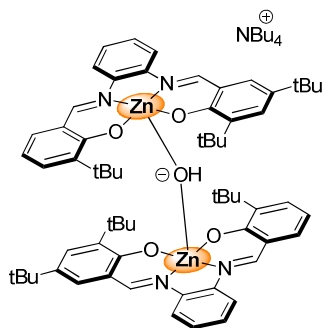


(1)₂·NBu₄OH: To a solution of Zn(salphen) complex **1** (75.0 mg, 0.152 mmol) in CH₃CN (5 mL) was added NBu₄OH (0.05 mL, 1M in MeOH). Shortly after adding the salt dark orange crystals deposited, which were collected by filtration and dried. Yield: 57.2 mg (0.00460 mmol, 92%). ¹H NMR (400 MHz, acetone-*d*₆): δ = 7.93 (s, 4H, CH=N), 7.25 (m, 8H, ArH), 7.03 (d, ³*J* = 7.2 Hz, ⁴*J* = 1.8 Hz, 4H, ArH), 6.75 (d, ³*J* = 7.8 Hz, ⁴*J* = 1.8 Hz, 4H, ArH), 6.26 (t, ³*J* = 7.5 Hz, 4H, ArH), 3.40 (m, 8H, NCH₂ of NBu), 1.74-1.82 (m, 8H, NBu), 1.50 (br s, 1H, OH), 1.35-1.44 (m, 8H, NBu), 1.29 (s, 36H, C(CH₃)₃), 0.95 (t, ³*J* = 7.4 Hz, 12H, CH₃ of NBu). ¹³C {¹H} NMR (100 MHz, acetone-*d*₆): δ = 173.75, 160.56, 142.15, 140.30, 134.06, 129.07, 125.19, 119.82, 115.51, 110.20, 58.43, 34.91, 23.49, 19.46, 12.94 (missing signal overlapping with solvent peaks). ESI-MS (MeOH, negative mode): *m/z* = 1013.2 (M – NBu₄OH + MeO)⁻ (calcd 1013.3), 1001.2 (M – NBu₄⁺)⁻ (calcd 1001.3), 521.1 (complex **1**·OMe)⁻ (calcd 521.2). Anal. calcd. for C₇₂H₉₇N₅O₅Zn₂·2H₂O: C 67.59, H 7.96, N 5.47. Found: C 67.46, H 8.48, N 5.63.

(2)₂·NBu₄OH: To a solution of Zn(salphen) complex **2** (184.2 mg, 0.305 mmol) in CH₃CN (5 mL) was added NBu₄OH (0.1 mL, 1M in MeOH). Shortly after adding the salt dark orange crystals deposited, which were collected by filtration and dried. Yield: 88.0 mg (0.0600 mmol, 60%). ¹H NMR (400 MHz, acetone-*d*₆): δ = 7.73 (s, 4H, CH=N), 7.25-7.32 (m, 8H, ArH), 7.21 (d, ⁴*J* = 2.7 Hz, 4H,



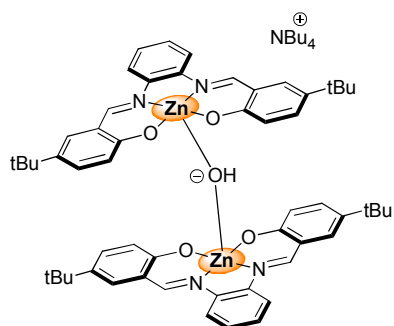
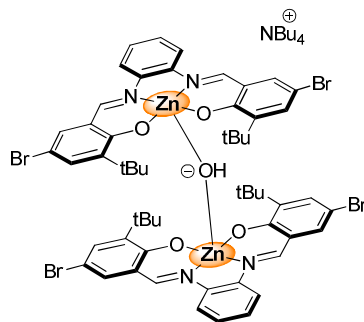
ArH), 6.62 (d, $^4J = 2.6$ Hz, 4H, ArH), 3.35-3.39 (m, 8H, NCH₂ of NBu), 1.73-1.77 (m, 8H, NBu), 1.52 (br s, 1H, OH), 1.40 (s, 36H, C(CH₃)₃), 1.32-1.38 (m, 8H, NBu), 1.29 (s, 36H, C(CH₃)₃), 0.93 (t, $^3J = 7.4$ Hz, 12H, CH₃ of NBu). ^{13}C { ^1H } NMR (100 MHz, acetone-*d*₆): $\delta = 173.36, 161.40, 142.75, 141.11, 131.86, 129.85, 128.32, 125.55, 119.27, 116.62, 59.37, 36.20, 34.52, 32.20, 30.19, 24.45, 20.41, 13.93$ (missing signal overlapping with solvent peaks). MALDI-TOF-MS (DCTB matrix, negative mode): $m/z = 1225.7$ (M - NBu₄⁺)⁻ (calcd 1225.6). Anal. calcd. for C₈₈H₁₂₉N₅O₅Zn₂: C 72.01, H 8.86, N 4.77. Found: C 71.52, H 9.68, N 4.76.



(3)₂-NBu₄OH: To a solution of Zn(salphen) complex **3** (0.17 g, 0.31 mmol) in CH₃CN (5 mL) was added NBu₄OH (0.2 mL, 1M in MeOH). The reaction mixture was cooled to -25°C which eventually yielded a bright orange solid. Yield: 95.6 mg (0.0705 mmol, 47%). ^1H NMR (400 MHz, acetone-*d*₆, mixture of isomers, major component)^[20]: $\delta = 7.97$ (s, 1H, CH=N), 7.86 (s, 1H, CH=N), 7.81 (s, 1H, CH=N), 7.79 (s, 1H, CH=N), 7.22-7.36 (m, ArH), 7.14 (d, $^3J = 7.3$ Hz, ArH), 7.04 (t, $^3J = 7.8$

Hz, $^4J = 1.8$ Hz, ArH), 6.72-6.75 (m, ArH), 6.65 (d, $^4J = 2.6$ Hz, ArH), 6.28 (t, $^3J = 7.5$ Hz, 1H, ArH), 6.23 (t, $^3J = 7.5$ Hz, 1H, ArH), 3.41 (m, 8H, NCH₂ of NBu), 1.75-1.83 (m, 8H, NBu), 1.44 (s, C(CH₃)₃), 1.40 (s, C(CH₃)₃), 1.34 (s, C(CH₃)₃), 1.31 (m, 8H, NBu, overlapping with tBu peaks), 1.30 (s, C(CH₃)₃), 1.29 (s, C(CH₃)₃), 1.25 (s, C(CH₃)₃), 0.96 (t, $^3J = 7.4$ Hz, 12H, CH₃ of NBu). ^{13}C { ^1H } NMR (100 MHz, acetone-*d*₆)^[21]: $\delta = 174.72, 173.27, 161.64, 161.50, 161.40, 161.34, 143.19, 143.07, 142.77, 142.69, 135.11, 135.07, 132.01, 131.94, 129.94, 129.91, 129.82, 128.61, 128.43, 126.08, 125.92, 125.79, 119.20, 119.10, 116.58, 116.55, 116.53, 111.19, 111.10, 59.34, 36.21, 36.15, 35.91, 35.89, 30.17, 29.98, 24.44, 20.40, 13.93$ (missing signals due to overlap with solvent peaks). ESI-MS (MeOH, negative mode): $m/z = 1169.3$ (M - NBu₄OH + BuO)⁻ (calcd 1169.5), 1139.3 (M - NBu₄OH + EtO)⁻ (calcd 1139.5), 1127.3 (M - NBu₄OH + MeO)⁻ (calcd 1127.5), 1113.3 (M - NBu₄⁺)⁻ (calcd 1113.4), 577.2 (complex **1**-OMe)⁻ (calcd 577.2). Anal. calcd. for C₈₀H₁₁₃N₅O₅Zn₂·2H₂O: C 69.05, H 8.47, N 5.03. Found: C 69.44, H 9.00, N 5.07.

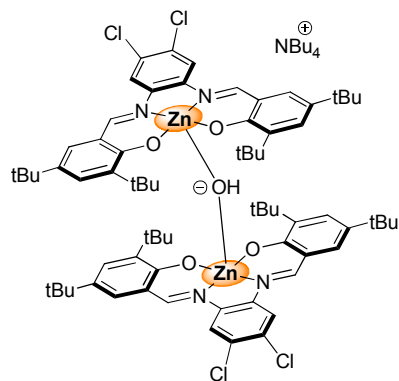
(4)₂·NBu₄OH: To a solution of Zn(salphen) complex **4** (244.4 mg, 0.376 mmol) in CH₃CN (8 mL) and CH₂Cl₂ (4 mL) was added NBu₄OH (0.3 mL, 1M in MeOH). The reaction mixture was concentrated to 6 mL upon which a bright orange, crystalline solid separated. The product was isolated by filtration yielding 244.5 mg (0.157 mmol, 83%). ¹H NMR (400 MHz, acetone-*d*₆): δ = 7.90 (s, 4H, CH=N), 7.38 (m, 8H, ArH), 7.09 (d, ⁴*J* = 2.8 Hz, 4H, ArH), 6.90 (d, ⁴*J* = 2.8 Hz, 4H, ArH), 3.40-3.44 (m, 8H, NCH₂ of NBu), 1.76-1.84 (m, 8H, NBu), 1.50 (br s, 1H, OH), 1.37-1.46 (m, 8H, NBu), 1.26 (s, 36H, C(CH₃)₃), 0.96 (t, ³*J* = 7.4 Hz, 12H, CH₃ of NBu). ¹³C {¹H} NMR (100 MHz, acetone-*d*₆): δ = 173.41, 160.46, 146.31, 140.45, 135.94, 132.96, 127.17, 122.12, 116.48, 102.31, 59.37, 36.12, 29.81, 24.43, 20.40, 13.92. MALDI-TOF-MS (DCTB matrix, negative mode): *m/z* = 1315.1 (M – NBu₄⁺)⁻ (calcd 1314.96). Anal. calcd. for C₇₂H₉₃N₅O₅Zn₂Br₄·H₂O: C 54.84, H 6.07, N 4.44. Found: C 54.69, H 6.00, N 4.65.



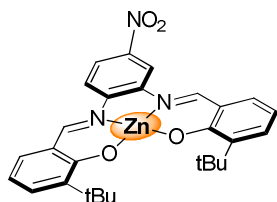
(5)₂·NBu₄OH: To a solution of Zn(salphen) complex **5** (191.8 mg, 0.390 mmol) in CH₃CN (3 mL) and CH₂Cl₂ (5 mL) was added NBu₄OH (0.5 mL, 1M in MeOH). The reaction mixture was concentrated to 3-4 mL upon which a slightly orange microcrystalline solid separated. The product was isolated by filtration yielding 162.5 mg (0.131 mmol, 67%). ¹H NMR (400 MHz, acetone-*d*₆): δ = 7.84 (s, 4H, CH=N), 7.30-7.33

(m, 4H, ArH), 7.19-7.23 (m, 8H, ArH), 6.88 (d, ⁴*J* = 2.8 Hz, 4H, ArH), 6.43 (d, ⁴*J* = 8.9 Hz, 4H, ArH), 3.38-3.42 (m, 8H, NCH₂ of NBu), 1.72-1.78 (m, 8H, NBu), 1.28-1.40 (m, 27H, OH+NBu+C(CH₃)₃), 0.92 (t, ³*J* = 7.4 Hz, 12H, CH₃ of NBu). ¹³C {¹H} NMR (100 MHz, acetone-*d*₆): δ = 173.02, 161.95, 141.15, 133.98, 132.26, 132.15, 126.52, 124.55, 119.55, 117.07, 59.32, 34.24, 32.07, 24.53, 20.37, 13.99. ESI(-)-MS (MeOH): *m/z* = 1013.3 (M – NBu₄OH + MeO)⁻ (calcd 1013.3), 1001.2 (M – NBu₄⁺)⁻ (calcd 1001.3), 521.1 (complex **5**-OMe)⁻ (calcd 521.2). Anal. calcd. for C₇₂H₉₇N₅O₅Zn₂·5H₂O: C 64.85, H 8.09, N 5.25. Found: C 64.36, H 7.42, N 5.57.

(6)₂·NBu₄OH: To a solution of Zn(salphen) complex **6** (153.6 mg, 0.228 mmol) in CH₃CN (5 mL) was added NBu₄OH (0.13 mL, 1M in MeOH). The reaction mixture was cooled to -30°C causing precipitation of a solid. The solid was isolated by filtration and dried to yield the product (131.2 mg, 0.0817 mmol, 63%) as an orange solid. ¹H NMR (400 MHz, acetone-*d*₆): δ = 7.87 (s, 4H, CH=N), 7.41 (s, 4H, ArH), 7.28 (d, ⁴J = 2.7 Hz, 4H, ArH), 6.78 (d, ⁴J = 2.7 Hz, 4H, ArH), 3.40-



3.44 (m, 8H, NCH₂ of NBu), 1.76-1.84 (m, 8H, NBu), 1.38-1.44 (m, 45H, OH+NBu+C(CH₃)₃), 1.30 (s, 36H, C(CH₃)₃), 0.96 (t, ³J = 7.4 Hz, 12H, CH₃ of NBu). ¹³C {¹H} NMR (100 MHz, acetone-*d*₆): δ = 174.00, 162.20, 143.04, 141.21, 132.98, 129.76, 129.38, 128.65, 119.15, 117.89, 59.30, 36.21, 34.58, 32.19, 30.09, 24.43, 20.37, 13.93. ESI(-)-MS (MeOH): *m/z* = 1375.4 (M - NBu₄OH + OMe)⁻ (calcd 1375.4), 1361.4 (M - NBu₄)⁻ (calcd 1361.4), 703.2 (complex **6**-OMe)⁻ (calcd 703.2). Anal. calcd. for C₈₈H₁₂₅N₅O₅Zn₂Cl₄: C 65.83, H 7.85, N 4.36. Found: C 66.26, H 7.72, N 4.52.

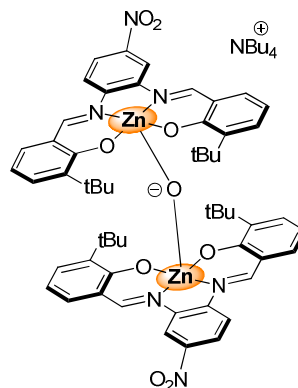


Zn(salphen) complex (8): To a solution of 4-nitro-1,2-phenylenediamine (0.25 g, 1.63 mmol) and 3-*tert*-butylsalicylaldehyde (0.69 g, 3.87 mmol) in MeOH (35 mL) was added a solution of Zn(OAc)₂·2H₂O (0.72 g, 3.28 mmol) in MeOH (10 mL). After 18 h, the mixture was filtered yielding a yellow solid

(215.0 mg). After 18 h, the reaction mixture was filtered to yield a red solid (282.3 mg). Then the mother liquor was cooled to -28°C to yield another 52.4 mg of product. Total yield: 334.7 mg (0.62 mmol, 38%). ¹H NMR (400 MHz, acetone-*d*₆): δ = 9.30 (s, 1H, CH=N), 9.21 (s, 1H, CH=N), 8.74 (d, ⁴J = 1.9 Hz, 1H, ArH), 8.20 (d, ³J = 9.0 Hz, ⁴J = 2.3 Hz, 1H, ArH), 8.13 (d, ³J = 9.1 Hz, 1H, ArH), 7.41 (d, ³J = 7.9 Hz, ⁴J = 1.5 Hz, 1H, ArH), 7.31-7.38 (m, 3H, ArH), 6.54 (t, ³J = 7.6 Hz, 2H, ArH), 1.53 (s, 18H, 2 × C(CH₃)₃). ¹³C {¹H} NMR (100 MHz, DMSO-*d*₆): δ = 173.48, 172.72, 165.16, 164.62, 145.30, 145.15, 141.96, 141.64, 139.83, 135.01, 131.36, 121.31, 119.47, 119.35, 117.10, 112.80, 35.05, 29.49. MS (MALDI+, dctb): *m/z* = 535.1 (M)⁺ (calcd. 535.1). Anal. calcd. for C₂₈H₂₉N₃O₄Zn·2H₂O: C 58.70, H 5.81, N 7.33; Found: C 58.81, H 6.22, N 7.21. As a minor product in this synthetic protocol, the mono-imine based on 4-nitro-phenylenediamine and 3-*tert*-butylsalicylaldehyde was obtained from a separate fraction. Yield: 116.0 mg (0.370 mmol, 23% based on diamine reagent). ¹H NMR (400 MHz, acetone-*d*₆): δ = 13.27 (s, 1H, OH), 9.02 (s, 1H, CH=N), 8.08 (d, ⁴J = 2.5 Hz, 1H, ArH), 7.99 (d, ³J = 9.0 Hz, ⁴J = 2.6 Hz, 1H, ArH), 7.56 (d, ³J = 7.6 Hz, ⁴J =

1.6 Hz, 1H, ArH), 7.45 (d, $^3J = 7.7$ Hz, $^4J = 1.4$ Hz, 1H, ArH), 6.94-6.97 (m, 2H, ArH), 6.24 (br s, 2H, NH₂), 1.45 (s, 9H, C(CH₃)₃). ¹³C {¹H} NMR (100 MHz, DMSO-*d*₆): $\delta = 165.81, 159.34, 149.57, 136.35, 133.14, 131.69, 130.44, 124.20, 119.31, 118.59, 115.22, 113.44, 34.45, 29.22$. MS (ESI+, MeOH): $m/z = 336.1$ (M+Na)⁺ (calcd. 336.1), 649.3 (2M+Na)⁺ (calcd. 649.3). Anal. calcd. for C₁₇H₁₉N₃O₃: C 65.16, H 6.11, N 13.41; Found: C 65.03, H 6.04, N 13.28.

(8)₂·NBu₄OH: To a solution of Zn(salphen) complex **8** (183.1 mg, 0.341 mmol) in CH₃CN (5 mL) was added NBu₄OH (0.15 mL, 1M in MeOH). The reaction mixture was concentrated and cooled to -30°C causing precipitation of a solid. The solid was isolated by filtration and dried to give an intensely colored, dark red solid (82.8 mg, 0.0531 mmol, 16%). ¹H NMR (400 MHz, acetone-*d*₆): $\delta = 8.33$ (s, 1H, CH=N), 8.32 (s, 1H, CH=N), 8.31 (s, 1H, CH=N), 8.27 (s, 1H, CH=N), 8.13 (d, $^4J = 2.5$ Hz, 1H, ArH), 7.99-8.05 (m, 3H, ArH), 7.58 (d, $^3J = 8.7$ Hz, 1H, ArH),



7.48 (d, $^3J = 9.0$ Hz, 1H, ArH), 7.05-7.12 (m, 5H, ArH), 6.98 (d, $^3J = 7.9$ Hz, $^4J = 1.7$ Hz, 1H, ArH), 6.90 (d, $^3J = 7.9$ Hz, $^4J = 1.8$ Hz, 1H, ArH), 6.86 (d, $^3J = 8.0$ Hz, $^4J = 1.8$ Hz, 1H, ArH), 6.27-6.38 (m, 4H, ArH), 3.44-3.48 (m, 8H, NCH₂ of NBu), 1.80-1.88 (m, 8H, NBu), 1.51 (br s, 1H, OH), 1.39-1.49 (m, 8H, NBu), 1.31 (s, 9H, C(CH₃)₃), 1.29 (s, 18H, 2 × C(CH₃)₃), 1.27 (s, 9H, C(CH₃)₃), 0.99 (t, $^3J = 7.4$ Hz, 12H, CH₃ of NBu). ¹³C {¹H} NMR (100 MHz, acetone-*d*₆): $\delta = 176.05, 176.04, 175.25, 175.12, 164.17, 164.11, 163.28, 163.22, 147.28, 145.83, 143.74, 143.64, 143.43, 143.39, 141.66, 141.56, 135.51, 135.40, 135.35, 135.18, 131.51, 131.46, 131.13, 131.05, 121.43, 121.36, 120.71, 120.67, 120.47, 120.43, 116.75, 112.58, 112.45, 112.35, 112.17, 111.64, 111.50, 59.43, 35.88, 30.04, 24.46, 20.45, 13.92$. MALDI(-)-MS (pyrene): $m/z = 1089.2$ (M - NBu₄)⁻ (calcd 1089.2). Anal. calcd. for C₇₂H₉₅N₇O₉Zn₂·½H₂O: C 64.42, H 7.21, N 7.30. Found: C 64.44, H 7.60, N 7.44.

Single crystal X-ray analysis data

Table 2. Crystal and structure determination data for $(1)_2 \cdot \text{NBu}_4\text{OH}$ and $1 \cdot \text{NBu}_3$.

Complex	$(1)_2 \cdot \text{NBu}_4\text{OH}$	$1 \cdot \text{NBu}_3$
Empirical formula	$\text{C}_{73}\text{H}_{99}\text{Cl}_2\text{N}_5\text{O}_5\text{Zn}_2$	$\text{C}_{40}\text{H}_{57}\text{N}_3\text{O}_2\text{Zn}$
Formula weight	1328.25	677.26
T / K	293(2)	100(2)
Crystal system	Orthorhombic	Orthorhombic
Space group	$Pbca$ (no.61)	$Pca2(1)$
Unit cell dimensions/ \AA	$a = 23.195(5)$ $b = 24.208(5)$ $c = 24.371(5)$	$a = 17.1860(9)$ $b = 19.0560(10)$ $c = 22.1544(11)$
Unit cell angles / $^\circ$	$\alpha, \beta, \gamma = 90$	$\alpha, \beta, \gamma = 90$
$V / \text{\AA}^3$	13684(5)	7255.5(6)
Z	8	8
$F(000)$	5648	2912
$\rho_{\text{calc}} / \text{g} \cdot \text{cm}^{-3}$	1.289	1.240
Crystal size / mm^3	$0.05 \times 0.05 \times 0.10$	$0.2 \times 0.15 \times 0.15$
$\lambda / \text{\AA}$	0.71073	0.71073
μ / mm^{-1}	0.832	0.714
$\theta_{\text{min}}, \theta_{\text{max}} / ^\circ$	3.6, 28.5	2.5, 28.1
Total reflections	16000	17462
Unique reflections	6395	15951
R_{int}	^a	0.0575
Data [$I > 2.0 \sigma(I)$]	6395	15951
$N_{\text{ref}}, N_{\text{par}}$	16000, 800	17462, 847
GOF on F^2	0.831	1.055
$R1, wR2$ (all data)	0.0541, 0.1118	0.0432, 0.0926
$R1, wR2$ [$I > 2.0 \sigma(I)$]	0.1487, 0.1241 ^b	0.0381, 0.0903 ^c
Flack x	—	0.002(7)
Larg. peak/hole ($e/\text{\AA}^3$)	0.879, -0.995	0.579, -1.019

^a The measured crystal was a twin and the structure was solved using TWINABS.^[15] ^b $w = 1/[\sigma^2(F_o^2) + (0.0181P)^2]$ where $P = (F_o^2 + 2F_c^2)/3$. ^c $w = 1/[\sigma^2(F_o^2) + (0.0309P)^2 + 4.5928P]$ where $P = (F_o^2 + 2F_c^2)/3$.

Table 3. Selected inter-atomic distances (Å) and bond angles (°) of $(1)_2\cdot\text{NBu}_4\text{OH}$ and $1\cdot\text{NBu}_3$.

$(1)_2\cdot\text{NBu}_4\text{OH}$		$1\cdot\text{NBu}_3$	
Zn(1A)-O(1A)	1.965(3)	Zn(1A)-O(1A)	1.9636(17)
Zn(1A)-O(2A)	1.993(2)	Zn(1A)-O(2A)	1.9811(16)
Zn(1A)-O(1)	1.941(2)	Zn(1A)-N(1AS)	2.180(2)
Zn(1A)-N(1A)	2.089(3)	Zn(1A)-N(1A)	2.180(2)
Zn(1A)-N(2A)	2.120(3)	Zn(1A)-N(2A)	2.092(2)
O(1A)-Zn(1A)-O(2A)	95.36(10)	O(1A)-Zn(1A)-O(2A)	91.89(7)
O(1A)-Zn(1A)-N(1A)	88.50(12)	O(1A)-Zn(1A)-N(1A)	87.49(8)
O(1A)-Zn(1A)-N(2A)	102.96(11)	O(1A)-Zn(1A)-N(2A)	142.29(8)
O(2A)-Zn(1A)-N(1A)	148.79(10)	O(2A)-Zn(1A)-N(1A)	154.88(8)
O(2A)-Zn(1A)-N(2A)	84.71(11)	O(2A)-Zn(1A)-N(2A)	88.19(7)
O(1A)-Zn(1A)-O(1)	103.79(11)	O(1A)-Zn(1A)-N(1AS)	111.82(8)
O(2A)-Zn(1A)-O(1)	103.15(9)	O(2A)-Zn(1A)-N(1AS)	102.59(8)
N(1A)-Zn(1A)-N(2A)	78.06(13)	N(1A)-Zn(1A)-N(2A)	77.30(8)

2.6 Notes and references

- [1] a) P. G. Cozzi, *Chem. Soc. Rev.*, 2004, **33**, 410; b) T. Katsuki, *Adv. Synth. Catal.*, 2002, **344**, 131; c) E. N. Jacobsen, *Acc. Chem. Res.*, 2000, **33**, 421; d) N. Madhavan, C. W. Jones and M. Weck, *Acc. Chem. Res.*, 2008, **41**, 1153; e) E. M. McGarrigle and D. G. Gilheany, *Chem. Rev.*, 2005, **105**, 1563.
- [2] S. J. Wezenberg and A. W. Kleij, *Angew. Chem. Int. Ed.*, 2008, **47**, 2354.
- [3] a) M. E. Germain and M. J. Knapp, *J. Am. Chem. Soc.*, 2008, **130**, 5422; b) A. Dalla-Cort, L. Mandolini, C. Pasquini, K. Rissanen, L. Russo and L. Schiaffino, *New. J. Chem.*, 2007, **31**, 1633; c) S. J. Wezenberg, E. C. Escudero-Adán, J. Benet-Buchholz and A. W. Kleij, *Org. Lett.*, 2008, **10**, 3311.
- [4] For a few selected examples: a) C. Mazet and E. N. Jacobsen, *Angew. Chem. Int. Ed.*, 2008, **47**, 1762; b) P. Goyal, X. Zheng and M. Weck, *Adv. Synth. Catal.*, 2008, **350**, 1816; c) R. N. Loy and E. N. Jacobsen, *J. Am. Chem. Soc.*, 2009, **131**, 2786.
- [5] A. W. Kleij, *Chem.–Eur. J.*, 2008, **14**, 10520.
- [6] See for instance: K. Matsumoto, B. Saito and T. Katsuki, *Chem. Commun.*, 2007, 3619.

- [7] K. E. Splan, A. M. Massari, G. A. Morris, S.-S. Sun, E. Reina, S. T. Nguyen and J. T. Hupp, *Eur. J. Inorg. Chem.*, 2003, 2348.
- [8] Self-dimerization for Zn(salphen) complexes is a general phenomenon for those complexes that lack large substituents at the 3/3' positions of the phenyl side rings. Apparently, preferential crystallization of **7** in the presence of NBu_4OH takes place under the applied conditions. For the use of this self-assembly behavior in supramolecular systems see: A. W. Kleij, *Dalton Trans.*, 2009, 4635.
- [9] For some examples see: a) A. W. Kleij, M. Kuil, D. M. Tooke, A. L. Spek and J. N. H. Reek, *Inorg. Chem.*, 2007, **46**, 5829; b) A. W. Kleij, M. Kuil, M. Lutz, D. M. Tooke, A. L. Spek, P. C. J. Kamer, P. W. N. M. van Leeuwen and J. N. H. Reek, *Inorg. Chim. Acta*, 2005, **359**, 1807; c) S. J. Wezenberg, E. C. Escudero-Adán, J. Benet-Buchholz and A. W. Kleij, *Inorg. Chem.*, 2008, **47**, 2925.
- [10] S. J. Wezenberg, E. C. Escudero-Adán, J. Benet-Buchholz and A. W. Kleij, *Chem. –Eur. J.*, 2009, **15**, 5695.
- [11] See for some examples: a) N. Halland, A. Braunton, S. Bachmann, M. Marigo and K. A. Jorgensen, *J. Am. Chem. Soc.*, 2004, **126**, 4790; b) A. Bøgevig, K. Juhl, N. Kumaragurubaran, W. Zhuang and K. A. Jorgensen, *Angew. Chem. Int. Ed.*, 2002, **41**, 1790.
- [12] The complex structurally resembles multinuclear Zn enzymes such as phospholipase C. For more details see: a) J. Weston, *Chem. Rev.*, 2005, **105**, 2151. For a recent example of a functional model for metallohydrolases see: b) Y.-H. Zhou, H. Fu, W.-X. Zhao, M.-L. Tong, C.-Y. Su, H. Sun, L.-N. Ji and Z.-W. Mao, *Chem.–Eur. J.* 2007, **13**, 2402.
- [13] N. Itagaki, M. Kimura, T. Sugahara and Y. Iwabuchi, *Org. Lett.*, 2005, **7**, 4185.
- [14] We were also able to obtain crystalline material for assembly $(\mathbf{2})_2\cdot\text{NBu}_4\text{OH}$ and X-ray diffraction in this case confirmed the presence of the sandwich structure. The crystal quality in this case proved, however, to be poor.
- [15] TWINABS Version 2008/4 Bruker AXS, R. H. Blessing, *Acta Cryst.*, 1995, **A51**, 33.
- [16] The coordination ability of (tertiary) amines to analogous Zn(salphen) structures was previously studied by Dalla Cort et al. showing a large steric effect, see reference 3b. For a more recent account on this subject: E. C. Escudero-Adán, J. Benet-Buchholz and A. W. Kleij, *Eur. J. Inorg. Chem.*, 2009, 3562.
- [17] We used a 80:20 v/v acetonitrile/water system with 12 mol% of $(\mathbf{2})_2\cdot\text{NBu}_4\text{OH}$ since this assembly proved to be more soluble than the one based on **1** under the applied conditions. The increase in intensity of the band related to *p*-nitro-phenolate anion formation ($\lambda \sim 400$

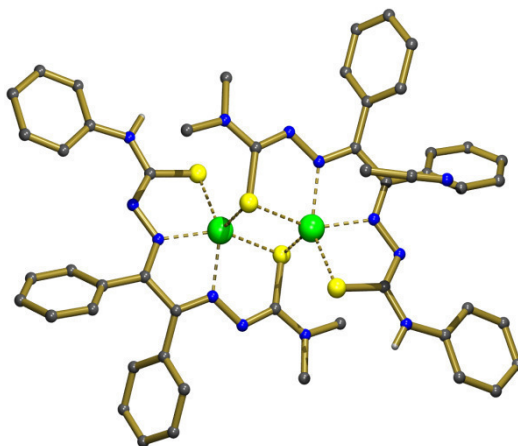
- nm) was monitored. See for more experimental details: H. Carlsson, M. Haukka and E. Nordlander, *Inorg. Chem.*, 2004, **43**, 5681.
- [18] For the synthesis of $\text{NBu}_4(p\text{-nitro-phenolate})$ see: N. Saki and E. U. Akkaya, *J. Incl. Phenom. Macrocycl. Chem.*, 2005, **53**, 269.
- [19] For details please refer to: a) A. W. Kleij, D. M. Tooke, M. Kuil, M. Lutz, A. L. Spek and J. N. H. Reek, *Chem. –Eur. J.*, 2005, **11**, 4743; b) A. W. Kleij, D. M. Tooke, M. Lutz, A. L. Spek and J. N. H. Reek, *Eur. J. Inorg. Chem.*, 2005, 4626; c) E. C. Escudero-Adán, J. Benet-Buchholz and A. W. Kleij, *Inorg. Chem.*, 2007, **46**, 7265.
- [20] Please note that the relative orientation of the two Zn(salphen) units in this assembly may give rise to multiple signals in the ^1H NMR spectrum as a consequence of the non-symmetrical nature of **3**. Nonetheless, the data are in line with those reported for the other assemblies, i.e., large upfield shifts are noted for the imine-H. Also, some de-assembled **3** may be present.
- [21] This compound crystallizes from deuterated acetone/benzene and affected the quality of the spectra. The data given are for the major component.
- [22] G. Salassa, M. J. J. Coenen, S. J. Wezenberg, B.L.M. Hendriksen, S. Speller, J. A. A. W. Elemans and A. W. Kleij, *J. Am. Chem. Soc.*, 2012, **134**, 7186.

Chapter III

Mild Formation of Cyclic Carbonates using Zn(II)

Complexes based on N₂S₂-Chelating Ligands

A series of Zn(II) complexes were prepared based on a versatile N₂S₂-chelating ligand abbreviated as btsc [btsc = bis-(thiosemicarbazonato)] derived from simple and accessible building blocks. These complexes comprise a Lewis acidic Zn(II) centre useful for substrate activation, and we have investigated the potential of these compounds in the cyclo-

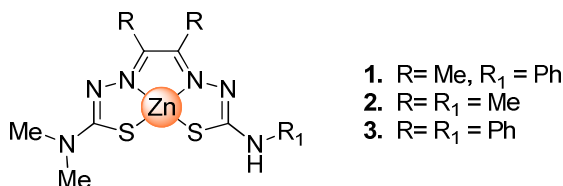


addition reaction of carbon dioxide to various epoxides yielding cyclic carbonate structures. Initial screening studies with complexes 1-3 showed that complex 3 is most suited for this CO₂ fixation reaction under particularly mild conditions (45°C, pCO₂ = 10 bar) and low catalyst loadings (1 mol%). Furthermore, upon examination of the substrate scope, complex 3 shows appreciable catalytic turnover for a range of terminal epoxides, while for the sterically more challenging epoxides almost no conversion was achieved under comparable conditions. Additional experiments indicated that higher yields of cyclic carbonates may be realized by simply increasing the (co)catalyst loading up to 3%, while maintaining mild reaction conditions. The use of a relatively non-toxic, abundant metal and an environmentally benign solvent system (MEK; methyl ethyl ketone) mark this protocol as an attractive way for organic carbonate production.

3.1 Introduction

The synthesis of organic carbonates is an area of research that has received a great deal of attention in the last decade.^[1-7] These carbonate structures find many useful applications including new non-protic solvents and they may serve as substitutes for toxic reagents in organic synthesis and as valuable precursors for their polymeric counterparts.^[1,2,4] Cyclic carbonates form a sub-family of carbonates which can be derived from epoxides; in the past these were primarily prepared by treatment of the oxiranes by phosgene followed by ring closure.^[8] This protocol, however, is characterized by the use of a highly toxic and hazardous reagent and concomitantly produces large amounts of corrosive by-products (HCl) which are difficult to handle. For this reason, alternative synthetic pathways have been investigated and the cycloaddition of carbon dioxide (CO₂) to epoxides represents an attractive and green process. Such a process has a number of advantages; CO₂ is an economical, abundant, non-toxic and renewable C1 reagent and the only by-product that is formed during the formation of the cyclic carbonate target is water. However, since CO₂ has a tremendously high kinetic and thermodynamic stability, conversion into a cyclic carbonate requires catalytic activation.^[9] Various research groups have explored homogeneous and heterogeneous catalytic solutions that are known to effectively catalyze this transformation.^[6] A major drawback of most of these proposed catalysts is the need for harsh reaction conditions which either translates into elevated CO₂ pressures, high reaction temperatures or a combination of both. Obviously, such demanding process conditions compromise the degree of sustainability, the net consumption of CO₂ and the overall energy balance. Recent breakthroughs have demonstrated the potential that metal catalysis can have for the design of more sustainable options focusing on (nearly) ambient conversion of CO₂.^[10-12] In this respect, metallosalen structures have emerged as powerful catalysts for cyclic carbonate synthesis^[6] with the Al(III),^[11] Co(III)^[13] and Cr(III) complexes^[14] among the most active systems. We have recently designed Zn-based salen complexes that have shown great promise in cyclic carbonate synthesis under extremely mild (25°C, *p*(CO₂) = 2 bar) and green reaction conditions.^[15-16] While the salen ligands result in typical N₂O₂ coordination environments around the complexed metal ion, other combinations of hetero-atoms within the ligand structure could give rise to new yet unexplored reactivity patterns. In our search for such ligands, we considered that bis-(thiosemicarbazonato) ligands (abbreviated as btsc) could be useful to construct N₂S₂-chelated complexes as these can be readily assembled from available precursors.^[17-20] It should be mentioned here that the choice for btsc ligands opposing

analogous salen systems having N₂S₂ donor sets can be justified from the viewpoint of their synthetic accessibility; as a testament of this postulation, only a few of these N₂S₂-salen ligands have been reported to date and their synthesis is less developed.^[21]

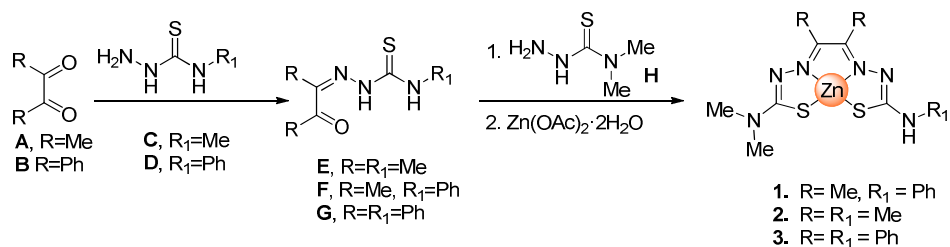


Scheme 1. Schematic structures for Zn(btsc) complexes 1-3.

Herein we report on the use of Zn(II)-btsc complexes (Scheme 1) as effective catalysts in cyclic carbonate synthesis under mild and environmentally friendly conditions using comparably low loadings of catalyst. This protocol features an easily synthesized catalyst comprising a cheap and abundant metal. The scope of cyclic carbonate synthesis has been investigated in detail and shows that the Zn(II) based complexes are active mediators for this synthetic conversion under mild conditions.

3.2 Results and discussion

Synthesis of N₂S₂ (btsc) complexes: The preparation of Zn(II)-btsc complexes **1-3** (68-77% yield) is straightforward and consists of two steps (Scheme 2). The first step involves preparation of the (pro)ligand by condensation of a dicarbonyl compound with two thiosemicarbazide molecules, followed by metallation with an appropriate metal salt. Full details on the synthesis of **1-3** are provided in the Experimental section, see also reference 22.



Scheme 2. Synthesis of Zn(btsc) complexes 1-3.

Structural studies: In order to establish the ability of complexes **1-3** to act as Lewis acid activators we first examined their structural properties. As a representative example, we combined complex **3** with various epoxides to obtain crystals suitable for X-ray diffraction. Crystals were obtained from CH₃CN upon heating **3** in the presence of an epoxide and allowing the mixture to cool to ambient temperature. Small, needle-shaped crystals were obtained which were, unfortunately, not suitable for X-ray diffraction. Recrystallization at 55°C afforded, however, better quality crystals in the case where epoxyhexane was utilized. These crystals were subjected to X-ray diffraction studies. An isolated sample of these crystals was dried *in vacuo* and then examined by ¹H NMR (DMSO-*d*₆); surprisingly, the spectrum did not show the expected signals for the epoxide substrate as only **3** was present.^[24] The crystal structure was then determined and the result is presented in Figure 1. In line with the ¹H NMR observation, the structure does not contain an axially ligated epoxide, but shows an unexpected self-assembled dimer mediated through μ₂-S bridging ligands.^[25,26-28]

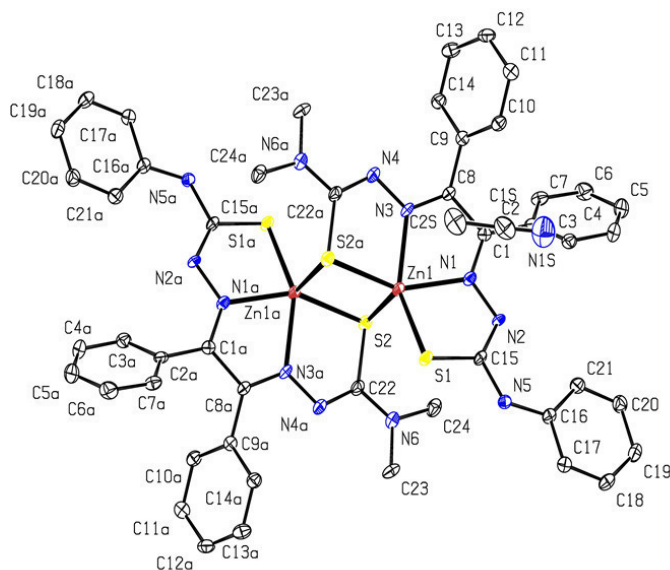
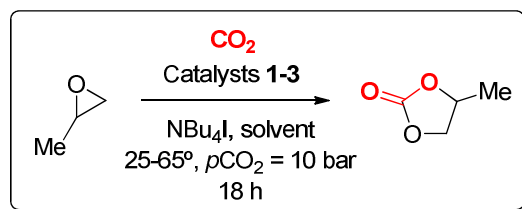


Figure 1. X-ray molecular structure for (**3**)₂ with the adopted numbering scheme. Co-crystallized solvent molecules and H-atoms are omitted for clarity. Selected bond lengths/angles: Zn(1)-S(1) = 2.3546(9) Å, Zn(1)-S(2a) = 2.4236(11) Å, Zn(1)-N(3) = 2.113(3) Å, Zn(1)-N(1) = 2.107(3) Å, Zn(1)-S(2) = 2.4592(13) Å, S(2a)-Zn(1)-S(1) = 108.82(4)°, S(2a)-Zn(1)-S(2) = 96.77(4)°, S(2a)-Zn(1)-N(3) = 80.91(9)°, S(2a)-Zn(1)-N(1) = 147.16(11)°, S(1)-Zn(1)-N(3) = 142.61(9)°, S(1)-Zn(1)-S(2) = 108.57(4)°, S(1)-Zn(1)-N(1) = 79.54(8)°.

Complex **3** crystallizes in the centro-symmetric space group P2(1)/c. The Zn ions in each of the two units of **3** are pentacoordinate with the chelating N₂S₂ fragment occupying the basal plane of the approximate square pyramidal geometry. Both S2 and S2a sulphur donor atoms act as anionic bridging ligands between the Zn1a and Zn1 metal centers completing the pentacoordination. The formation of the central S₂Zn₂ unit causes the Zn center to displace from the N₂S₂ coordination plane as illustrated by the difference in Zn-S bond distances (Zn1-S1 = 2.35 Å and Zn1-S2a = 2.42 Å) within each monomeric unit. This “self-dimerization” resembles the well-known self-assembly behavior of Zn(salen) complexes (having N₂O₂ donor sets) for which exists ample literature precedent.^[29-31] We recently reported extensive studies on the features that control the strength of this self-assembly process;^[32,33] one key feature is the steric control when, *ortho* to the O-donor atoms, large fragments are introduced. In these cases dimer formation may be minimized and monomeric complexes prevail. Connected with the substitution pattern of these salen ligands is their ability to act as Lewis acid activators. We have reported on a series of Zn(II)salphen complexes [salphen = *N,N*-bis(salicylidene)imine-1,2-diaminobenzene] that were applied as efficient catalysts for the cycloaddition of carbon dioxide (CO₂) to terminal epoxides under ambient conditions.^[15,16] Within these studies, those Zn-complexes comprising sterically demanding groups near the O-donor atoms showed the highest activities, whereas Zn(salphen) building blocks with smaller groups proved to be less efficient ascribed to their competing self-dimerization. This self-assembly behavior thus limits the effectiveness in Lewis acid mediated catalysis. The occurrence of Zn(salphen) self-assembly is easily recognized by UV-Vis spectroscopy and titration of these complexes with pyridine leads to significantly different absorption spectra.^[32,33] Therefore, the possible dimer formation of Zn complex **3** was additionally studied by UV-Vis titration with a suitable titrant (epoxyhexane) in different solvents (methyl ethyl ketone) to evaluate the formation of monomeric **3** upon addition of the epoxide. The addition of epoxide did not lead to any observable changes in the UV-Vis spectrum which may be interpreted as **3** already existing as a monomer under these conditions. Alternatively, when we titrated complex **3** with pyridine (see Experimental section), clear 1:1 complexation was observed and the stability constant K_s ($1.6 \pm 0.1 \times 10^5 \text{ M}^{-1}$) is in the same order as for pyridine binding at Zn(salphen) structures that prefer to be monomeric. This further supports the preferential presence of monomeric **3** in solution.

Catalysis studies: Complexes **1-3** were screened as catalysts for the formation of cyclic carbonates using CO₂ and propylene oxide as reagents, under relatively mild reaction conditions

Table 1. Screening of reaction conditions and catalysts (**1-3**) using propylene oxide as standard substrate, a $p(\text{CO}_2)$ of 10 bar, NBu_4I as co-catalyst and a reaction time of 18 h, $[\text{Zn}(\text{btsc})] = 3.7 - 11.1 \text{ mM}$.

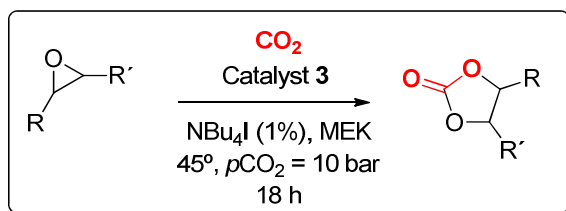


Entry	Complex (mol%)	Co-cat (mol%)	T (°C)	Solvent	Yield ^a (%)
1	1 (1)	1	45	MEK	15 ^b
2	1 (1)	2.5	45	MEK	72 ^b
3	1 (1)	1	65	MEK	70 ^b
4	2 (1)	1	45	MEK	18 ^b
5	2 (1)	2.5	45	MEK	54 ^b
6	2 (1)	1	65	MEK	52 ^b
7	3 (1)	-	45	MEK	0
8	-	1	45	MEK	0
9	3 (1)	1	25	MEK	18
10	3 (1)	1	45	MEK	66
11	3 (1)	1	65	MEK	89
12	3 (2)	1	45	MEK	76
13	3 (3)	1	45	MEK	90
14	3 (1)	1	45	THF	16
15	3 (1)	1	45	DCM	5 ^c
16	3 (1)	1	45	CH_3CN	19
17	3 (1)	1	45	Acetone	54

^a Yield determined by $^1\text{H NMR}$ ($\text{DMSO}-d_6$) using mesitylene as an internal standard. No other products were observed and therefore the selectivity toward the cyclic carbonate is $>99\%$. ^b Note that in these cases only partial dissolution of the complexes is achieved before as well as after the reaction. ^c After the reaction a heterogeneous mixture was observed.

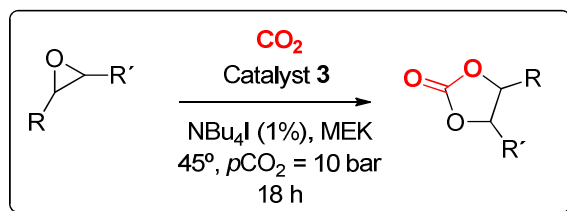
($T = 45^{\circ}\text{C}$, $p(\text{CO}_2) = 10$ bar) as a starting point using tetrabutylammonium iodide as co-catalyst and methyl ethyl ketone (MEK) as medium. All three complexes proved to be active, although in those reactions employing either complex **1** or **2** (Table 1, entries 1-6) heterogeneous mixtures were noted that may have affected catalytic turnover.^[34] In all cases conversion to propylene carbonate was achieved, with the best performance noted for complex **3** (see entries 9-11). It should be noted that in the absence of either the catalyst (**3**) or co-catalyst (entries 7-8) no conversion was observed, which emphasized the need for both catalyst components for effective turnover. As may be expected, increasing co-catalyst concentration (entries 2 and 5), increasing the reaction temperature (entries 3, 6 and 11) or increasing the catalyst loading (entries 12 and 13) gives higher yield of propylene carbonate. The influence of other solvents on the product yield was also observed (entries 14-17); unlike in previous work,^[16] both DCM as well as CH_3CN turned out to be poor solvents, whereas acetone proved to be a rather good alternative.

The catalyst **3** was further employed to study the substrate scope in the formation of cyclic carbonates using various terminal epoxides (Table 2), MEK as solvent and using mild reaction conditions (45°C , $p(\text{CO}_2) = 10$ bar) and a low catalyst loading. When using 1 mol% (3.7 mM) of **3**, yields of up to 66% are achieved (entry 1). These yields can simply be improved by increasing the catalyst loading up to 3 mol% (11.1 mmol/l) giving, for instance, propylene carbonate in high(er) yield (entry 3, 90%). The same effect is observed for the conversion of other epoxides (entries 7 and 15). As also previously observed with Zn(salphen) based catalysts with sterically more congested epoxides,^[15,16] conversion of 2,2-dimethyl- and 2,3-dimethyl-oxirane (entries 17 and 18) proved to be difficult, which relates to the steric impediment in the ring-opening step of the coordinated epoxide upon using a bulky nucleophile (i.e., iodide). As may be expected for the less reactive epoxidic substrates (entries 11 and 19) lower yields under comparable conditions are achieved, while conversely, the benchmark substrate 1,2-epoxyhexane unexpectedly gives only 27% yield (entry 12). This is lower than achieved with a similar substrate (entry 5) or using Zn(salphen) under similar reaction conditions.^[15,16]

Table 2. Screening of the substrate scope at 45°C, $p\text{CO}_2 = 10$ bar, NBu_4I as co-catalyst (1 mol%), MEK as solvent and a reaction time of 18 h using catalyst **3** (1 mol%).

Entry	Substrate (R)	Substrate (R')	Catalyst (mol%)	Product	Yield ^a (%)
1	Me	H	1		66
2	Me	H	2		76 ^b
3	Me	H	3		90 ^c
4	Me	H	2.5		90 ^d
5	$\text{CH}_2\text{CH}_2\text{CH}=\text{CH}_2$	H	1		62
6	Bn	H	1		64
7	Bn	H	2		94 ^{b,e}
8	CH_2OH	H	1		54
9	CH_2Cl	H	1		60
10	CH_2OMe	H	1		37
11	Ph	H	1		29
12	<i>n</i> -Bu	H	1		27 ^f

Table 2. (Continued)



Entry	Substrate (R)	Substrate (R')	Catalyst (mol%)	Product	Yield ^a (%)
13	<i>n</i> -Bu	H	2.5		80 ^d
14	CH ₂ OCH ₂ Ph	H	1		57
15	CH ₂ OCH ₂ Ph	H	2		98 ^{b,g}
16	CH ₂ OCH ₂ Ph	H	2.5		83 ^d
17	1,1-di-Me	H	1		1
18	Me	Me	1		1
19	CH=CH ₂	H	1		30

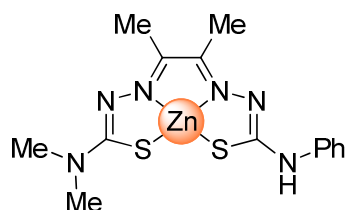
^a Yield determined by ¹H NMR (DMSO-*d*₆) using mesitylene as an internal standard. ^b 2 mol% of co-catalyst used. ^c 3 mol% of co-catalyst used. ^d Taken from reference 15; here a Zn(salphen) complex was used. ^e The calculated conversion using signal integration for both the remaining epoxide as well the carbonate product was 92%. ^f The duplicate experiment gave a 29% yield of the product. ^g The calculated conversion was 97%.

3.3 Conclusions

In this work we have presented application of a new type of Zn complex based on btsc [btsc = bis-(thiosemicarbazonato)] ligands as effective catalysts for the cyclo-addition of CO₂ to various terminal epoxides under relatively mild reaction conditions. Complex **3** proved to be the most useful among the series **1-3** under our reaction conditions. Although X-ray diffraction revealed the formation of an unexpected dimeric assembly, the monomeric form is dominant in solution,

as only the monomer is catalytically active. Also the UV-Vis experiments suggest that in solution the monomeric complex likely prevails. The use of a cheap and abundant metal in combination with an environmentally tolerable solvent such as MEK and mild reaction conditions further mark this catalytic process as a potentially sustainable way for cyclic carbonate synthesis.

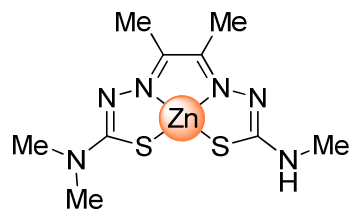
3.4 Experimental section



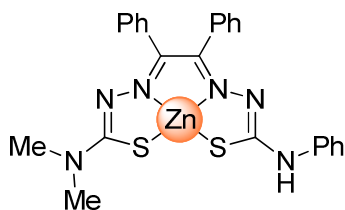
Zn(btsc) complex (1): This complex was prepared according to procedure described by Cowley et al.^[35] Compound **H** (253 mg, 2.12 mmol) was dissolved in tetrahydrofuran (THF) and treated with glacial acetic acid (0.2 ml) for ca. 20 minutes. Compound **F** (500 mg,

2.12 mmol) was added to the solution and the mixture was stirred at room temperature for 3 h. Zinc(II) acetate dihydrate (559 mg, 2.54 mmol) was dissolved in 15 ml of methanol and then added to the reaction mixture, followed by triethylamine (0.74 ml, 5.30 mmol). After 18 h at room temperature the solvents were evaporated and the residue suspended in ca. 10 ml methanol. The yellow solid was filtered off, washed with methanol (3 × 5 ml) and dried in vacuo. Yield: 647 mg (76%) of a yellow powder, whose purity was estimated $\geq 95\%$ by NMR. ^1H NMR (300 MHz, DMSO- d_6 , 25°C): δ = 9.35 (s, 1H, NH), 7.57 (dd, 3J = 8.2 Hz, 5J = 1.2 Hz, 2H, ArH), 7.31 (t, 3J = 8.0 Hz, 2H, ArH), 7.04 (dt, 3J = 7.6 Hz, 5J = 1.2 Hz, 1H, ArH), 3.23 (s, 6H, N(CH $_3$) $_2$), 2.31 (s, 6H, CH $_3$), 2.25 (s, 6H, CH $_3$). $^{13}\text{C}\{^1\text{H}\}$ NMR (75 MHz, DMSO- d_6 , 25°C): δ = 178.2, 172.4, 149.1, 144.0, 141.2, 128.3 (2C), 121.2, 119.7 (2C), 39.6 (2C), 14.7, 13.8. HRMS (FAB+): m/z = 399.0396 found, calculated: 399.0404.

Zn(btsc) complex (2): This compound was prepared analogously to complex **1** from **H** (119 mg, 1.00 mmol), **E** (173 mg, 1.00 mmol), and zinc (II) acetate dihydrate (231 mg, 1.05 mmol); glacial acetic acid and triethylamine were added in corresponding amounts as



described above. Yield: 260 mg (77%) of yellow powder, NMR purity $\geq 95\%$. ^1H NMR (300 MHz, DMSO- d_6 , 25°C): δ = 7.20 (s, br, 1H, NH), 3.17 (s, 6H, N(CH $_3$) $_2$), 2.81 (s, 3H, NHCH $_3$), 2.17 (s, 6H, 2 × CH $_3$). $^{13}\text{C}\{^1\text{H}\}$ NMR (100 MHz, DMSO- d_6 , 25°C): δ = 178.0 (2C), 145.0 (2C), 48.9, 29.6 (2C), 14.2, 14.1. HRMS (FAB+): m/z = 337.6256 found, calculated: 337.6300.



Zn(btsc) complex (3): The reactants **H** (50 mg, 0.42 mmol) and **G** (151 mg, 0.42 mmol) were stirred in THF (ca. 7 ml) at 50°C for 2 h. The reaction mixture was cooled down to room temperature and zinc (II) acetate dehydrate (92 mg, 0.46 mmol) dissolved in 5 ml methanol was added. After stirring for 18 h at room

temperature the solvents were evaporated, the red residue suspended in ca. 5 ml cold methanol, filtered off, washed twice with methanol and dried under vacuum. Yield: 150 mg (68%) of a bright red solid, NMR purity $\geq 95\%$. ^1H NMR (300 MHz, $\text{DMSO-}d_6$, 25°C): δ = 9.47 (s, 1H, NH), 7.60 (d, 3J = 8.0 Hz, 2H, ArH), 7.34 – 7.19 (m, 10H, ArH), 7.08 (t, 3J = 7.8 Hz, 2H, ArH), 6.83 (t, 3J = 7.7 Hz, 2H, ArH), 3.17 (s, 6H, $\text{N}(\text{CH}_3)_2$). $^{13}\text{C}\{^1\text{H}\}$ NMR (75 MHz, $\text{DMSO-}d_6$, 25°C): δ = 180.4, 173.7, 150.2, 143.8, 141.4 (2C), 134.8 (2C), 134.0 (2C), 130.8 (2C), 130.5 (2C), 129.1, 128.8 (2C), 128.0 (2C), 127.8, 122.2, 120.6, 39.6 (2C). HRMS (FAB+): m/z = 522.0586 found, calculated: 522.0600.

Typical procedure for the catalysis experiments: Catalyst **3** (2.0×10^{-5} mol, 10.4 mg) and (co-catalyst) NBu_4I (2×10^{-5} mol, 7.4 mg) were added in a two-necked round-bottomed flask under a gentle flux of argon. Then, methyl ethyl ketone (5.0 mL) and mesitylene (280 μL , 2.0×10^{-3} mol) were added and the solution stirred until complete dissolution occurred. To this mixture, propylene oxide (140 μL , 2.0×10^{-3} mol) was added and the solution transferred to a 25 mL stainless-steel reactor previously purged with argon. Three cycles of pressurization and depressurization of the reactor (with CO_2 at 5 bar) were carried out before finally stabilizing the pressure at 10 bar and the solution left stirring at 45°C for 18 h. A sample of the solution was then analyzed by means of ^1H NMR spectroscopy ($\text{DMSO-}d_6$) and the yield determined using mesitylene as an internal standard.

Titration studies of complex (3) with pyridine: To 2.500 ml 50.0×10^{-6} M solution of complex **3** in a quartz cuvette, aliquots (5 μl for first 25 points, 10 μl for all following points) of 2.50×10^{-3} M solution of pyridine were added. After each addition, the solution was shaken; left to equilibrate for 1 minute and a UV-Vis spectrum was recorded. A blue-shift of the band at 487 nm and of the valley at 420 nm, as well as the appearance of the new absorption band at 343 nm was observed upon addition of pyridine. Absorbance values at 529 nm were taken to create a $(A_0 - A)$ vs c_{pyridine} plot, shown in Figure 2. The binding constant was calculated using the curve fitting procedure for the 1:1 complexation case, developed in the Hunter Group^[36] by having A_{end} and K as unknowns, what resulted with $A_0 - A_{\text{end}} = 0.0826771$ and $K_s = 1.4 \pm 0.2 \times 10^5 \text{ M}^{-1}$. The fitting

using in-house developed curve-fitting scripts gave a value of $1.6 \pm 0.1 \times 10^5 \text{ M}^{-1}$, which was more accurate and therefore given in the text.

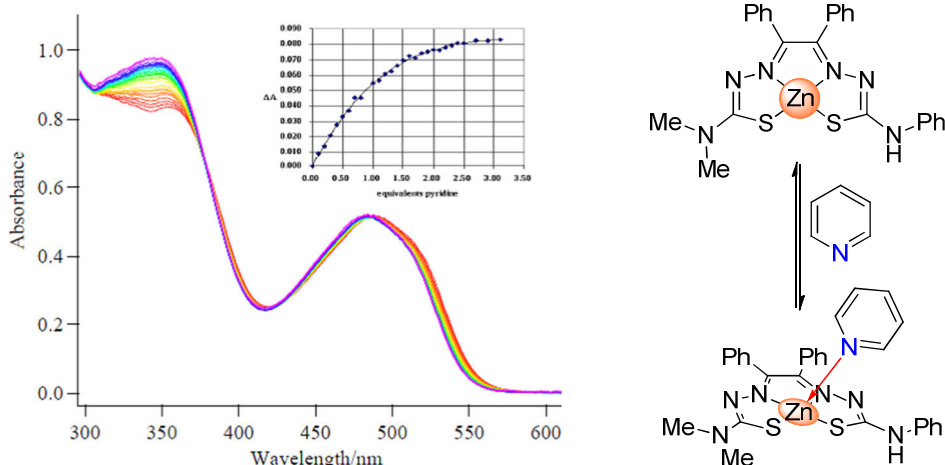
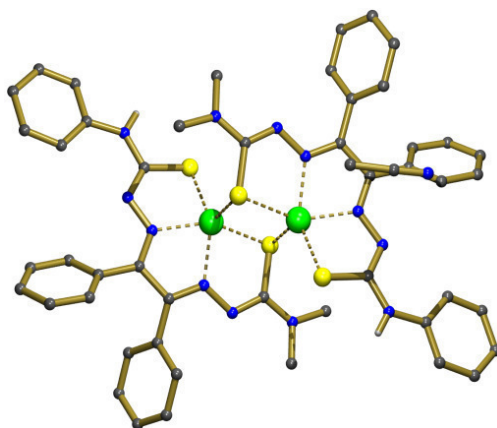


Figure 2. Spectral changes of complex **3** upon the addition of pyridine with $[3] = 50.0 \times 10^{-6}$ and the corresponding titration curves and data fits at $\lambda = 529 \text{ nm}$.

X-ray structure determination: Crystals of compound **3** were obtained by slow evaporation of a solution in CH_3CN at 55°C . The measured crystals were stable under atmospheric conditions; nevertheless they were prepared under inert conditions immersed in perfluoropoly-ether as protecting oil for manipulation. **Data Collection:** Measurements were made on a Bruker-Nonius diffractometer equipped with an APPEX 2 4K CCD area detector, a FR591 rotating anode with MoK_α radiation, Montel mirrors and a Kryoflex low temperature device ($T = -173^\circ\text{C}$). Full-sphere data collection was used with ω and φ scans. **Programs used:** Data collection Apex2 V2011.3 (Bruker-Nonius 2008), data reduction Saint + Version 7.60A (Bruker AXS 2008) and absorption correction SADABS V. 2008-1 (2008). **Structure Solution:** SHELXTL Version 6.10 (Sheldrick, 2000) was used.^[23] **Structure Refinement:** SHELXTL-97-UNIX VERSION.



Crystal data for **3** at 100 K: C₂₆H₂₅N₇S₂Zn₁,
 Fw = 565.02 g mol⁻¹, monoclinic, P2₁/c, *a* =
 7.7782(6) Å, *b* = 32.165(2) Å, *c* =
 10.1938(8) Å, *V* = 2549.8(3) Å³, *Z* = 4, ρ_{calcd}
 = 1.472 Mg/m³, *R*₁ = 0.0437 (0.0705), *wR*₂
 = 0.1007 (0.1200), for 3193 reflections
 with *I* > 2σ(*I*) (for 4240 reflections [*R*_{int}:
 0.0671] with a total measured of 14756
 reflections), 332 parameters, goodness-of-
 fit on *F*² = 1.088, largest diff. peak (hole) =
 0.455 (-0.748) e·Å⁻³.

3.5 Notes and references

- [1] T. Sakakura and K. Kohno, *Chem. Commun.*, 2009, 1312.
- [2] T. Sakakura, J.-C. Choi and H. Yasuda, *Chem. Rev.*, 2007, **107**, 2365.
- [3] M. R. Kember, A. Buchard and C. K. Williams, *Chem. Commun.*, 2011, **47**, 141.
- [4] D. J. Darensbourg, *Chem. Rev.*, 2007, **107**, 2388.
- [5] M. North, R. Pasquale and C. Young, *Green Chem.*, 2010, **12**, 1514.
- [6] A. Decortes, A. M. Castilla and A. W. Kleij, *Angew. Chem. Int. Ed.*, 2010, **49**, 9822.
- [7] M. Aresta and A. Dibenedetto, *Dalton Trans.*, 2007, 2975.
- [8] A.-A. G. Shaikh and S. Sivaram, *Chem. Rev.*, 1996, **96**, 951.
- [9] For an early example on direct CO₂ activation see: M. Aresta, C. F. Nobile, V. G. Albano, E. Forni and M. Manassero, *J. Chem. Soc. Chem. Commun.*, 1975, 636.
- [10] I. I. F. Boogaerts and S. P. Nolan, *J. Am. Chem. Soc.*, 2010, **132**, 8858.
- [11] W. Clegg, R. W. Harrington, M. North and R. Pasquale, *Chem. Eur. J.*, 2010, **16**, 6828.
- [12] M. R. Kember, P. D. Knight, P. T. R. Reung and C. K. Williams, *Angew. Chem. Int. Ed.*, 2009, **48**, 931.
- [13] R. L. Paddock and S. T. Nguyen, *Chem. Commun.*, 2004, 1622.
- [14] D. J. Darensbourg and R. M. Mackiewicz, *J. Am. Chem. Soc.*, 2005, **127**, 14026.
- [15] A. Decortes, M. Martínez Belmonte, J. Benet-Buchholz and A. W. Kleij, *Chem. Commun.*, 2010, **46**, 4580.
- [16] A. Decortes and A. W. Kleij, *ChemCatChem*, 2011, **3**, 831.

- [17] A. R. Cowley, J. R. Dilworth, P. S. Donnelly, J. M. Heslop and S. J. Ratcliffe, *Dalton Trans.*, 2007, 209.
- [18] M. Christlieb, A. R. Cowley, J. R. Dilworth, P. S. Donnelly, B. M. Paterson, H. S. R. Struthers and J. M. White, *Dalton Trans.*, 2007, 327.
- [19] E. Hess and G. Baehr, *Z. Anorg. Allg. Chem.*, 1952, **268**, 351.
- [20] E. Hess, E. Steinkopf, G. Schleitzer and G. Baehr, *Z. Anorg. Allg. Chem.*, 1953, **273**, 325.
- [21] P.A. Stenson, A. Board, A. Marin-Becerra, A. J. Blake, E. S. Davies, C. Wilson, J. McMaster and M. Schroder, *Chem. Eur. J.*, 2008, **14**, 2564.
- [22] V. Bocokić, M. Lutz, A. L. Spek and J. N. H. Reek, *Dalton Trans.*, 2012, **41**, 3740. Note that the used complexes **1-3** were prepared by these authors and used in this collaborative project.
- [23] G. M. Sheldrick (1998) SHELXTL Crystallographic System Ver. 5.10, Bruker AXS, Inc.: Madison, Wisconsin.
- [24] This results contrasts our previous findings for related Zn(salphen) complexes where the coordination of various epoxides was crystallographically characterized (see ref. 15). Apparently, under these conditions the Zn(btsc) complex **3** preferentially crystallizes as a dimer.
- [25] For a related Cu(btsc) dimer see: A. R. Cowley, J. R. Dilworth, P. S. Donnelly, E. Labisbal and A. Sousa, *J. Am. Chem. Soc.*, 2002, **124**, 5270. Please note that in this case the S-atoms are *not* used in the formation of a dinuclear species.
- [26] The chemistry of btsc ligands and their (Zn) complexes is well-documented, see: T. S. Lobana, R. Sharma, G. Bawa and S. Khanna, *Coord. Chem. Rev.*, 2009, **253**, 977.
- [27] For other multinuclear Zn(btsc) systems see: D. Dayal, D. Palanimuthu, S. V. Shinde, K. Somasundaram and A. G. Samuelson, *J. Biol. Inorg. Chem.*, 2011, **16**, 621.
- [28] For other multinuclear Zn(btsc) systems see: M. Christlieb, A. R. Cowley, J. R. Dilworth, P. S. Donnelly, B. M. Paterson, H. S. R. Struthers and J. M. White, *Dalton Trans.*, 2007, 327.
- [29] A. W. Kleij, *Dalton Trans.*, 2009, 4635.
- [30] J. K.-H. Hui, Z. Yu and M. J. MacLachlan, *Angew. Chem. Int. Ed.*, 2007, **46**, 7980.
- [31] A. W. Kleij, M. Kuil, M. Lutz, D. M. Tooke, A. L. Spek, P. C. J. Kamer, P. W. N. M. van Leeuwen and J. N. H. Reek, *Inorg. Chim. Acta*, 2006, **359**, 1807.
- [32] M. Martínez Belmonte, S. J. Wezenberg, R. M. Haak, D. Anselmo, E. C. Escudero-Adán, J. Benet-Buchholz and A. W. Kleij, *Dalton Trans.*, 2010, **39**, 4541.

- [33] J. A. A. W. Elemans, S. J. Wezenberg, E. C. Escudero-Adán, J. Benet-Buchholz, D. den Boer, M. J. J. Coenen, S. Speller, A. W. Kleij and S. De Feyter, *Chem. Commun.*, 2010, **46**, 2548.
- [34] Attempts to solubilize complexes **1-2** at higher temperatures failed which indicates that during the reactions with these catalysts only partial dissolution is achieved. Furthermore, we analyzed these precipitates in order to identify any possible decomposition products: in these cases only the starting complexes **1-2** were identified by ¹H NMR spectroscopy.
- [35] A. R. Cowley, J. R. Dilworth, P. S. Donnelly, J. M. Heslop and S. J. Ratcliffe, *Dalton Trans.*, 2007, 209.
- [36] P. A. Bisson, C. A. Hunter, C. J. Morales and K. Young, *Chem. Eur. J.*, 1998, **4**, 845.

UNIVERSITAT ROVIRA I VIRGILI

LEWIS ACIDIC ZN(II) SCHIFF BASE COMPLEXES IN HOMOGENEOUS CATALYSIS

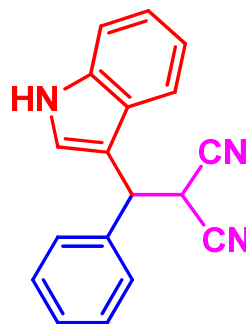
Daniele Anselmo

Dipòsit Legal: T. 1564-2013

Chapter IV

Zn-Mediated Synthesis of 3-Substituted Indoles using a Three-Component Reaction Approach

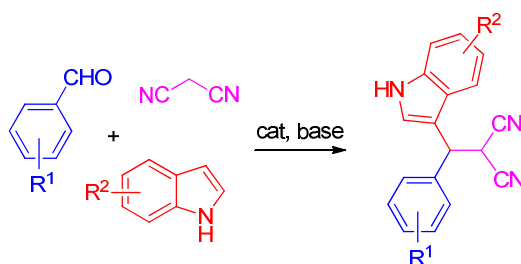
The synthesis of 3-substituted indoles has been investigated through a multi-component reaction (MCR) approach using aldehydes, indole and malononitrile as reagents. The reaction is catalyzed by Lewis acidic Zn(salphen) complexes and their performance was compared against a number of other Zn(II) structures and M(salphen)s showing the Zn(salphen)s to be superior. However, the complex nature of this three-component reaction (3-CR) results in substantial by-product formation arising from the intermediate benzylidene malononitrile species. The 3-CR has been studied in detail covering the influence of base, solvent, reagent stoichiometry and also involved stability studies. The results have led to a mechanistic proposal in which the benzylidene malononitrile intermediate plays a central role; it is one of the major species formed in most of the catalytic reactions studied, and furthermore provides also a prelude for in situ reaction with the malononitrile reagent to likely afford complex mixtures of N-containing heterocycles.



4.1 Introduction

Multi-components reaction (MCR) strategies represent a powerful tool in organic synthesis to create diversity-oriented libraries of scaffolds with potentially interesting biological activities.^[1] The attractiveness of the MCR approach is undoubtedly the simple operation by which organic structures with impressive molecular complexity can be assembled into targets with, ideally, high selectivity and yield using minimal synthetic requirements. In this context, indole scaffolds have conquered a prominent position as these structures are known for their importance in the development of new compounds of pharmaceutical interest.^[2] For the family of substituted

indoles there exist a number of MCRs that comprise of efficient procedures towards these structures.^[3] Recent interest in this field focusing on 3-substituted indoles has revealed that such MCR approaches may be also feasible in environmentally benign solvents such as water.^[4] Zhou and co-workers reported that water-soluble Cu(salphen)s [salphen = *N,N'*-bis(salicylidene)imine-1,2-phenylenediamine] in the presence of a suitable base are excellent catalysts converting various combinations of aldehydes, malononitrile and indoles into the respective 3-component reaction (3-CR) products (Scheme 1) providing high yields using water as the reaction medium. The fact that Cu(salphen) complexes are able to catalyze this 3-CR triggered our attention, as we recently reported that Zn(salphen) complexes are excellent Lewis acid activators in the catalytic conversion of oxiranes and carbon dioxide to afford organic carbonates.^[5] Whereas Cu(salphen)s are coordinatively saturated, Zn(salphen)s show propensity to form pentacoordinated structures due to the high Lewis acidity these systems possess.^[6] Therefore, we envisioned that the use of Zn(II) rather than Cu(II)salphen complexes would be beneficial for effective synthesis of 3-substituted indoles. Of particular note is that recent work has shown that Cu- and Zn(salen)s show tendency to decompose under aqueous conditions providing access to “half-salen” type intermediates.^[7] This stability issue therefore raises the question if water as a medium is truly the best solvent for this 3-CR process, as the organic products unfortunately also needed to be isolated and purified using organic solvents.

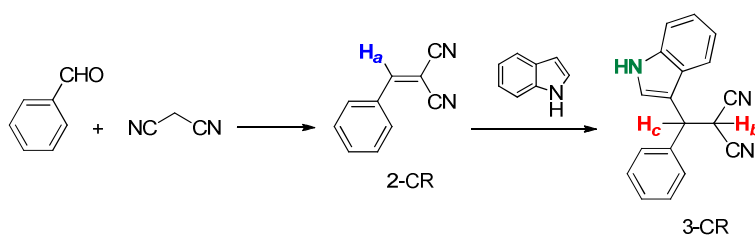


Scheme 1. A 3-CR affording 3-substituted indoles.

Here, we report an extensive investigation of the use of Zn(salphen) complexes as mediators for the 3-CR affording 3-substituted indoles. Process parameters such as temperature, solvent, type of base, catalyst structure, stability of intermediates and the final 3-CR product, and comparison with previously reported data^[4] has been carried out: the results show that the 3-CR approach toward 3-substituted indoles (Scheme 1) is much more complicated than reported before, and the selectivity toward the desired target is compromised by side-product formation that encompasses the reaction between an intermediate 2-CR compound and malononitrile.

4.2 Results and discussion

As part of our screening strategy, we have used a number of Zn-based structures/salts to reveal their potential as catalysts for the 3-CR reported in Scheme 1. Using the reaction conditions reported previously for water-soluble Cu(salphen) complexes,^[4] the influence of base, solvent and catalyst structure was examined and the results are reported in Table 1. First of all, we tested complexes **1-4** as catalyst candidates and used benzaldehyde, malononitrile and indole as standard reagents. As base we selected a relatively non-nucleophilic tertiary amine (DIPEA = diisopropyl ethylamine) as tertiary amines have been shown to have negligible competing interaction with the Lewis acidic Zn(II) ions in salen or salphen structures.^[8] In all the reactions that we performed we observed the formation of several species but the major identified components proved to be a 2-CR intermediate,^[9] and the 3-CR target; the amount of each component depended highly on the reaction conditions and the catalyst employed. The 2-CR and 3-CR products are easily recognized in the ¹H NMR spectra through the H_a, H_b-H_c and NH protons (Scheme 2, below).



Scheme 2. Reaction scheme with indicated H-atoms used to recognize each product by ¹H NMR.

In the absence of base and catalyst, already low amounts of 2-CR were noted (Table 1, 11%) whereas the presence of DIPEA or catalyst **1** afforded much higher levels of this intermediate. When **1** and DIPEA were combined, the highest amount of 3-CR was observed (56%) together with low amounts of 2-CR (19%) and unreacted aldehyde (11%). Hence, it seems that complex **1** is particularly effective for mediating the conversion of the 2-CR into the 3-CR compound. Other Lewis acidic Zn-complexes such as **2**, **3**,^[10] and **4** were also tested but showed inferior behavior, i.e. significantly lower amounts of the 3-CR product were noted. Interestingly, upon examination of the mass balance (i.e., converted aldehyde + free aldehyde against the normalized amount of indole-based components) it is clear that some aldehyde remains unaccountable. Despite the fact that in some reactions this amount is rather high, no clear evidence for other side-products can be derived from the recorded ¹H NMR spectra as many

peak are overlapping. Since the stable 2-CR intermediate seems to play a key role, one can envision that it may be involved in side-reactions.

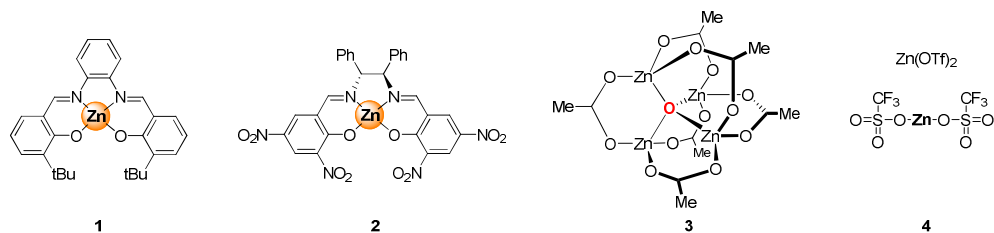


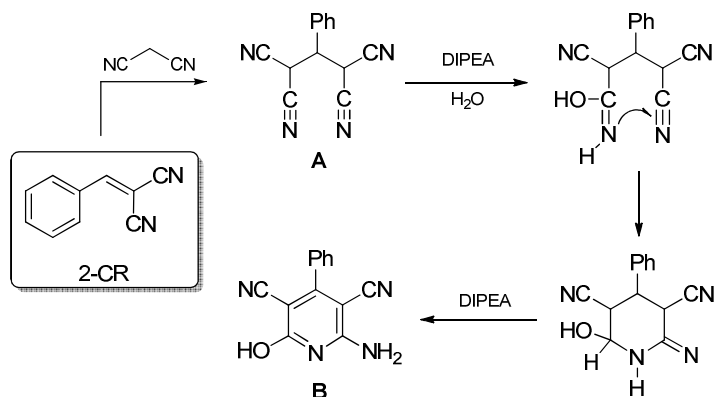
Table 1. Screening of various Zn-based catalysts in the 3CR towards 3-substituted indoles.^[a]

Catalyst	Base	Solvent	T [°C]	3-CR [%] ^[b]	2-CR [%] ^[b]	PhCHO [%] ^[b]	MB [%] ^[c]
–	–	dcm	25	0	11	76	87
–	DIPEA	dcm	25	2	56	<1	58
1	–	dcm	25	0	69	31	100
1	DIPEA	dcm	25	56	19	11	86
1 ^[d]	DIPEA	dcm	25	28	42	1	71
1 ^[e]	DIPEA	dcm	25	2	86	0	88
1	DIPEA	dcm	40	57	0	1	58
1	DIPEA	tce	25	0	100	0	100
1	DIPEA	ace	25	<1	0	44	<45
1 ^[f]	DIPEA	thf	60	0	42	7	49
1 ^[f]	DIPEA	tol	60	0	59	8	67
2	DIPEA	dcm	25	27	58	1	86
3	DIPEA	dcm	25	20	43	3	66
4	DIPEA	dcm	25	12	63	6	81
1	DBU	dcm	25	24	4	4	32
1	NEt ₃	dcm	25	11	57	<1	<69
1	TBAH	dcm	25	0	0	7	7
1	PS	dcm	25	23	50	1	74

[a] All reactions were carried out using 0.11 mmol of indole, 0.11 mmol of malononitrile and 0.10 mmol of benzaldehyde using 5 mol% of catalyst and 1 equiv of base, in 3.0 mL of solvent, 24 h. Abbreviations used: DIPEA = di-iso-propyl ethylamine, DBU = 1,8-Diazabicyclo[5.4.0]undec-7-ene, TBAH = tetrabutylammonium hydroxide, PS = proton sponge, 1,8-bis(dimethylamino)naphthalene. [b] Determined by ¹H NMR in DMSO-*d*₆ and related to [3-CR] + free [Indole]; the 2-CR and 3-CR structures are provided in the Scheme above Table 1. [c] MB = mass balance based on [3-CR] + [2-CR] + free [PhCHO] versus total indole, i.e. normalized [3-CR] + free [indole]. [d] Using 0.5 equiv of base. [e] Using 0.05 equiv of base. [f] Reaction time was 6 h.

A recent contribution from Chao-Guo and co-workers^[11] has revealed that the 2-CR (2-benzylidenemalononitrile) intermediate may further react with malononitrile to afford a

tetracyano derivative (Scheme 3, **A**), and depending on the reaction conditions even the formation of penta-substituted pyridines (**B**) should be considered.



Scheme 3. Side-product formation starting from the intermediate 2-CR resulting in loss of 3-CR selectivity.

The use of other bases such as DBU (1,8-diazabicyclo[5.4.0]undec-7-ene), NEt_3 , NBu_4OH or proton sponge [1,8-bis(dimethylamino)naphthalene] did not improve the selectivity towards the 3-CR product. Furthermore, lower than stoichiometric amounts of DIPEA had a detrimental effect on the formation of the 3-CR compound. Other solvents including dichloroethane (DCE), THF, acetone and MeOH were also probed but the results were poor in terms of the formation of the 3-CR target (Table 1) even at elevated temperatures. Therefore, the next step was to investigate whether the Zn(salphen) structure could be further optimized using DCM as solvent and DIPEA as stoichiometric base additive (see Table 2 and Scheme 4). A number of differently substituted Zn(salphen)s were prepared comprising of electron-withdrawing groups installed at different positions on the salphen backbone (**1** and **7-12**). A comparison was made with appropriate Al(III) and Cu(II)salphen)s (**5**, **6** and **13**) to evaluate the relative efficacies in this MCR. Of one representative Zn(salphen) (**8**) the X-ray molecular structure was determined (Figure 1);^[12] the structure serves to demonstrate that the Lewis acidic Zn ion shows axial binding for potential O- or N- based substrates. The Zn(salphen)s equipped with NO_2 and/or Br substituents were tested as catalysts for the MCR towards 3-substituted indoles, with the primary objective to increase the selectivity for the target 3-CR product. As can be deduced from Table 2, Zn(salphen) **8** showed the highest selectivity for the 3-CR derivative (60%) at 25°C, a result that could not be improved by increasing the reaction temperature (40°C: 41%). However, complexes **1**, **10** and **11** showed rather similar results indicating that the structure of the catalyst does not impart a significant influence under these reaction conditions. Water-soluble Cu(salphen)s have

recently been reported as efficient catalysts for the same MCR leading to high isolated yields of the 3-CR product.^[4]

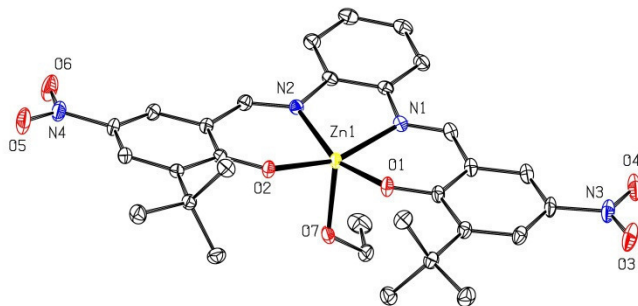
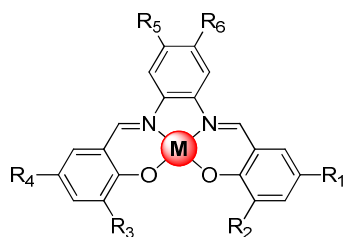


Figure 1. X-ray molecular structure determined for Zn(salphen) complex **8**. H-atoms and co-crystallized solvent are omitted for clarity, and a partial numbering scheme is provided. Selected bond lengths [Å] and angles [°]: Zn(1)-O(1) = 1.9765(8), Zn(1)-O(2) = 1.9769(8), Zn(1)-N(1) = 2.0948(9), Zn(1)-N(2) = 2.0759(9), Zn(1)-O(7) = 2.0712(9); O(1)-Zn(1)-O(2) = 98.54(3), N(1)-Zn(1)-N(2) = 78.34(4), O(1)-Zn(1)-N(2) = 158.64(4), O(2)-Zn(1)-N(1) = 160.17(4), O(1)-Zn(1)-N(1) = 88.07(4), N(2)-Zn(1)-O(7) = 104.63(4), O(2)-Zn(1)-O(7) = 93.79(3).



1. M = Zn; R¹ = R⁴ = H; R² = R³ = tBu; R⁵ = R⁶ = H
5. M = AlCl; R¹ = R⁴ = H; R² = R³ = tBu; R⁵ = R⁶ = H
6. M = Cu; R¹ = R⁴ = H; R² = R³ = tBu; R⁵ = R⁶ = H
7. M = Zn; R¹ = R⁴ = tBu; R² = R³ = NO₂; R⁵ = R⁶ = H
8. M = Zn; R¹ = R⁴ = NO₂; R² = R³ = tBu; R⁵ = R⁶ = H
9. M = Zn; R¹ = R⁴ = NO₂; R² = R³ = tBu; R⁵ = R⁶ = Br
10. M = Zn; R¹ = R² = NO₂; R³ = R⁴ = tBu; R⁵ = R⁶ = H
11. M = Zn; R¹ = R² = NO₂; R³ = tBu; R⁴ = H; R⁵ = R⁶ = H
12. M = Zn; R¹ = R⁴ = SO₃Na; R² = R³ = R⁵ = R⁶ = H
13. M = Cu; R¹ = R⁴ = SO₃Na; R² = R³ = R⁵ = R⁶ = H

Scheme 4. M(salphen) catalyst structures **1** and **5-13** used in this work.

Therefore, we also tested both complexes **12** (M = Zn) and **13** (M = Cu; made in situ by transmetalation of **12** with Cu(OAc)₂)^[13] using H₂O as medium at 60°C and KH₂PO₄ as base, which are the original conditions. In our hands, we failed to reproduce these original results; on the contrary, we observed rather similar features as compared with the data for the other Zn(salphen)s. Much lower amounts of the 3-CR (**14**) product were formed, and concomitantly higher amounts of 2-CR (**15**) were present (Table 2). In general, these latter results are thus in line with the general impression that the formation of the 3-CR product is significantly compromised by side-product formation as indicated in Scheme 3.

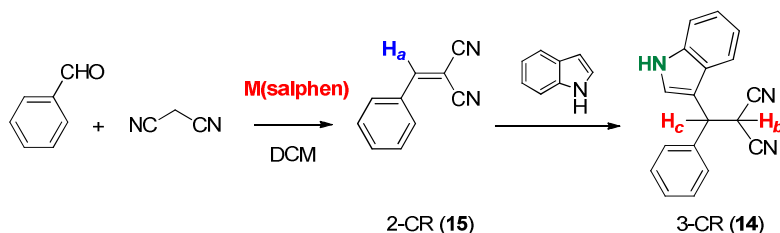


Table 2. Screening of various *M(salphen)* catalysts in the 3-CR toward 3-substituted indoles.^[a]

Catalyst	T [°C]	3-CR (14) [%] ^[b]	2-CR (15) [%] ^[b]	PhCHO [%] ^[b]	MB. [%] ^[c]
1	25	56	19	11	86
5	25	5	46	7	58
6	25	6	75	1	84
7	25	8	17	0	25
8	25	60	10	1	71
8	40	41	31	6	78
9	25	25	40	1	66
10	25	49	37	8	94
11	25	52	29	5	86
12 ^[d]	60	36	48	<1	<85
13 ^[d]	60	9	34	7	50

[a] All reactions were carried out using 0.11 mmol of indole, 0.11 mmol of malononitrile and 0.10 mmol of benzaldehyde using 5 mol% of catalyst and 1 equiv of DIPEA, in 3.0 mL of DCM. [b] Determined by ¹H NMR in DMSO-*d*₆ and related to [3-CR] + free [Indole]. [c] MB = mass balance based on [3-CR] + [2-CR] versus total indole, i.e. normalized [3-CR] + free [indole]. [d] The base was KH₂PO₄ and the reaction time was 6 h.

We then screened some other aldehydes and monitored the formation of both the 2-CR (Table 3, **15-19**) and the 3-CR products. We found that in the case of the more electron-deficient aldehydes the amount of 3-CR product was comparable with that noted in the case of benzaldehyde (54-55%) while (very) low amounts of 2-CR intermediate could be observed. This indicates that the respective 2-CR derivatives **16** and **17** are more prone to formation of either the 3-CR target but likely also react in situ with malononitrile to form side-products. This is in line with the mass balance data for these substrates, as lower amounts of accountable aldehyde-based components are noted in the reactions that involve 3,5-dibromobenzaldehyde, 4-bromobenzaldehyde or benzaldehyde. To further test this hypothesis, we used the relative

electron-rich 4-methoxy- and 4-methylbenzaldehyde as substrates (Table 3); in these cases much higher amounts of 2-CR intermediates **18** and **19** were found together with small amounts of 3-CR products. More importantly, a nearly closed mass balance is apparent using these substrates. In order to further evaluate the formation of both the 2-CR intermediate as well as the 3-CR indole product, we followed this MCR in time using ^1H NMR spectroscopy (CD_2Cl_2 ,

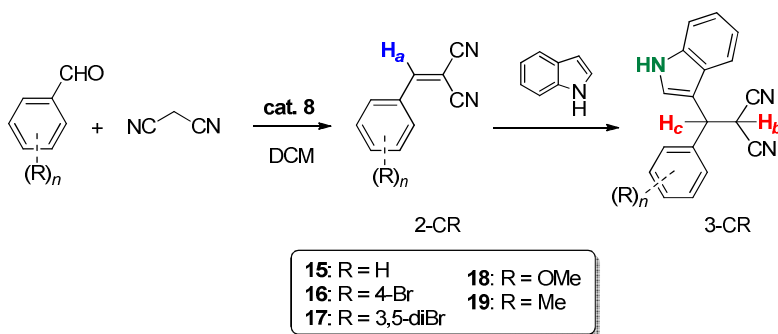


Table 3. Screening of various aldehydes in the 3-CR toward 3-substituted indoles^[a] catalyzed by complex **8** and influence of reaction stoichiometry.

Catalyst	T [°C]	R	3-CR [%] ^[b]	2-CR [%] ^[b]	RCHO [%] ^[b]	MB. [%] ^[c]
8 ^[d]	25	H	48	26	<1	<75
8 ^[e]	25	H	13	56	0	69
8 ^[f]	25	H	22	35	–	–
8	25	3,5-Br ₂	54	0	0	54
8	25	4-Br	55	11	1	67
8	25	H	60	10	1	71
8	25	4-Me	16	73	2	91
8	25	4-MeO	15	84	1	100

[a] All reactions were carried out using 0.11 mmol of indole, 0.11 mmol of malononitrile and 0.10 mmol of benzaldehyde using 5 mol% of **8** and 1 equiv of DIPEA, in 3.0 mL of DCM, unless stated otherwise. [b] Determined by ^1H NMR in $\text{DMSO}-d_6$ and related to [3-CR] + free [Indole]. [c] MB = mass balance based on [3-CR] + [2-CR] versus total indole, i.e. normalized [3-CR] + free [indole]. [d] The ratio indole-aldehyde-malononitrile was 2:1:1. [e] The ratio indole-aldehyde-malononitrile was 1:1:2. [f] The ratio indole-aldehyde-malononitrile was 1:2:1.

Figure 2) and three different aldehyde reagents. As for benzaldehyde, the reaction is slow (as expected) and low levels of the 3-CR product are formed (ca. 25%) after 22.5 h. Interestingly, under these conditions there is a slow decay of the 2-CR intermediate after a fast initial formation. Significantly larger amounts of 3-CR product (50–55%) are formed for the more reactive aldehydes (4-bromobenzaldehyde and 3,5-dibromobenzaldehyde, compounds **16** and **17**; Figure 2), and the decay in 2-CR intermediate is also notably faster. In the case of 3,5-dibromobenzaldehyde, after 22.5 h the amount of the 2-CR derivative had been lowered to around 4%. Then, preformed 2-benzylidenemalononitrile **15** (i.e., the 2-CR intermediate of the reaction that involved benzaldehyde) was treated with indole under the catalytic conditions to see whether larger amounts of product could be formed. In 24 h, the amount of the 3-CR product noted was 33%, and remarkably some free aldehyde (3% by integration) was also present.

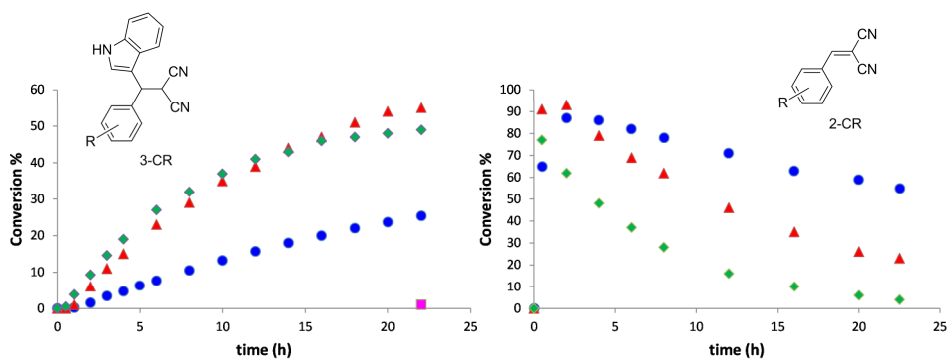


Figure 2. ^1H NMR analysis (DCM-d_2 , 30°C) in time of the 3-CR reactions catalyzed by **8** involving benzaldehyde ($R = \text{H}$, **15**; blue traces), 4-bromobenzaldehyde ($R = 4\text{-Br}$, **16**; red traces) and 3,5-dibromobenzaldehyde ($R = 3,5\text{-diBr}$, **17**; green traces). Note that both the formation of the 3-CR product (left) as well the decay of the 2-CR intermediate compounds **15-17** was examined (right) using normalized NMR integrals. The purple dot at $t = 22.5$ h indicates the reaction without any catalyst.

The free aldehyde probably arises from some decomposition of the 2-CR reagent rather than from the 3-CR product, as the stability of the 3-CR derivative was confirmed by separate NMR studies showing no observable changes under similar conditions during 24 h. Finally, the reaction of 2-benzylidenemalononitrile (**15**) with one equivalent of malononitrile in dichloromethane was carried out to study the possible formation of side-products. After 24 h, NMR analysis showed the presence of other species (see asterisks in Figure 3, red trace). Compared with the reaction stoichiometry 1:2:1 (i.e., benzaldehyde:malononitrile:indole, Table

3 and blue trace in Figure 3) similar peaks at $\delta = 3.5$, 4.8 and 5.05 ppm were noted. Thus, it seems likely that the 2-CR intermediate **15** in the presence of malononitrile can lead to side-product formation with chemical structures related to those in Scheme 3. Although here an excess of malononitrile was probed, in other reactions carried out with various catalysts we have seen similar by-products (though in most cases in reduced amounts) indicating that in the course of 3-CR product formation, the formation of these side-products indeed effectively lowers the selectivity for the desired product.

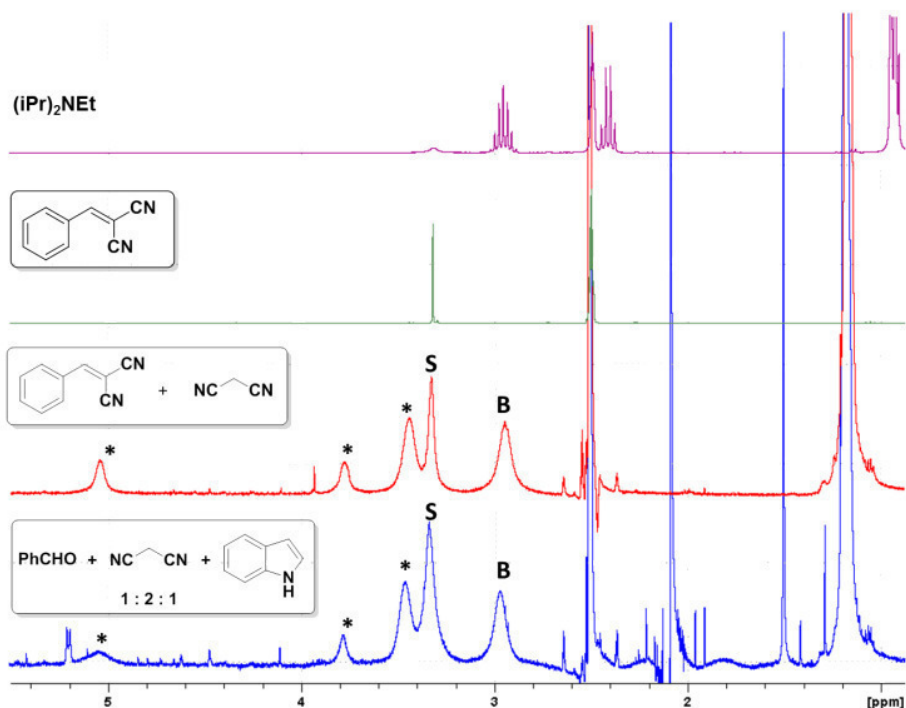


Figure 3. The region 1-5.5 ppm of the ¹H NMR comparison (DMSO-*d*₆) between DIPEA, the 2-CR derivative **15**, the spectrum recorded for the reaction between isolated **15** and 1 equiv of malononitrile at 24 h, and the NMR trace for the 1:2:1 reaction between benzaldehyde, malononitrile and indole after 24 h. Abbreviations used: B = base [(iPr)₂NEt], S = residual solvent signals. The asterisks denote side-products.

We also checked the stability of **15** in the presence of DIPEA and we found also in this case that some decomposition of the alkene intermediate **15** takes place as several traces of other components (cf., Figure 3) were present after 24 h. Thus, an in situ “retro” Knoevenagel

condensation reaction of **15** followed by irreversible formation of side-products may lead to diminished selectivity for the 3-CR product.

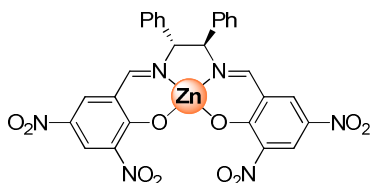
4.3 Conclusions

In summary, the MCR between (substituted) benzaldehydes, malononitrile and indole catalyzed by Zn(salphen) complexes in the presence of DIPEA as base affords mixtures of reaction products. Whereas the 3-CR target can be obtained with reasonable selectivity, the reactivity of the intermediate 2-CR derivative (i.e., the benzyldenemalononitrile) causes significant side-product formation that is a probable result of in situ conversion into N-heterocyclic structures. The (irreversible) side-product formation depends on the type of benzaldehyde used, as larger amount of side-products seem to be evident when using electron-poor reagents. This work thus demonstrates that this MCR reaction is not as straightforward as previously communicated.^[4] Further research is thus required to increase the overall selectivity towards the 3-CR target, and since the MCR products contain a chiral centre the development of asymmetric versions also remains a highly attractive objective.

4.4 Experimental section

General remarks

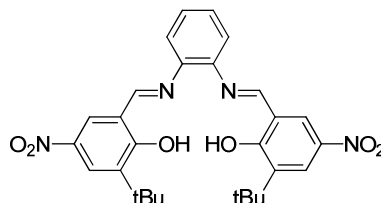
NMR spectra were recorded on a Bruker AV-400 or AV-500 spectrometer and referenced to the residual deuterated solvent signals. Elemental analysis was performed by the Unidad de Análisis Elemental at the Universidad de Santiago de Compostela. Mass spectrometric analysis and X-ray diffraction studies were performed by the Research Support Group at the ICIQ. The intermediate compounds **15**,^[14] **16**,^[15] **18**^[14] and **19**^[14] have been previously reported. Complexes **1**,^[16] **3**,^[10a] **5**,^[5b] **6**,^[5b] **7**,^[5b] **10**,^[13] and **11**^[13] were prepared according to previously reported procedures.



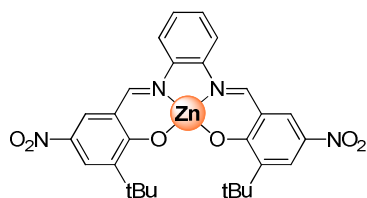
Zn(salen) complex (2): A solution of (1R,2R)-(+)-1,2-diphenylethylenediamine (96 mg, 0.45 mmol), 3,5-dinitro-salicylaldehyde (200 mg, 0.94 mmol) and Zn(OAc)₂·2H₂O (110 mg, 0.50 mmol) in MeOH (35 ml) was stirred for 4 h at room temperature. The desired compound was isolated by filtration and dried in vacuo to

yield an orange solid. Yield: 214 mg (72 %). ^1H NMR (400 MHz, acetone- d_6): δ = 8.59 (d, 4J = 3.1 Hz, 2H; ArH), 8.43 (s, 2H; CH=N), 8.35 (d, 4J = 3.1 Hz, 2H; ArH), 7.32-7.45 (m, 10H; ArH), 5.54 (s, 2H, CH-CH); $^{13}\text{C}\{^1\text{H}\}$ NMR (100 MHz, acetone- d_6): δ = 168.36, 166.98, 137.15, 134.95, 132.37, 129.22, 129.03, 128.55, 123.64, 121.75, 83.25, 72.61; MS (MALDI-, dctb): m/z = 662.2 [M^-] (calcd 662.0); elemental analysis calcd for $\text{C}_{28}\text{H}_{18}\text{N}_6\text{O}_{10}\text{Zn}\cdot\text{H}_2\text{O}$: C 49.32, H 2.96, N, 12.32; found: C 49.42, H 2.79, N 12.23.

Ligand precursor to (8): 3-*tert*-Butyl-5-nitro-salicylaldehyde (147 mg, 0.66 mmol) was solubilized in MeOH (20 mL). Then ortho-phenylenediamine (36 mg, 0.33 mmol) was added and the mixture stirred for 6 h. The orange precipitate that had formed was isolated by filtration and dried in vacuo. Yield: 118 mg (69%).



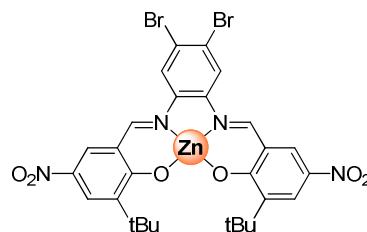
^1H NMR (400 MHz, DMSO- d_6): δ = 15.40 (s, 2H; OH), 9.30 (s, 2H; CH=N), 8.61 (d, 4J = 2.7 Hz, 2H; ArH), 8.15 (d, 4J = 2.7 Hz, 2H; ArH), 7.69 (m, 2H; ArH), 7.56 (m, 2H; ArH), 1.41 (s, 18H, $\text{C}(\text{CH}_3)_3$); $^{13}\text{C}\{^1\text{H}\}$ NMR (100 MHz, DMSO- d_6): δ = 161.52, 158.20, 155.75, 136.43, 134.67, 135.17, 124.14, 122.10, 121.05, 114.93, 30.64, 24.25; HRMS (ESI-, MeOH): m/z = 517.2093, calcd for $\text{C}_{28}\text{H}_{30}\text{N}_4\text{O}_6$: 517.2087.



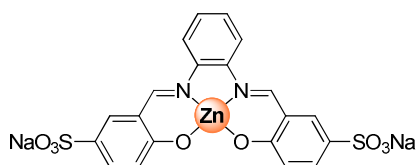
Zn(salphen) complex (8): To a solution of the ligand precursor (110 mg, 0.21 mmol) in MeOH (15 ml) was added $\text{Zn}(\text{OAc})_2\cdot 2\text{H}_2\text{O}$ (60 mg, 0.27 mmol). The reaction mixture was stirred for 6 h during which an orange precipitate slowly formed. Filtration and drying in vacuo gave an orange solid. Yield: 118 mg (97%). ^1H NMR (400

MHz, DMSO- d_6): δ = 9.28 (s, 2H; CH=N), 8.56 (d, 4J = 3.0 Hz, 2H; ArH), 8.05 (d, 4J = 3.3 Hz, 2H; ArH), 8.02-8.04 (m, 2H; ArH), 7.47-7.50 (m, 2H; ArH), 1.50 (s, 18H; $\text{C}(\text{CH}_3)_3$); $^{13}\text{C}\{^1\text{H}\}$ NMR (100 MHz, DMSO- d_6): δ = 176.85, 163.60, 143.02, 139.34, 133.87, 133.33, 128.83, 124.78, 119.02, 117.51, 35.76, 29.48; MS (MALDI-, pyrene): m/z = 580 [M^-] (calcd 580); elemental analysis calcd (%) for $\text{C}_{28}\text{H}_{28}\text{N}_4\text{O}_6\text{Zn}\cdot\text{H}_2\text{O}$: C 56.06, H 5.04, N 9.34; found: C 56.19, H 5.35, N 9.04.

Zn(salphen) complex (9): A mixture of 4,5-dibromo-*ortho*-phenyldiamine (40 mg, 0.15 mmol), 3-tert-butyl-5-nitro-salicylaldehyde (70 mg, 0.31 mmol) and Zn(OAc)₂·2H₂O (40 mg, 0.18 mmol) in MeOH (20 ml) was stirred for 4 h at room temperature. The orange product was then isolated by filtration and dried.



Yield: 69 mg (62 %). ¹H NMR (400 MHz, acetone-*d*₆): δ = 9.37 (s, 2H; CH=N), 8.49 (d, ⁴J = 3.0 Hz, 2H; ArH), 8.45 (s, 2H; ArH); 8.16 (d, ⁴J = 3.0 Hz, 2H; ArH), 1.55 (s, 18H, C(CH₃)₃); ¹³C{¹H} NMR (100 MHz, acetone-*d*₆): δ = 164.49, 143.50, 141.34, 139.72, 134.69, 132.63, 125.05, 123.30, 122.04, 118.33, 39.84, 35.46; MS (MALDI-, DCTB): m/z = 739.7 [M⁺] (calcd 739.9); elemental analysis calcd (%) for C₂₈H₂₆Br₂N₄O₆Zn·3.5H₂O: C 41.43, H 4.22, N 6.90; found: C 41.83, H 3.61, N 6.72.



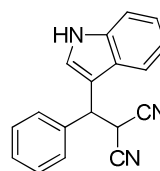
Zn(salphen) complex (12): To a solution of sodium 3-formyl-4-hydroxybenzenesulfonate (0.63 g, 2.38 mmol) in H₂O (10 mL) was added *ortho*-phenylenediamine (0.13 g, 1.20 mmol) dissolved in MeOH (15 mL). The initial suspension quickly turned into a clear solution, after which a solution

Of Zn(OAc)₂·2H₂O (0.28 g, 1.28 mmol) in H₂O (10 mL) was added. Instantaneously a suspension was obtained which was filtered after 1 h giving 253.9 mg of product. From the mother liquor, after dilution by acetone, a second crop of product (164.0 mg) was obtained. Yield: 417.9 mg (60% based on the diamine reagent). ¹H NMR (400 MHz, DMSO-*d*₆/pyridine-*d*₅ = 9:1 v/v): δ = 8.95 (s, 2H, CH=N), 7.82 (d, ⁴J = 2.4 Hz, 2H; ArH), 7.77-7.80 (m, 2H; ArH), 7.59 (d, ³J = 8.9 Hz, ⁴J = 2.4 Hz, 2H; ArH), 7.34-7.36 (m, 2H; ArH), 6.78 (d, ³J = 8.9 Hz, 2H, ArH); ¹³C{¹H} NMR (100 MHz, DMSO-*d*₆/pyridine-*d*₆ = 7:3 v/v): δ = 173.11, 163.50, 139.89, 134.41, 134.38, 132.98, 127.83, 123.01, 118.10, 117.03; MS (ESI-, MeOH): m/z = 559.0 (M - Na)⁺ (calcd 558.9); HRMS (ESI-, MeOH): m/z = 267.9654 (M - 2Na)²⁺, C₂₀H₁₂N₂O₈S₂Zn requires 267.9669.

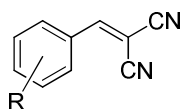
Catalytic reactions: In a typical procedure, the catalyst (0.005 mmol), indole (0.11 mmol) and malononitrile (0.11 mmol) were dissolved in dichloromethane (3 mL). Then, the aldehyde (0.1 mmol) and DIPEA (0.1 mmol) were added to the solution. The resulting mixture was stirred at 40°C for 24 h and then cooled to room temperature. Sampling after appropriate time intervals was done by taking aliquots, concentration and NMR analysis in DMSO-*d*₆. Identification of the reaction components was done by comparison with authentic samples. For the isolation of pure

3-CR product, the reaction mixture was dried over Na_2SO_4 and the solvent was removed under reduced pressure. The residue was purified by silica gel flash column chromatography (hexane/AcOEt: 8:1 to 4:1)^[4] to give the desired product, see below for a typical example.

Synthesis of 2-((1*H*-indol-3-yl)(phenyl)methyl)malononitrile (14): Zn-(salphen) complex **1** (25 mg, 0.05 mmol), indole (129 mg, 1.1 mmol) and malononitrile (73 mg, 0.11 mmol) were added to dichloromethane (6.0 mL). Then salicylaldehyde (106 mg, 1.0 mmol) and DIPEA (129 mg, 1.0 mmol) were added to the solution. The resulting mixture was stirred at 40°C for 24



h and then cooled to room temperature. The solution was dried over Na_2SO_4 and the solvent was removed under reduced pressure. The residue was purified by silica gel flash column chromatography (hexane/AcOEt: gradient from 8:1 to 4:1 v/v) to give the desired product. Yield: 72.5 mg (30%). ^1H NMR (400 MHz, acetone- d_6): δ = 11.21 (s, 1H; NH), 7.55 (d, 4J = 2.3 Hz, 1H; ArH), 7.51 (d, 3J = 7.1 Hz, 2H; ArH), 7.47 (d, 3J = 8.1 Hz, 1H; ArH), 7.34-7.39 (m, 3H; ArH), 7.26-7.30 (m, 1H; ArH), 7.08 (t, 3J = 7.5 Hz, 1H; ArH), 6.95 (t, 3J = 7.6 Hz, 1H; ArH), 5.84 (d, 3J = 9.3 Hz, 1H; CH=CH), 5.21 (d, 3J = 9.3 Hz, 1H; CH=CH); $^{13}\text{C}\{^1\text{H}\}$ NMR (100 MHz, acetone- d_6): δ = 139.68, 136.52, 129.07, 128.46, 126.34, 123.19, 122.09, 119.33, 119.00, 114.50, 114.27, 112.80, 112.11, 42.89, 29.10; HRMS (ESI+, MeOH): m/z = 294.1012 (M+Na)⁺, calcd for $\text{C}_{18}\text{H}_{13}\text{N}_3\cdot\text{Na}$: 294.1007.



NMR studies: The NMR studies were conducted following the same conditions adopted for the catalysis experiments except for the use of deuterated dichloromethane as solvent. After initial mixing of the reagents a 0.7 ml sample was withdrawn and then inserted in the NMR apparatus for analysis. The NMR sample was examined during 24 h acquiring a ^1H NMR spectrum every 30 min at 30°C.

Synthesis of intermediate alkenes (15-19): The (substituted) benzylidene malononitriles were prepared by a standard method. In a typical example, malononitrile (444.3 mg, 6.73 mmol) was dissolved in EtOH (10 ml), then benzaldehyde was added (713.9 mg, 6.73 mmol) followed by 2 drops of piperidine, and the reaction mixture was shortly refluxed. The precipitate that formed upon cooling of the reaction mixture to room temperature was isolated by filtration and dried in vacuo, following analysis by NMR spectroscopy. A second fraction (cf., **15**) was obtained by cooling the mother liquor to -30°C. Yield: 729.3 mg (4.73 mmol, 70%). Note that compounds **15**, **16**, **18** and **19** are known, see the section 'General'.

2-benzylidenemalononitrile (15): Yield: 0.73 g (70%). ^1H NMR (300 MHz, DMSO- d_6): δ = 8.55 (s, 1H; CH=C), 7.94-7.97 (m, 2H; ArH), 7.62-7.72 (m, 3H; ArH); $^{13}\text{C}\{^1\text{H}\}$ NMR (100 MHz, DMSO- d_6): δ = 162.05, 134.85, 131.78, 130.97, 130.00, 114.69, 113.70, 82.09.

2-(4-bromobenzylidene)malononitrile (16): Yield: 0.94 g (84%). ^1H NMR (400 MHz, DMSO- d_6): δ = 8.54 (s, 1H; CH=C), 7.87 (m, 4H; ArH). $^{13}\text{C}\{^1\text{H}\}$ NMR (100 MHz, DMSO- d_6): δ = 160.75, 133.15, 132.60, 130.86, 128.79, 114.55, 113.48, 82.78.

2-(3,5-dibromobenzylidene)malononitrile (17): Yield: 1.15 g (74%). ^1H NMR (500 MHz, DMSO- d_6): δ = 8.49 (s, 1H; CH=C), 8.20 (d, 4J = 2.2 Hz, 1H; Ar-H), 8.10 (d, 4J = 1.9 Hz, 2H; Ar-H); $^{13}\text{C}\{^1\text{H}\}$ NMR (125 MHz, DMSO- d_6): δ = 158.75, 138.47, 135.20, 132.02, 123.65, 114.02, 112.94, 85.75; HRMS (APCI+, MeOH): m/z = 342.9091, calcd for $\text{C}_{11}\text{H}_9\text{N}_2\text{OBr}_2$: 342.9082 [$\text{M} + \text{MeOH} + \text{H}$] $^+$; elemental analysis calcd (%) for $\text{C}^{10}\text{H}^4\text{Br}^2\text{N}^2$: C 38.50, H 1.29, N 8.98; found: C 38.39, H 1.12, N 8.80.

2-(4-methoxybenzylidene)malononitrile (18): Yield: 0.82 g (88%). ^1H NMR (500 MHz, DMSO- d_6): δ = 8.44 (s, 1H; CH=C), 7.85 (d, 3J = 8.2 Hz, 2H; ArH), 7.41 (d, 3J = 8.2 Hz, 2H; ArH), 2.40 (s, 3H; Me). $^{13}\text{C}\{^1\text{H}\}$ NMR (125 MHz, DMSO- d_6): δ = 164.82, 160.84, 133.83, 124.58, 115.63, 115.25, 114.34, 77.27, 56.36.

2-(4-methylbenzylidene)malononitrile (19): Yield: 0.84 g (87%). ^1H NMR (500 MHz, DMSO- d_6): δ = 8.36 (s, 1H; CH=C), 7.96 (d, 3J = 8.9 Hz, 2H; ArH), 7.16 (d, 3J = 8.9 Hz, 2H; ArH), 3.98 (s, 3H; OMe). $^{13}\text{C}\{^1\text{H}\}$ NMR (125 MHz, DMSO- d_6): δ = 161.68, 146.13, 131.16, 130.59, 129.20, 114.84, 113.87, 80.32, 21.92.

X-ray crystallography: The measured crystals of **8** (CCDC 865459) were stable under atmospheric conditions; nevertheless they were treated under inert conditions immersed in perfluoropoly-ether as protecting oil for manipulation. Data Collection: Measurements were made on a Bruker-Nonius diffractometer equipped with an APPEX 2 4K CCD area detector, a FR591 rotating anode with Mo- K_α radiation, Montel mirrors and a Kryoflex low temperature device ($T = -173$ °C). Full-sphere data collection was used with ω and φ scans. Programs used: Data collection Apex2 V2011.3 (Bruker-Nonius 2008), data reduction Saint + Version 7.60A (Bruker AXS 2008) and absorption correction SADABS V. 2008-1 (2008). Structure Solution: SHELXTL Version 6.10 (Sheldrick, 2000)^[17] was used. Structure Refinement: SHELXTL-97-UNIX VERSION.

4.5 Notes and references

- [1] For reviews and seminal contributions see: a) I. Ugi, A. Dömling and B. J. Werner, *Heterocyclic Chem.*, 2000, **37**, 647; b) I. Ugi, R. Meyr and U. Fetzter, *Angew. Chem.*, 1959, **71**, 386; c) O. Kappe, *Acc. Chem. Res.*, 2000, **33**, 879; d) A. Dömling and I. Ugi, *Angew. Chem. Int. Ed.*, 2000, **39**, 3168; e) R. V. A. Orru and M. de Greef, *Synthesis*, 2003, 1471; f) T. Ngouansavanh, J. Zhu, *Angew. Chem. Int. Ed.*, 2006, **45**, 3495; g) A. Dömling, *Chem. Rev.*, 2006, **106**, 17; h) D. Tejedor and F. Garcia-Tellado, *Chem. Soc. Rev.*, 2007, **36**, 484.
- [2] See for instance: a) M. Somei and F. Yamada, *Nat. Prod. Rep.*, 2005, **22**, 73; b) A. C. Kinsman and M. A. Kerr, *J. Am. Chem. Soc.*, 2003, **125**, 14120; c) F. J. Chang, J. B. Rangisetty, M. Dukat, V. Setola, T. Raffay, B. Roth and R. A. Glennon, *Bioorg. Med. Chem. Lett.*, 2004, **14**, 1961.
- [3] a) K. Diker, M. Döé de Maindreville, D. Royer, F. Le Provost and J. Lévy, *Tetrahedron Lett.*, 1999, **40**, 7463; b) G. W. Zhang, L. Wang, J. Nie and J. A. Ma, *Adv. Synth. Catal.*, 2008, **350**, 1457; c) P. Galzerano, F. Pesciaoli, A. Mazzanti, G. Bartoli and P. Melchiorre, *Angew. Chem., Int. Ed.*, 2009, **48**, 7892; d) S. Shirakawa and S. Kobayashi, *Org. Lett.*, 2006, **8**, 4939.
- [4] Y. Qu, F. Ke, L. Zhou, Z. Li, H. Xiang, D. Wua and X. Zhou, *Chem. Commun.*, 2011, **47**, 3912.
- [5] a) A. Decortes, M. Martínez Belmonte, J. Benet-Buchholz and A. W. Kleij, *Chem. Commun.*, 2010, **46**, 4580; b) A. Decortes and A. W. Kleij, *ChemCatChem*, 2011, **3**, 831.
- [6] For some contributions: a) A. W. Kleij, *Dalton. Trans.*, 2009, 4635; b) A. W. Kleij, *Chem. Eur. J.*, 2008, **14**, 10520; c) E. C. Escudero-Adán, J. Benet-Buchholz and A. W. Kleij, *Chem. Eur. J.*, 2009, **15**, 4233; d) S. J. Wezenberg, G. Salassa, E. C. Escudero-Adán, J. Benet-Buchholz and A. W. Kleij, *Angew. Chem. Int. Ed.*, 2011, **50**, 713.
- [7] E. Delahaye, M. Diop, R. Welter, M. Boero, C. Massobrio, P. Rabu and G. Rogez, *Eur. J. Inorg. Chem.*, 2010, 4450.4450.
- [8] A. Dalla Cort, L. Mandolini, C. Pasquini, K. Rissanen, L. Russo and L. Schiaffino, *New J. Chem.*, 2007, **31**, 1633.
- [9] In fact, the 2-CR constitutes the product of a well-known base-assisted Knoevenagel condensation.
- [10] Complex **3** represent the “basic zinc acetate” structure that has been known for decades. Its preparation can be found at: a) A. C. Poshkus, *Ind. Eng. Chem. Prod. Res. Dev.*, 1983, **22**, 381. Furthermore, Mashima and co-workers have recently reported numerous catalytic applications for this Lewis acidic Zn₄ structure. See for instance: b) T. Ohshima, T. Iwasaki, Y.

- Maegawa, A. Yoshiyama and K. Mashima, *J. Am. Chem. Soc.*, 2008, **130**, 2944; c) T. Ohshima, T. Iwasaki and K. Mashima, *Chem. Commun.*, 2006, 2711.
- [11] C. Jiao, M. Zhen and Y. Chao-Guo, *Chem. Res. Chinese Universities*, 2010, **26**, 937.
- [12] Crystallographic data for complex **8**: Formula = C₃₂H₃₇N₅O₇Zn, Fw = 669.04 g·mol⁻¹, monoclinic, space group: P2₁/c, a = 10.6855(5) Å, b = 16.6868(7) Å, c = 17.9841(8) Å, α = 90°, β = 103.532(2)°, γ = 90°, V = 3117.7(2) Å³, Z = 4, ρ_{calcd} = 1.425 Mg/m³, crystal size = 0.20 × 0.10 × 0.02 mm³, F(000) = 1400, μ = 0.844 mm⁻¹, θ range = 1.69–28.41°, R₁ (R all data) = 0.0240 (0.0267), wR2 = 0.0686 (0.0704), reflections collected = 49495, independent reflections = 7822 [R_{int}: 0.0249], data/restraints/parameters = 7822 / 4 / 445, goodness-of-fit on F² = 1.053, largest diff. peak (hole) = 0.428 (–0.306) e·Å⁻³.
- [13] We recently reported a versatile procedure for the in situ transmetalation of Zn(salphen)s: E. C. Escudero-Adán, J. Benet-Buchholz and A. W. Kleij, *Inorg. Chem.*, 2007, **46**, 7265.
- [14] C. Yue, A. Mao, Y. Wei and M. Lu, *Catal. Commun.*, 2008, **9**, 1571.
- [15] U. R. Pratap, D. V. Jawale, R. A. Waghmare, D. L. Lingampalle and R. A. Mane, *New J. Chem.*, 2011, **35**, 49.
- [16] A. W. Kleij, D. M. Tooke, M. Kuil, M. Lutz, A. L. Spek and J. N. H. Reek, *Chem. Eur. J.*, 2005, **11**, 4743.
- [17] G. M. Sheldrick, SHELXTL Crystallographic System Version 5.10, Bruker AXS, Inc. Madison (Wisconsin) 1998.

UNIVERSITAT ROVIRA I VIRGILI

LEWIS ACIDIC ZN(II) SCHIFF BASE COMPLEXES IN HOMOGENEOUS CATALYSIS

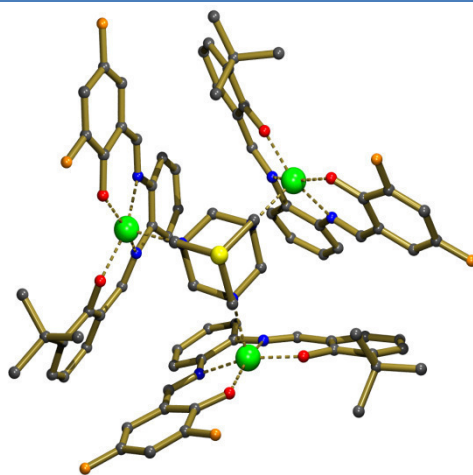
Daniele Anselmo

Dipòsit Legal: T. 1564-2013

Chapter V

Supramolecular Bulky Phosphines Comprising of 1,3,5-triaza-7-phosphaadamantane and Zn(salphen)s: Structural Features and Application in Hydrosilylation Catalysis

The use of the commercially available, bifunctional phosphine 1,3,5-triaza-7-phosphaadamantane (abbreviated as PN_3) in conjunction with a series of Zn(salphen) complexes leads to sterically encumbered phosphine ligands as a result of (reversible) coordinative Zn–N interactions. The solid state and solution phase behaviour of these supramolecular



ligand systems have been investigated in detail and revealed their stoichiometries in the solid state observed by X-ray crystallography, and those determined in solution by NMR and UV-Vis spectroscopy. Also, upon application of these supramolecular bulky phosphines in hydrosilylation catalysis employing 1-hexene as substrate, the catalysis data infer the presence of an active Rh species with two coordinated, bulky PN_3 /Zn(salphen) assemblies having a maximum of three Zn(salphen)s associated per PN_3 scaffold, with an excess of bulky phosphine hardly affecting the overall activity.

5.1 Introduction

Supramolecular catalysis has witnessed the development of a wide variety of catalyst structures showing unprecedented activity, selectivity and/or stability behaviour.^[1] The common feature in all these catalysts is that the individual components self-assemble into the desired structures with high efficiency and little synthetic effort, which is highly attractive in cases where modular changes are (or tend) to be rapidly evaluated through the use of large libraries of ligands.^[2] Structural diversity and accessibility are important parameters for the individual building blocks of a supramolecular catalyst. In this respect, several groups have reported on the use of various supramolecular strategies that involve Schiff base derived chiral diols,^[3] phosphine-based pyridones,^[4] porphyrin,^[5] salen^[6] and other types of modular synthons^[7] useful for catalyst optimization. Previously, the use of bis- and tris-(pyridyl)phosphines and their coordination chemistry towards various Lewis acidic Zn-based building blocks was reported providing partially encapsulated supramolecular phosphines that show unusual reactivity and/or selectivity behaviour in hydroformylation catalysis.^[5,6,8]

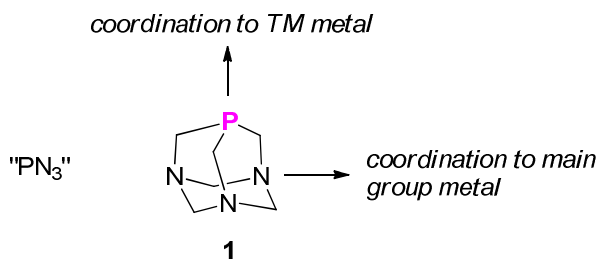
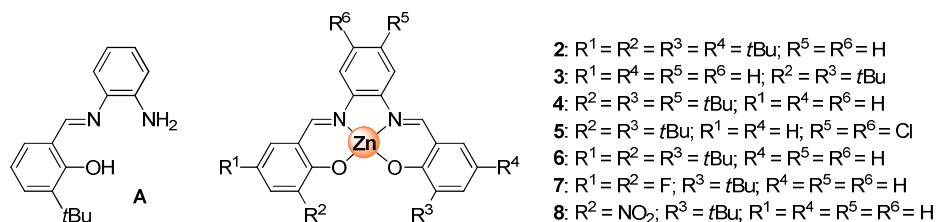


Figure 1. Structure of the "PN₃" ligand scaffold **1** used in this work. TM stands for transition metal.

The key factor adding to the success of this coordination chemistry driven strategy is the selective nature of formation of the Zn–N motifs, thereby leaving the phosphine donor available for coordination to transition metal ions and subsequent catalytic applications. Thus, these pyridylphosphines may be regarded as bifunctional ligands able to coordinate to a combination of (both) main group and transition metal ions. A minor drawback of the pyridylphosphine scaffold is that variations of the ligand backbone are limited. In order to be able to further increase the potential of the encapsulation strategy, other bifunctional *P,N*-derived scaffolds would be interesting to be considered. Despite the fact that 1,3,5-triaza-7-phosphaadamantane is a commercially available compound and its use as phosphine ligand in homogeneous catalysis is well-documented (Figure 1),^[9] no prior use of this "PN₃" ligand scaffold has been reported to

date in the context of supramolecular catalysis. In view of the closer mutual distance between the P- and N-donor atoms of this system and the objective to access an encapsulated phosphine ligand that can potentially show markedly different catalytic behaviour compared with the non-encapsulated ligand, we envisioned that combination with Zn(salphen) complexes (salphen = *N,N'*-bis(salicylidene)imine-1,2-phenylenediamine) would result in high potential in this perspective. These Zn(salphen) complexes are readily available, modular building blocks^[10] that allow for easy fine-tuning of the supramolecular assemblies, and thus their catalytic performance.^[6] Herein we report a detailed study on the assembly formation of the PN₃ ligand scaffold (Fig. 1) and a series of Zn(salphen)s with different substitution patterns (Scheme 1), both in solution phase as well as in the solid state. The results from various Job plot analyses, UV-Vis titrations and application of these supramolecular PN₃ assemblies in hydrosilylation catalysis show that the steric properties of these encumbered ligands can be used for catalyst reactivity control.



Scheme 1. Line drawings of Zn(salphen) complexes **2-8** and mono-imine **A**.

5.2 Results and discussion

Synthesis: Whereas **4** (yield: 68%) was prepared using 4-*tert*-butyl-1,2-phenylenediamine, 3-*tert*-butylsalicylaldehyde and Zn(OAc)₂·2H₂O in a one-pot approach, non-symmetrically substituted complexes **7** (yield: 89%) and **8** (yield: 70%) were derived from the reaction of mono-imine **A** (Scheme 1)^[11] and 3,5-di-fluorosalicylaldehyde and 3-nitro-salicylaldehyde, respectively, in the presence of Zn(OAc)₂·2H₂O. All other Zn(salphen) complexes (**2**, **3**, **5** and **6**) have been reported previously (see the Experimental Section).^[12,13]

NMR studies: First a series of various Zn(salphen)s (Scheme 1) were combined in solution (acetone-*d*₆) with the PN₃ ligand to investigate the binding properties. As a representative case, increasing amounts of complex **2** were added to the PN₃ ligand **1** with stoichiometries ranging from 1:1 to 3:1, and their ¹H and ³¹P{¹H} NMR spectra were recorded.

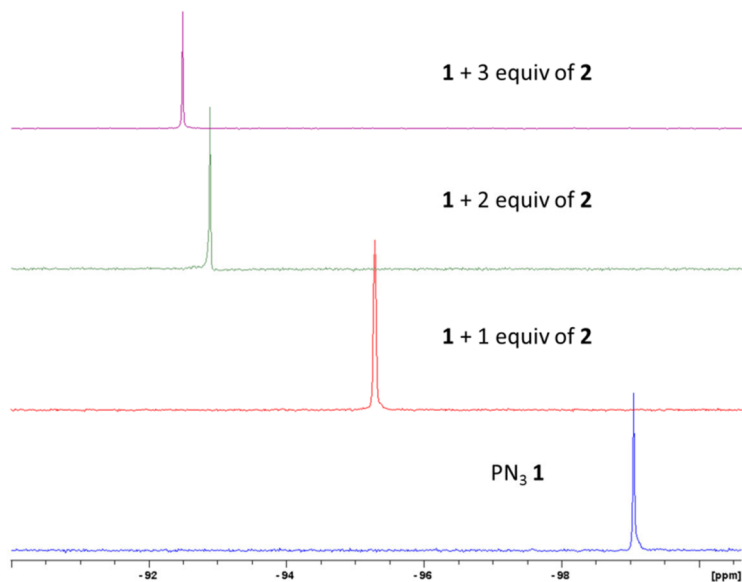


Figure 2. ^{31}P NMR (acetone- d_6) spectral changes for the addition of complex **2** to the PN_3 ligand

The results were compared with the individual components (i.e., “free” PN_3 **1** and **2**) and clearly showed features of a binding event (Fig. 2). For instance, while the free phosphine PN_3 **1** shows a resonance at -99.0 ppm, the 1:1 ($\delta = -95.3$ ppm), 2:1 ($\delta = -92.8$ ppm) and 3:1 ($\delta = -92.5$ ppm) combinations of **2** and PN_3 **1** show distinct values. It is important to notice that the addition of a third equivalent of **2** does not significantly change the ^{31}P chemical shift observed with a 2:1 ratio, which clearly suggests the weak influence of a possible third Zn(salphen) binding on the phosphorus nuclei. Similar features were noted in the ^1H NMR spectra recorded for these combinations (Fig. 3), and a typical up-field shift was observed for the imine-H of **2** ($\Delta\delta = -0.38$) for the 2:1 stoichiometry. Interestingly, further addition of **2** to **1** (i.e., having a 3:1 ratio) caused the imine-H to a downfield shifted value from 8.73 to 8.82 ppm, suggesting the presence of free, unbound **2** and observation of an average value for the imine-H resonances of the 2:1 assembly and free **2**. To gain more insight in the molecular structures, a series of crystallographic analyses were performed for assemblies based on **1** and various Zn(salphen)s (*vide infra*).

X-ray diffraction studies: Suitable crystals were obtained from either hot solutions in CH_3CN , from $\text{CH}_3\text{CN}/\text{DCM}$ or from acetone (see Experimental section). The molecular structures for the assemblies based on **1** and complexes **2** and **7** are presented in Figures 4 and 5.

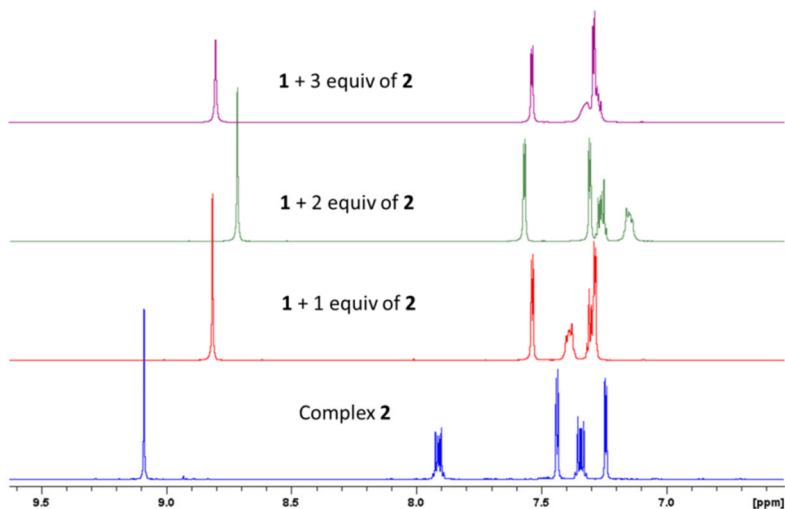


Figure 3. ^1H NMR (acetone- d_6) spectral changes for the addition of complex **2** to the PN_3 ligand

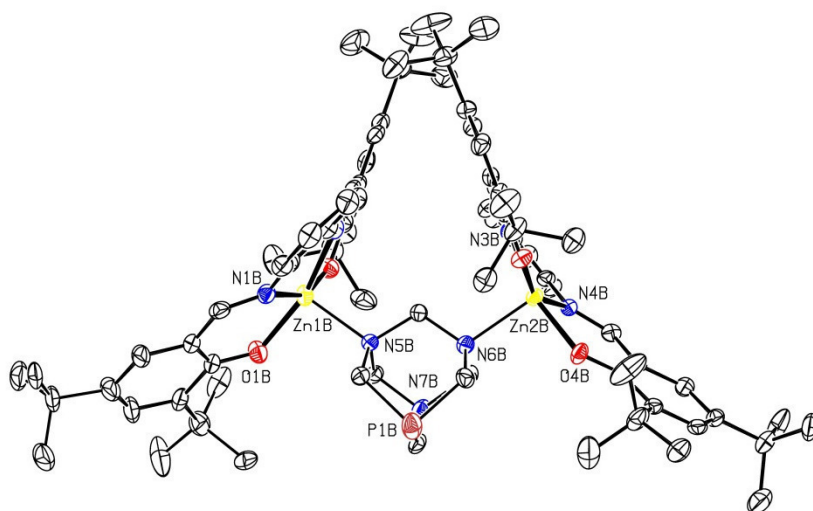


Figure 4. Molecular structure for $1 \cdot (2)_2$ with a partial numbering scheme provided. H-atoms and co-crystallized solvent molecules are not shown for clarity reasons. Selected bond lengths (\AA) and angles ($^\circ$) with *esd*'s in parentheses: $\text{Zn}(1\text{B})\text{-O}(1\text{B}) = 1.976(3)$, $\text{Zn}(1\text{B})\text{-O}(2\text{B}) = 1.967(3)$, $\text{Zn}(1\text{B})\text{-N}(1\text{B}) = 2.091(4)$, $\text{Zn}(1\text{B})\text{-N}(2\text{B}) = 2.099(4)$, $\text{Zn}(1\text{B})\text{-N}(5\text{B}) = 2.103(6)$, $\text{Zn}(2\text{B})\text{-N}(6\text{B}) = 2.172(7)$; $\text{O}(1\text{B})\text{-Zn}(1\text{B})\text{-O}(2\text{B}) = 102.58(13)$, $\text{N}(1\text{B})\text{-Zn}(1\text{B})\text{-N}(2\text{B}) = 77.31(15)$, $\text{O}(1\text{B})\text{-Zn}(1\text{B})\text{-N}(2\text{B}) = 162.78(14)$, $\text{O}(2\text{B})\text{-Zn}(1\text{B})\text{-N}(1\text{B}) = 156.30(14)$.

The structures for $1 \cdot (3)_3$, $1 \cdot (4)_2$, $1 \cdot (5)_2$, $1 \cdot (6)_2$ and $1 \cdot (8)_2$ were also determined and these are provided in the experimental section as they are rather similar to those reported in Figures 4

and 5. These structures confirm the preferred coordination of the N-atoms to the Zn centres of the Zn(salphen) complexes. In the case of complexes **2**, **4**, **5** and **6**, 2:1 coordination complexes were formed whereas for Zn(salphen)s **3** and **7**, 3:1 stoichiometries are present in the solid state. Upon comparing the structures in Figures 4 and 5, being representative examples of 2:1 and 3:1 assemblies, some differences can be noted for the Zn(salphen) complexes bound to PN₃ **1**. First, the Zn–N(PN₃) bond lengths in the 2:1 assembly **1**·(**2**)₂ are slightly shorter on average (2.103(6) and 2.172(7) Å) compared with those observed within **1**·(**7**)₃ (2.194(4), 2.201(4) and 2.200(3) Å). Also, a clear difference for the O–Zn–O angle in the Zn(salphen) units is apparent in both assemblies: whereas in **1**·(**2**)₂ this angle is 102.58(13)°, in **1**·(**7**)₃ the value is much smaller (95.68(14)°).

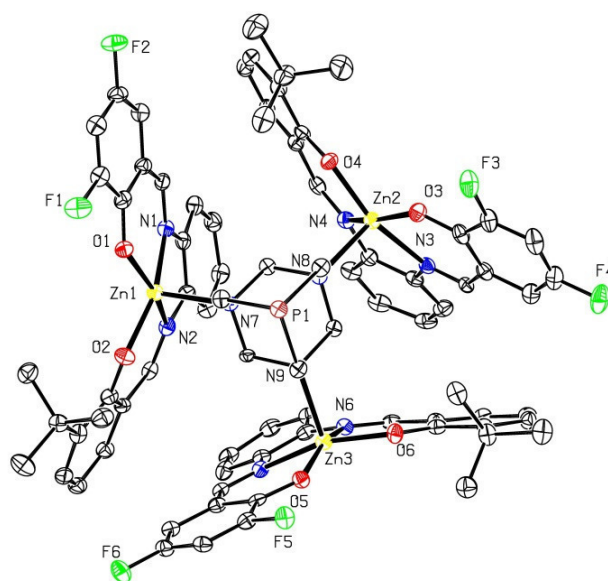


Figure 5. Molecular structure for **1**·(**7**)₃ with a partial numbering scheme provided. H-atoms and co-crystallized solvent molecules are not shown for clarity reasons. Selected bond lengths (Å) and angles (°) with esd's in parentheses: Zn(1)–O(1) = 1.957(3), Zn(1)–O(2) = 1.976(3), Zn(1)–N(1) = 2.107(4), Zn(1)–N(2) = 2.071(4), Zn(1)–N(7) = 2.194(4), Zn(2)–N(8) = 2.201(4), Zn(3)–N(9) = 2.200(3); O(1)–Zn(1)–O(2) = 95.68(14), N(1)–Zn(1)–N(2) = 78.93(15), O(1)–Zn(1)–N(2) = 159.16(14), O(2)–Zn(1)–N(1) = 157.88(14).

Such differences could be the result of some unfavourable steric impediment between the salphen units in the latter assembly, leading to a higher distortion from the standard encountered square pyramidal geometry around the Zn centres in these Zn(salphen) structures.^[14] Notably, the Zn(salphen) units in **1**·(**7**)₃ are arranged such that the different

substituents (F and tBu groups) of the individual complexes are pointing towards each other as to minimize this steric penalty.

Stoichiometry in solution and titration studies: Next, we examined the stoichiometry of all assemblies in solution using ^1H NMR Job plot analyses and UV-Vis titration data. The results of these studies have been combined with those obtained in the solid state, and are listed in Table 1. A representative Job plot (for assembly **1**·(**2**)₂) is shown in Figure 6. For all Zn(salphen)s used we found that the preferred stoichiometry upon combination with PN_3 **1** is 2:1, which is a bit unexpected if the 3:1 stoichiometries for **1**·(**3**)₂ and **1**·(**7**)₂ are considered.

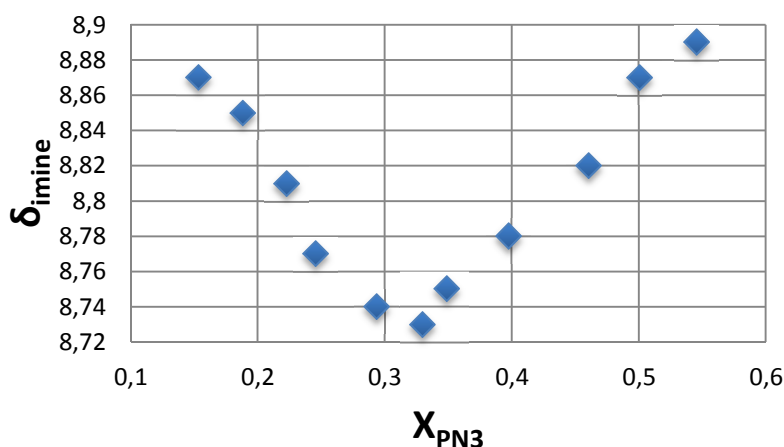


Figure 6. Job plot analysis (^1H NMR, acetone- d_6) using PN_3 **1** and Zn(salphen) complex **2**.

We therefore investigated the binding of several of these Zn(salphen) complexes by UV-Vis titrations carried out in toluene. First of all, to get insight in the strength of the Zn–N interaction, we used Zn(salphen) complex **2** and titrated a solution thereof in toluene with PN_3 **1** (see also the experimental section). The titration curve at $\lambda = 438$ nm and the corresponding data fit using Specfit/32^[15] software is presented in Figure 7. The model used for data-fitting considers four coloured species namely **2** and the 1:1, 2:1 and 3:1 assemblies. Specfit/32 was used to simulate both the UV-Vis traces for all these species as well as their concentration profiles (see experimental section). From the data fit the stepwise constants $K_{1:1}$, $K_{1:1 \rightarrow 2:1}$, and $K_{2:1 \rightarrow 3:1}$ were calculated as well as the cooperativity factors. As may be expected both $K_{1:1}$ ($8,45 \times 10^5 \text{ M}^{-1}$) as well as $K_{1:1 \rightarrow 2:1}$ ($8,85 \times 10^5 \text{ M}^{-1}$) are quite similar with negligible cooperativity ($\alpha = 1,05$), while the

binding of a third Zn(salphen) complex to PN_3 **1** ($K_{2:1 \rightarrow 3:1} = 7.51 \times 10^3 \text{ M}^{-1}$; $\alpha = 0.05$) is shown to be much weaker probably as a result of steric infringement.

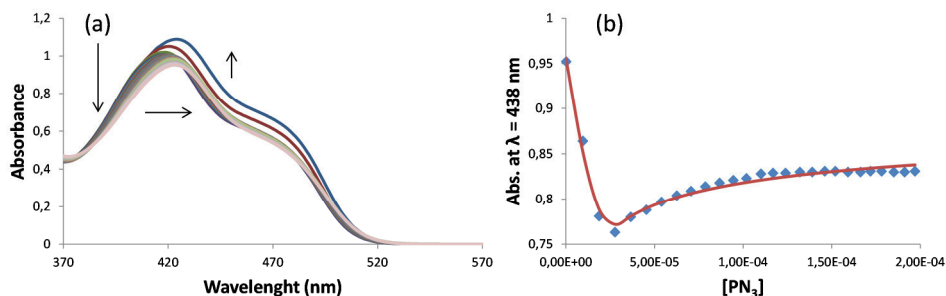


Figure 7. (a) Spectral changes upon the addition of PN_3 **1** to complex **2** in toluene (**2** at $5.38 \times 10^{-5} \text{ M}$); (b) Titration data (blue squares) at $\lambda = 438 \text{ nm}$; in red the corresponding data fit.

Highly similar titration curves were obtained for assemblies $\mathbf{1} \cdot (\mathbf{n})_2$ ($n = 3, 4$ or 5); thus it seems reasonable to assume that also in these cases the 2:1 stoichiometry is preferred in solution as indicated in Table 1. It also suggests that the binding of a third Zn(salphen) complex to **1** is comparatively weak in solution, whereas in the solid state stabilization of 3:1 stoichiometries (i.e., in the case of **3** and **7**) through intermolecular interactions/packing effects may be important for the observation of 3:1 species. As a final control experiment, the use of a generally more strongly binding Ru(CO)(salphen) complex **9**^[14b,16] with a similar molecular size (Fig. 8) was probed in the presence of PN_3 **1** to see whether this would lead to higher stability of a possible 3:1 stoichiometry in solution.

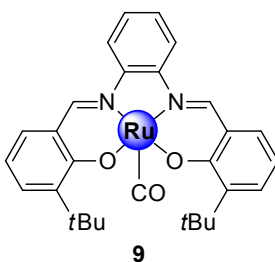


Figure 8. Line drawing of the Ru(salphen) complex **9**.

The combination of three equivalents of complex **9** with one equivalent PN_3 in acetone- d_6 solution resulted in a mixture of several compounds as deduced from the ^1H NMR spectrum, and the $^{31}\text{P}\{^1\text{H}\}$ NMR showed two signals at $\delta = -31.1$ and -48.9 ppm. These results sharply contrast

the findings of tris-pyridylphosphine binding at Ru(salphen)s, where only one single peak in the NMR spectrum was observed.^[14b] Detailed inspection of the NMR spectra revealed that beside the presence of assembled species also “free” Ru(salphen) **9** was present demonstrating that ex-

Table 1. Zn(salphen) complexes **2-8** used in this work and the stoichiometries of the PN₃ assemblies. S.S. = solid state stoichiometry, Sol = solution phase stoichiometry. See Scheme 1 for structural details. [Zn] stands for the Zn(salphen) complex used.

[Zn]	R ¹	R ²	R ³	R ⁴	R ⁵	R ⁶	S.S. ^a	Sol. ^b
2	<i>t</i> Bu	<i>t</i> Bu	<i>t</i> Bu	<i>t</i> Bu	H	H	2:1	2:1
3	H	<i>t</i> Bu	<i>t</i> Bu	H	H	H	3:1	2:1 ^c
4	H	<i>t</i> Bu	<i>t</i> Bu	H	<i>t</i> Bu	H	2:1	2:1 ^c
5	H	<i>t</i> Bu	<i>t</i> Bu	H	Cl	Cl	2:1	2:1 ^c
6	<i>t</i> Bu	<i>t</i> Bu	<i>t</i> Bu	H	H	H	2:1	2:1
7	F	F	<i>t</i> Bu	H	H	H	3:1	2:1
8	H	NO ₂	<i>t</i> Bu	H	H	H	2:1	2:1

^a Obtained by X-ray diffraction studies. ^b Obtained via Job plot analyses using ¹H NMR in acetone-*d*₆ at 25°C. ^c

Extrapolated value from a UV-Vis titration experiment in pre-dried toluene.

clusive 3:1 stoichiometries in solution phase can also not be obtained using a more strongly binding complex. Furthermore, the ³¹P{¹H} NMR also showed that the binding process is not selective, as clear indications of Ru–P coordination were apparent from ³¹P resonances found in the region –50 to –30 ppm.^[9] The occurrence of Ru–to–P coordination can be tentatively explained by the fact that the PN₃ ligand **1** is a much more basic phosphine than previously used tris-pyridylphosphines.^[17] Addition of 20% v/v of a competing ligand (i.e., pyridine-*d*₆) furnished both the ¹H and ³¹P{¹H} traces more easy to interpretate, and confirmed the initial and only partial P–coordination mode of the PN₃ ligand **1**.

Catalysis studies: In order to evaluate the supramolecular phosphines in catalysis, first hydroformylation reactions were carried out using styrene, 1-octene and *trans*-2-octene as substrates as the aldehyde product selectivity has shown to be a function of the steric and electronic properties of the phosphine ligand. The use of PN₃ **1** and various Zn(salphen) complexes (**2-4**) combined with [Rh(acac)(CO)₂] (acac = acetylacetonate) to form complexes coordinated by bulky phosphine ligands that can stir catalyst activity and/or product selectivity

gave poor results and in general with the three substrates tested only small changes in product selectivity were noted (Table 2).

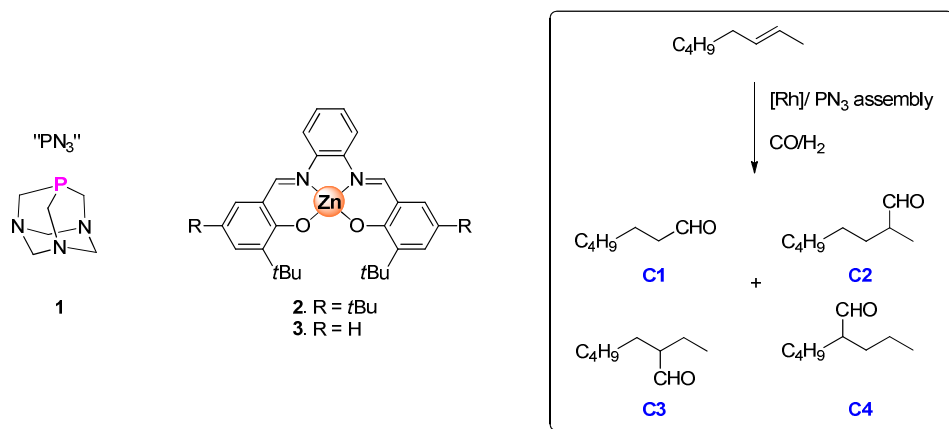


Table 2. Rhodium-catalyzed hydroformylation of *trans*-2-octene using the supramolecular PN_3 assemblies as ligands.^[a]

Entry	Ligand	Eq. [Zn]	Conv. [%] ^[b]	C1 [%]	C2 [%]	C3 [%]	C4 [%]
1	—	0	>99.9	9	52	23	16
2	1	0	0	0	0	0	0
3	2	10	0	0	0	0	0
4	1·2 ^[c,d]	2	94.1	8	50	20	11
5	1·2 ^[e]	12	0	0	0	0	0
6	1·2 ^[f]	5	0	0	0	0	0
7	1·2 ^[f]	10	0	0	0	0	0
8	3	10	0	0	0	0	0
9	1·3 ^[c,d]	3	64	0	53	35	4
10	1·3 ^[e]	13	0	0	0	0	0
11	1·3 ^[f]	5	21	0	57	43	0
12	1·3 ^[f]	10	34	0	49	51	0
13	4	10	0	0	0	0	0
14	1·4 ^[f]	3	40	0	57	43	0
15	1·4 ^[f]	10	48	0	57	43	0

[a] Conditions: [Rh] = 0.5 mM in toluene, ligand/metal ratio = 5, substrate/rhodium = 200, 40 °C, 20 bar, CO/H_2 = 1:1, 96 h. [b] Conversion and products distribution determined by GC. [c] Discrete/pre-isolated assembly used. [d] 11% (entry 4) and 8% (entry 9) of 2-octene isomerization noted. [e] Discrete assembly combined with 10 equiv of Zn(salphen) **2**, **3** or **4**. [f] In situ prepared assembly using the indicated amount of Zn(salphen) **2**, **3** or **4**.

Only in the case of *trans*-2-octene (Table 2) some increase in product selectivity (C3:C2 aldehyde ratio = 51:49) was observed reminiscent of previous results using a porphyrin-derived supramolecular phosphoroamidite ligand.^[18] Therefore, we decided to apply the supramolecular bulky phosphines in another reaction, and hydrosilylation was then chosen to evaluate the influence of the steric bulk of the $\text{PN}_3/\text{Zn}(\text{salphen})$ ligand assemblies given the precedent provided by the work of Tsuji and co-workers.^[19]

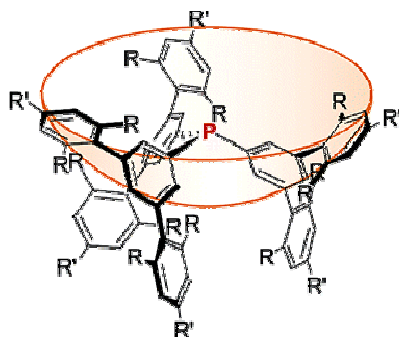


Figure 9. Bulky bowl shaped phosphines used by Tsuji and co-workers in rhodium-catalyzed hydrosilylation.

It should be noted that Tsuji used covalent bulky phosphines, of which the steric influence was evaluated in terms of activity, and particularly when using excess of phosphine ligand. The more sterically demanding phosphines did not allow for more than two P-ligands to be simultaneously coordinated to the Rh metal centre and thus catalytic activity was preserved unlike noted for less bulky phosphines such as PPh_3 . This hydrosilylation protocol may serve as a tool to assess whether the supramolecular phosphines based on PN_3 **1** and $\text{Zn}(\text{salphen})$ s show similar sterically controlled reactivity and thus can give synthetically more easily accessible alternative bulky P-ligands. 1-Hexene and dimethylphenylsilane were selected as reaction partners and the catalytic reactions were performed in toluene at room temperature for 1 h (Table 3). The results were compared to those obtained for a typical phosphine ligand (PPh_3) using various phosphine-to-metal ratios. The presence of two equiv of PPh_3 is known to produce an active catalyst,^[19] and excess of PPh_3 (entry 2, Table 3) shuts down catalytic turnover completely. The same trend is noted for PN_3 **1** (entries 3 and 4). Then, the influence of an increasing amount of $\text{Zn}(\text{salphen})$ **2** (entries 5-7) was evaluated first using two equiv of PN_3 **1** with respect to the Rh precursor. In the presence one equiv (on average) of $\text{Zn}(\text{salphen})$ per phosphine, a much higher conversion level (52%) and yield of product was observed (51%) and further addition of two equiv of $\text{Zn}(\text{salphen})$ **2** caused some decrease in activity, which we

ascribe to a steric effect that results in a less efficient activation of the silylating agent by the Rh complex.

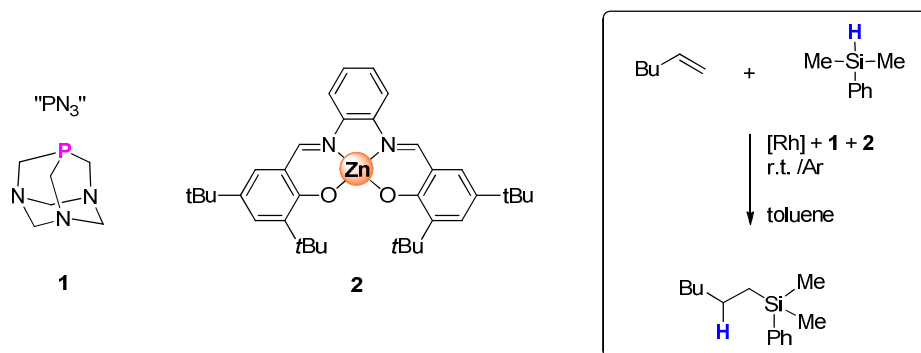


Table 3. Hydrosilylation catalysis carried out with the supramolecular bulky phosphine based on PN₃ **1** and Zn(salphen) complex **2**. [Rh] stands for the rhodium precursor [Rh-μ-Cl(C₂H₄)₂]₂.

Entry	[P]	Equiv [P]	Equiv ^b [Zn]	Conv. ^c (%)	Yield ^c (%)
1	PPh ₃	2	0	100	98
2	PPh ₃	4	0	0	0
3	1	2	0	83	82
4	1	4	0	0	0
5	1	2	2	52	51
6	1	2	4	30 ^d	29 ^d
7	1	2	6	79	76
8	1	2	8	43 ^e	42 ^e
9	1	4	4	0	0
10	1	4	8	27	25
11	1	4	12	74 ^d	73 ^d
12	1	4	16	0 ^e	0 ^e
13^f	–	–	2	0	0

^a Reaction conditions: 1-hexene (1.0 mmol), silane (1.2 mmol), [Rh-μ-Cl(C₂H₄)₂]₂ (5 μmol), toluene (1.0 mL), r.t., Ar-atmosphere, 1 h. ^b [Zn] = Zn(salphen) complex **2**. ^c Conversions/yields determined by ¹H NMR; yield determined using mesitylene as internal standard. ^d Average of two runs with both runs within 1-2%. ^e Heterogeneous mixture observed. ^f Reaction without the Rh precursor present.

When 3 equiv. of Zn(salphen) per PN_3 **1** are present (entry 7) the intermediate may be more prone to phosphine dissociation giving, on average, a more active system. Thus, in presence of six equiv. of Zn(salphen) complex (entry 7) the PN_3 ligands likely become saturated with Zn(salphen)s through $\text{N} \rightarrow \text{Zn}$ coordination but the original activity (entry 3) is nearly fully recovered (79% conversion; yield 76%) as a result of an increasing steric impediment posed by the coordinated, bulky $\text{PN}_3/\text{Zn(salphen)}$ ligand assemblies. In the work of Tsuji,^[19] covalent bulky phosphines (Fig. 9) still provided high activity catalyst systems even when excess (4 equiv) of the phosphine was present. Therefore, we also tested the activity of the catalyst prepared in situ using 4 equiv of PN_3 **1** and 4–12 equiv of Zn(salphen) **2** (entries 9–11, Table 3). The highest conversion/yield was again noted when 3 equiv (on average) of Zn complex per PN_3 ligand **1** were used (entry 11) close to the yield reported when only two equiv of the supramolecular phosphine were combined with the Rh precursor. The presence of an excess of Zn(salphen) (i.e., 4 equiv. per PN_3 **1**) either using a total of two equiv of four equiv of PN_3 **1** per Rh precursor (entries 8 and 12) did not lead to higher conversions/yields; on the contrary, a much less efficient system was obtained and the heterogeneous character (red solid formation) of the reaction mixture in these cases is likely the principal reason for this observation. Apparently, upon using an excess of Zn(salphen) **2** (part of) the (pre)catalytic species precipitates. Following the observations from Tsuji,^[19] the most likely precursor catalyst to be formed in the presence of two equiv of phosphine is a *trans*-bis-phosphine Rh complex having an additional chloride and alkene coordinating. While an increase in the relative amount of Zn(salphen) versus PN_3 **1** first leads to a decrease in activity (Table 3, entry 5 \rightarrow entry 6), further saturation of the PN_3 scaffold with the Zn complex **2** may give rise to a more dynamic inter-conversion between four- and three-coordinated Rh species thus creating vacant coordination sites for catalytic turnover and thus higher activity. The latter situation was also studied by $^{31}\text{P}\{^1\text{H}\}$ NMR (Figure 10c) and compared with the free $\text{PN}_3/\text{Zn(salphen)}$ assembly (Figure 10b, $\delta = -92.5$ ppm) and showed the presence of a single complex (see inset Figure 10c; $\delta = -47.2$ ppm) with a characteristic $^1J_{(\text{P-Rh})}$ of 131 Hz close to the ones reported for *trans*-diphosphine complexes Rh complexes derived from either the bulky P-ligand communicated by Tsuji ($^1J_{(\text{P-Rh})} = 130$ Hz)^[19] or PPh_3 ($^1J_{(\text{P-Rh})} = 129$ Hz).^[20] Since the presence of excess of $\text{PN}_3/\text{Zn(salphen)}$ ligand assembly (Table 3, entry 11) also showed high reactivity, this case was also studied in more detail using $^{31}\text{P}\{^1\text{H}\}$ NMR (see Figure 10d). Two species were detected, with one being easily identified as the free $\text{PN}_3/\text{Zn(salphen)}$ ligand assembly ($\delta = -92.5$ ppm; cf. Fig. 2) showing that not all the supramolecular phosphine interacts with the Rh metal centre. The second species ($\delta = -54.6$ ppm), a Rh-containing complex

different from the one observed in the presence of only two equiv of supramolecular ligand, pertains to a double doublet (dd, $^1J_{(P-Rh)} = 142$ Hz; $^2J_{(P-P)} = 36.8$ Hz). The $^2J_{(P-P)}$ coupling is typical for *cis*-diphosphine-Rh complexes,^[21] and the formation of a dinuclear Rh complex (see inset Figure 10d) as proposed by Tsuji for his bulky phosphine complexes is anticipated. The presence of bridging chlorides effectively prevents the formation of *trans*-bis-phosphine complexes. The presence of tris-phosphine Rh complexes can be ruled out as in that case a more complicated ^{31}P NMR would be expected. Apparently, the bulkiness of the $PN_3/Zn(salphen)$ ligand assembly does not allow for the formation of (catalytically inactive) tri- or tetra-phosphine species, and signal integration for both P-containing compounds present (Figure 10d; ~1:1) is in good agreement with the hypothesis that only two phosphines can be simultaneously bind to the Rh metal centre.

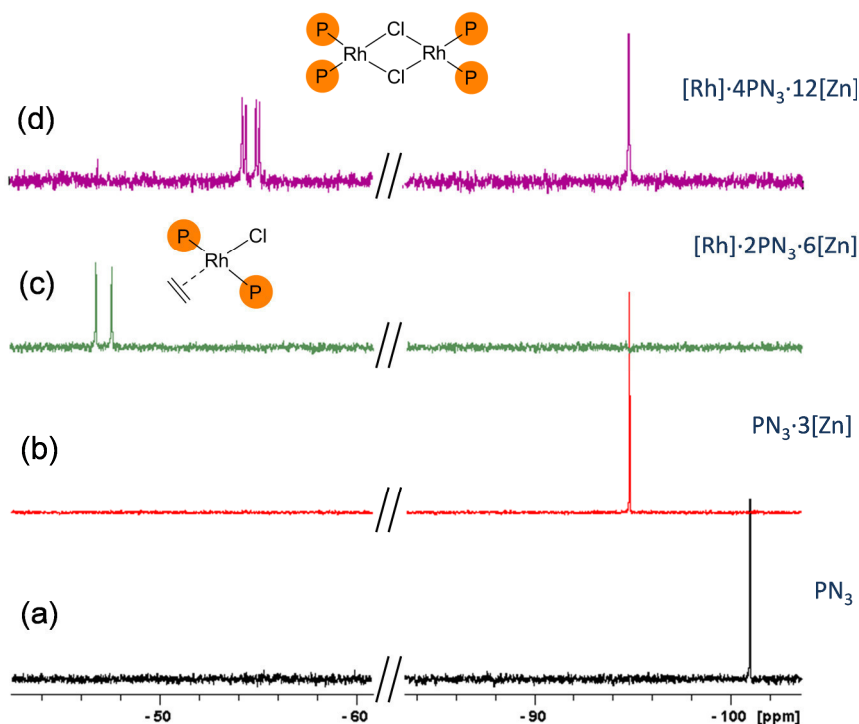


Figure 10. NMR details of the hydrosilylation pre-catalysts using different amounts of PN_3 **1** and/or $Zn(salphen)$ **2**. Conditions: acetone- d_6 , r.t., stirred for two hours in those cases where the Rh salt was added. (a) Only PN_3 **1** present; (b) mixture of PN_3 **1** and 3 equiv of $Zn(salphen)$ **2**; (c) mixture of 1 equiv of $[Rh(\mu-Cl)(C_2H_4)_2]_2$, 2 equiv of PN_3 **1** and 6 equiv of $Zn(salphen)$ **2**; (d) mixture of 1 equiv of $[Rh(\mu-Cl)(C_2H_4)_2]_2$, 4 equiv of PN_3 **1** and 12 equiv of $Zn(salphen)$ **2**. The graphical insets show the proposed structures.

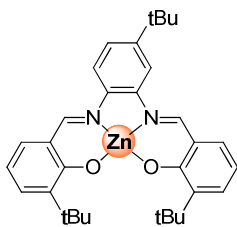
The observed P–P coupling is probably a result of a geometrical distortion (as in the case of Tsuji's P-ligands)^[19] caused by the steric impediment of the $\text{PN}_3/\text{Zn}(\text{salphen})$ ligand assembly, with both magnetically distinct P centres in fast equilibrium.

5.3 Conclusions

This work has shown that supramolecular phosphines based on the PN_3 scaffold are indeed easily prepared by simple combination of a series of $\text{Zn}(\text{salphen})$ complexes and PN_3 **1** in solution giving rise to assembled structures with a preferable 2:1 stoichiometry. The latter has been supported by various analyses (Job plot analysis, UV-Vis titrations, and control experiments). The catalytic results, and in particular those obtained using the $\text{PN}_3/\text{Zn}(\text{salphen})$ ligand assemblies in hydrosilylation, clearly show that the supramolecular formation of bulky phosphines with little synthetic effort may be useful as an alternative for covalent, bulky phosphines,^[19] and the hydrosilylation catalysis data for 1-hexene has shown comparable effects between covalent and supramolecular phosphine ligands. Thus, this implies that assemblies of the type $\text{PN}_3/\text{Zn}(\text{salphen})$ may hold promise to direct catalyst reactivity and potentially process selectivity. Further catalytic studies are now underway to exploit the bulkiness of such P-ligands in other catalysed organic transformations.

5.4 Experimental section

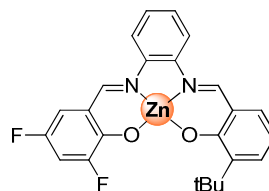
General: NMR spectra were recorded with a Bruker AV-400 or AV-500 spectrometer and were referenced to the residual deuterated solvent signals. Elemental analysis was performed by the Unidad de Análisis Elemental at the Universidad de Santiago de Compostela. Mass spectrometric analysis and X-ray diffraction studies were performed by the Research Support Group at the ICIQ. Complexes **2**,^[12] **3**,^[12] and **5**^[12] and **6**^[13] were prepared according to previously reported procedures. Mono-imine **A**^[11] and Zn(TPP) **10**^[22] were prepared according to known procedures.



Synthesis of Zn(salphen) (4): A mixture of 3-tert-butylsalicylaldehyde (390 mg, 2.19 mmol), 4-tert-butyl-ortho-phenyldiamine (180 mg, 1.09 mmol) and Zn(OAc)₂·2H₂O (360 mg, 1.64 mmol) in MeOH (25 ml) was stirred at room temperature for 48 h. Then the product was collected by filtration to furnish a light orange product (406 mg, 68%).

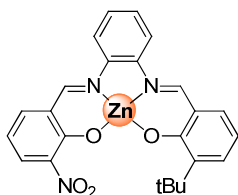
¹H NMR (400 MHz, acetone-*d*₆): δ = 9.14 (s, 1H, CH=N), 9.04 (s, 1H, CH=N), 7.96 (d, 4J = 2.0 Hz, 1H, ArH), 7.83 (d, ³J = 8.6 Hz, 1H, ArH), 7.44 (d, ⁴J = 2.0 Hz, ³J = 8.6 Hz, 1H, ArH), 7.23-7.28 (m, 4H, ArH), 6.46 (t, ³J = 7.6 Hz, 2H, ArH), 1.52 (s, 18H, C(CH₃)₃), 1.41 (s, 9H, C(CH₃)₃); ¹³C{¹H} NMR (125 MHz, acetone-*d*₆): δ = 182.58, 162.34, 161.91, 150.12, 141.99, 139.21, 137.35, 134.23, 130.35, 124.09, 119.66, 115.17, 112.41, 49.0, 35.12, 34.79, 30.72; MS (MALDI+, DCTB): *m/z* = 546.1 [M]⁺ (calcd. 546.2); elemental analysis calculated for C₃₂H₃₈N₂O₂Zn·2H₂O: C 65.80, H 7.25, N 4.80; found: C 65.53, H 8.27, N 4.61.

Synthesis of Zn(salphen) (7): To a solution of mono-imine **A** (73 mg, 0.27 mmol) in MeOH (15 ml) were added 3,5-difluoro-salicylaldehyde (46 mg, 0.29 mmol) and Zn(OAc)₂·2H₂O (99 mg, 0.45 mmol). The solution was left stirring for 18 hours while an orange precipitate was slowly forming. The desired compound



was isolated by filtration and dried in vacuo to yield an orange solid (114 mg, 89%). ¹H NMR (500 MHz, acetone-*d*₆): δ = 8.99 (s, 1H, CH=N), 8.92 (s, 1H, CH=N), 7.84-7.81 (m, 2H, ArH), 7.47-7.37 (m, 2H, ArH), 7.25 (d, ⁴J = 1.8 Hz, ³J = 7.4 Hz, 1H, ArH), 7.20 (d, ⁴J = 1.8 Hz, ³J = 8.0 Hz, 1H, ArH), 7.03-6.97 (m, 2H, ArH), 6.43 (t, ³J = 7.6 Hz, 1H, ArH), 1.45 (s, 9H, C(CH₃)₃); ¹³C{¹H} NMR (125 MHz, acetone-*d*₆): δ = 172.74, 163.86, 161.76, 141.94, 140.69, 139.39, 134.76, 130.80, 128.20, 126.98, 119.67, 119.25, 116.77, 113.57, 112.58, 107.93, 48.74, 35.12 + 29.46; MS (MALDI+,

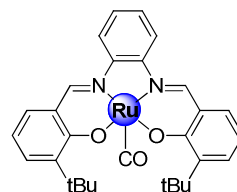
DCTB): $m/z = 470.1$ $[M]^+$ (calcd. 407.1); elemental analysis calculated for $C_{24}H_{20}F_2N_2O_2Zn \cdot 1/3H_2O$: C 60.33, H 4.36, N 5.86; found: C 60.36, H 4.19, N 5.81.



Synthesis of Zn(salphen) (8): To a solution of mono-imine **A** (134 mg, 0.49 mmol) in MeOH (20 ml) were added 3-nitrosalicylaldehyde (90 mg, 0.54 mmol) and $Zn(OAc)_2 \cdot 2H_2O$ (300 mg, 1.37 mmol). The resulting solution was stirred for 18 h at room temperature. In due course, a light orange suspension was

obtained, which was filtered to furnish the product as a light orange solid (164 mg, 70 %). 1H NMR (500 MHz, acetone- d_6): $\delta = 9.11$ (s, 1H, CH=N), 8.97 (s, 1H, CH=N), 7.88 (t, $^3J = 8.5$ Hz, 2H, ArH), 7.79 (d, $^4J = 2.0$ Hz, $^3J = 7.9$ Hz, 1H, ArH), 7.69 (d, $^4J = 1.7$ Hz, $^3J = 7.7$ Hz, 1H, ArH), 7.47 (t, $^3J = 7.6$ Hz, 1H, ArH), 7.40 (t, $^4J = 7.6$ Hz, 1H, ArH), 7.29 (d, $^4J = 1.8$ Hz, $^3J = 7.3$ Hz, 1H, ArH), 7.24 (d, $^4J = 1.9$ Hz, $^3J = 8.0$ Hz, 1H, ArH), 6.60 (t, $^3J = 7.7$ Hz, 1H, ArH), 6.47 (t, $^3J = 7.6$ Hz, 1H, ArH), 1.47 (s, 9H, $C(CH_3)_3$); $^{13}C\{^1H\}$ NMR (125 MHz, acetone- d_6): $\delta = 163.85, 162.23, 142.26, 140.72, 140.29, 139.14, 134.46, 130.96, 129.16, 128.49, 126.95, 123.35, 116.46, 112.91, 111.18, 48.93, 34.94, 29.15$; MS (MALDI+, pyrene): $m/z = 478.9$ $[M]^+$ (calcd. 479.1); elemental analysis calculated for $C_{24}H_{21}N_3O_4Zn \cdot 1/2H_2O$: C 58.85, H 4.53, N 8.58; found: C 58.66, H 4.27, N 8.63.

Synthesis of Ru(CO)(salphen) (9): A solution of *N,N'*-bis(3-*tert*-butylsalicylidene)-1,2-phenylenediamine (459 mg, 1.07 mmol) and $Ru_3(CO)_{12}$ (310 mg, 0.48 mmol) in toluene (25 mL) was heated under reflux for 18 h under argon.^[16] The reaction mixture was cooled to room temperature, filtered through Celite, and



concentrated under reduced pressure. The resulting dark red residue was chromatographed on alumina (II) eluting first with toluene to remove an orange band, followed by CH_2Cl_2 to remove a yellow band, and then with a mixture of EtOH/acetone (5:95 v/v) to remove a red-pink band. The red-pink band was concentrated to dryness under vacuum affording the compound as a glassy red solid that was recrystallized from aqueous EtOH. Yield: 52 mg (9 %). 1H NMR (500 MHz, acetone- d_6): $\delta = 9.31$ (s, 2H, CH=N), 8.29-8.27 (m, 2H, ArH), 7.44 (d, $^4J = 1.7$ Hz, $^3J = 8.1$ Hz, 2H, ArH), 7.36-7.32 (m, 4H, ArH), 6.51 (t, $^3J = 7.4$ Hz, 2H, Ar-H), 1.54 (s, 18H, $C(CH_3)_3$); $^{13}C\{^1H\}$ NMR (125 MHz, acetone- d_6): $\delta = 216.51, 156.50, 142.50, 135.26, 130.65, 126.16, 115.36, 113.16, 35.51, 29.35$; UV-Vis (6.12×10^{-5} M in toluene): λ (ϵ) = 306 nm (17712), 379 nm (24020), 480 nm (7500), 527 (shoulder, 6280); Selected IR (solid): $\nu = 1924$ (CO) cm^{-1} ; MS (MALDI+, pyrene): $m/z =$

528.3 [M–CO]⁺ (calcd. 528.1), 1056.5 [(M–CO)₂]⁺ (calcd. 1056.3); elemental analysis calculated for C₂₉H₃₀N₂O₃Ru·H₂O: C 60.72, H 5.62, N 4.88; found: C 60.91, H 5.82, N 4.32.

Hydrosilylation catalysis: A slightly modified literature procedure was applied:^[19] In a typical experiment, under an argon atmosphere, the phosphine ligand, the Zn(salphen) complex **2** and [Rh(μ-Cl)(C₂H₄)₂]₂ were placed in a Schlenk flask and 1 mL of anhydrous, degassed solvent was added by a syringe. The mixture was then stirred at room temperature for 2 h. Then 1-hexene, mesitylene (used as an internal standard) and dimethyl-phenylsilane were added by a syringe. After 1 h the conversion and yield were determined by ¹H NMR using signal integration and comparison.

Coordination studies: As a primary analysis tool ³¹P{¹H} NMR was used. In a typical experiment, the phosphine ligand, Zn(salphen) complex **2** and [Rh(μ-Cl)(C₂H₄)₂]₂ were placed in a Schlenk flask and 1 mL of anhydrous, degassed toluene was added by a syringe. The mixture was stirred at room temperature for 2 h. Then an aliquot was introduced in an NMR tube equipped with a capillary containing acetone-*d*₆ and a ³¹P NMR spectrum was recorded.

UV-Vis titrations: A typical example is as follows: aliquots between 20–520 μL of a solution of PN₃ **1** (9.54 × 10⁻⁴ M) and Zn(salphen) complex **2** (5.38 × 10⁻⁵ M) in dry toluene were added stepwise to 2.00 mL of a solution of the host **2** in dry toluene in a 1.00 cm quartz cuvette. After each addition, a UV-Vis spectrum was acquired. UV-Vis spectra were recorded on a Shimadzu UV-1800 spectrophotometer.

Determination of the stability constants for the assembly 1·(2)₂: In order to describe the behaviour of assembly (1)·(2)₂ in non-polar media and to obtain the stepwise binding constants of **2** to **1** we used the model described in Scheme 2 which includes four colored species (free Zn(salphen) **2** and the assembled species with stoichiometries 1:1, 1:2 and 1:3). For a first estimate of K_{1:1} (=K_m), we titrated **2** with quinuclidine (Fig. 11). From these data we obtained a titration curve (Fig. 11b), which was fitted to a 1:1 model using Specfit/32^[15], giving K_{1:1} as 2.82 × 10⁵ M⁻¹. This value was successively as a starting point for the data-fit of the titration of **2** with PN₃ **1**.

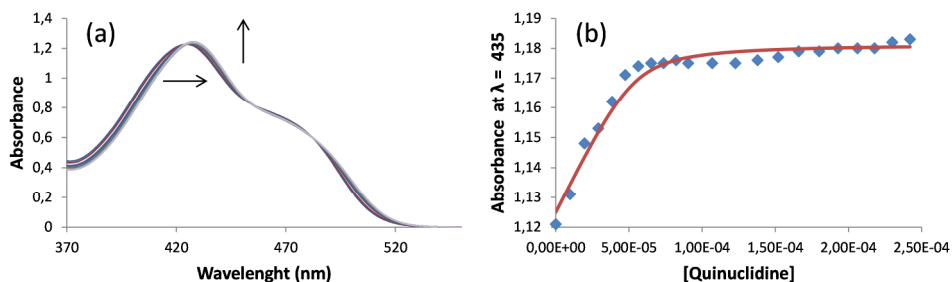
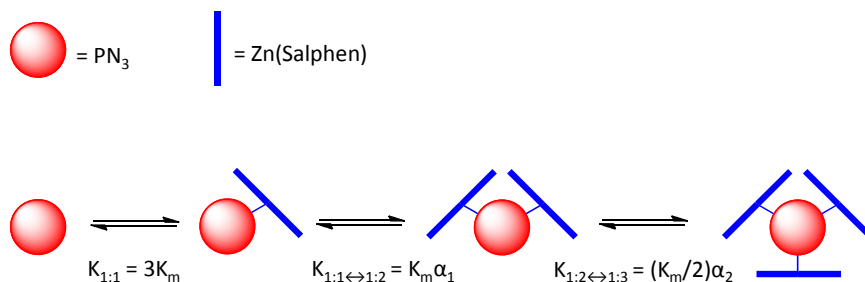


Figure 11. (a) Spectral changes of complex Zn(salphen) **2** upon the addition of quinuclidine carried out in toluene at $[2] = 5.46 \times 10^{-5} \text{ M}$; (b) Titration curve and data fits at $\lambda = 435 \text{ nm}$.

Aliquots between 20–520 μL of a solution of PN_3 ($9.54 \times 10^{-4} \text{ M}$) and Zn(salphen) complex **2** ($5.38 \times 10^{-5} \text{ M}$) in dry toluene were added stepwise to 2.00 mL of a solution of the host **2** in dry toluene in a 1.00 cm quartz cuvette. After each addition, a UV-Vis spectrum was acquired. The titration data obtained (Fig. 12) were analyzed using Specfit/32^[15] by fitting to the binding model reported in Scheme 2 resulting in the stepwise binding constants and cooperativity factors (α) reported in Table 4.



Scheme 2. Involved species in the titration of PN_3 **1** to Zn(salphen) complex **2**. $K_{1:1}$ is the stability constant of the 1:1 complex, $K_{1:1 \leftrightarrow 1:2}$ and $K_{1:2 \leftrightarrow 1:3}$ are the stepwise constants. All constants are related to statistical correction factors, the microscopic binding constant (K_m) and the cooperativity factor (α).

Table 4. Step-wise stability constants and cooperativity factors (α) for the PN_3 -Zn(salphen) assemblies based on the direct titration of Zn(salphen) **2** with PN_3 **1**.

	1:1	1:1 \leftrightarrow 1:2	1:2 \leftrightarrow 1:3
$K (\text{M}^{-1})$	8.45×10^5	8.85×10^5	7.51×10^3
α	-	1.047	0.053

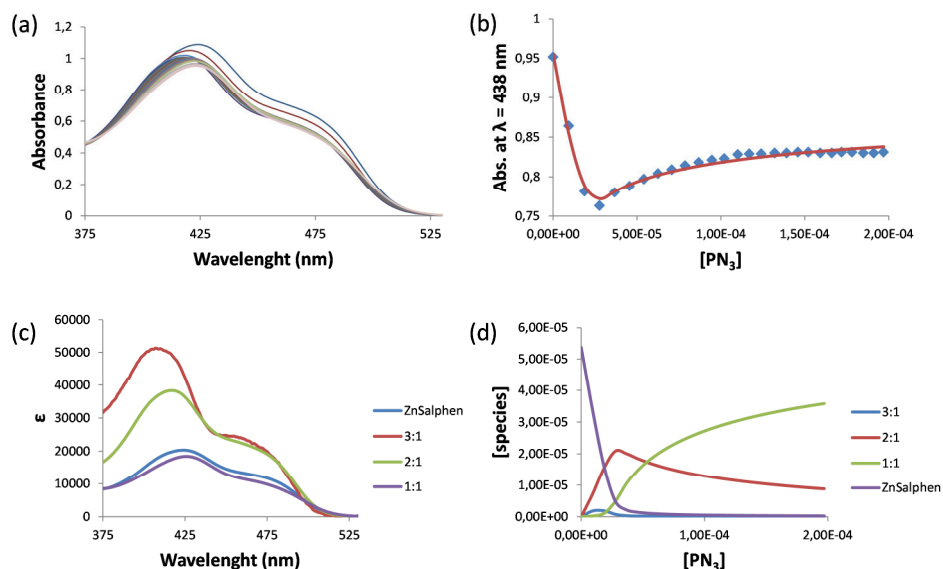


Figure 12. (a) Spectral changes upon the addition of PN₃ 1 to complex 2 carried out in toluene at [2] = 5.38×10^{-5} M; (b) Titration curve and data fit at $\lambda = 438$ nm; (c) Simulated spectra for this titration at the specified equilibrium constants; (d) Simulated concentration profiles for this titration at the specified equilibrium constants.

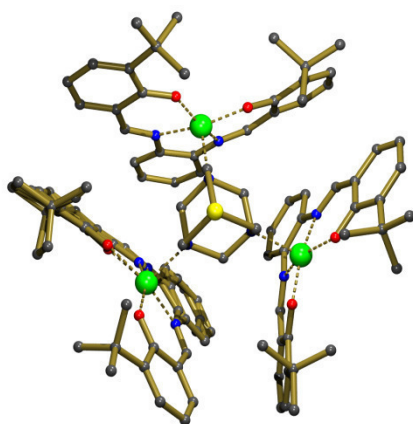
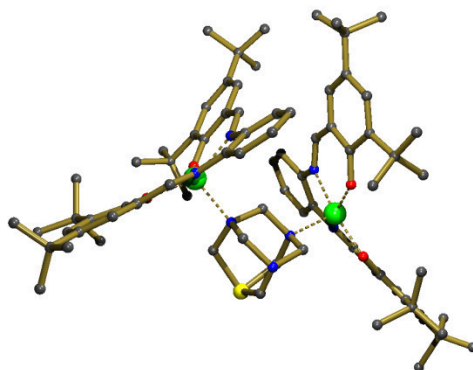
Job-plot analyses: Samples for NMR Job plot analysis were prepared by mixing weighed amounts of different Zn(salphen) complexes and PN₃ 1 (typically the concentration of the Zn(salphen) was $1.1\text{--}2.0 \times 10^{-2}$ M, and concentration of PN₃ 1 typically in the range 3.6×10^{-3} to 1.3×10^{-2} M) in 0.7 mL of acetone-*d*₆ following analysis by ¹H NMR spectroscopy. The δ_{imine} (CH=N) of the metal complexes was plotted against the relative molar fraction (X) of PN₃ 1 of each sample.

X-ray diffraction studies: The measured crystals were stable under atmospheric conditions; nevertheless they were treated under inert conditions immersed in perfluoropoly-ether as a protecting oil for manipulation. Data collection: Measurements were made on a Bruker-Nonius diffractometer equipped with an APPEX 2 4K CCD area detector, an FR591 rotating anode with MoK α radiation, Montel mirrors and a Kryoflex low temperature device (T = -173 °C). Full-sphere data collection was used with ω and ϕ scans. Programs used: Data collection Apex2 V2011.3 (Bruker-Nonius 2008), data reduction Saint + Version 7.60A (Bruker AXS 2008) and absorption correction SADABS V. 2008-1 (2008). Structure solution: SHELXTL Version 6.10

(Sheldrick, 2000)^[23] was used. Structure refinement: SHELXTL-97-UNIX VERSION. Structure resolution was done with SIR2011.^[24]

Crystallographic details for assembly 1·(2)₂:

$C_{84}H_{113}N_{10}O_4PZn_2$, $M_r = 1485.55$, triclinic, $P-1$, $a = 15.4322(9) \text{ \AA}$, $b = 18.2236(12) \text{ \AA}$, $c = 31.756(2) \text{ \AA}$, $\alpha = 84.459(3)^\circ$, $\beta = 83.048(3)^\circ$, $\gamma = 74.347(3)^\circ$, $V = 8517.2(9) \text{ \AA}^3$, $Z = 4$, $\rho = 1.161 \text{ mg}\cdot\text{M}^{-3}$, $\mu = 0.634 \text{ mm}^{-1}$, $\lambda = 0.71073 \text{ \AA}$, $T = 100(2) \text{ K}$, $F(000) = 3176$, crystal size = $0.20 \times 0.20 \times 0.03 \text{ mm}$, $\vartheta(\text{min}) = 0.65^\circ$, $\vartheta(\text{max}) = 25.07^\circ$, 90843 reflections collected, 29658 reflections unique ($R_{\text{int}} = 0.0565$), $\text{GoF} = 1.048$, $R_1 = 0.0648$ and $wR_2 = 0.1650$ [$I > 2\sigma(I)$], $R_1 = 0.0942$ and $wR_2 = 0.1772$ (all indices), min/max residual density = $-1.053/1.334 \text{ [e}\cdot\text{\AA}^{-3}]$. Completeness to $\vartheta(25.07^\circ) = 98.0\%$. The structure has been deposited at the CCDC with reference number 893436. This structure was solved using a disorder model for the tBu groups of the complex and for the PN_3 part of one of the crystallographic independent molecules. There are six acetonitrile co-crystallized solvent molecules present in the asymmetric unit, three of them were modelled with disorder and the program Squeeze^[25] was applied.

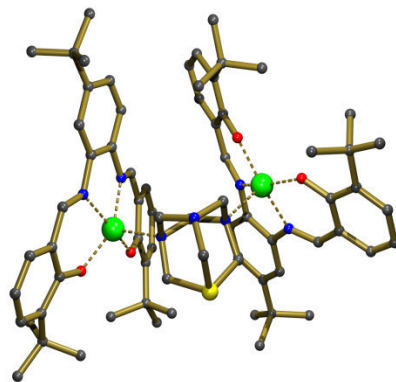


Crystal data for assembly 1·(3)₃:

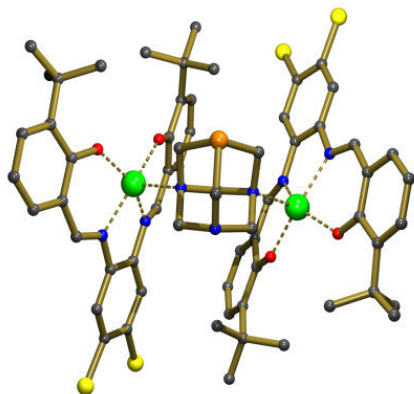
$C_{181}H_{206}N_{18}Cl_2O_{12}P_2Zn_6$, $M_r = 3350.70$, monoclinic, Cc , $a = 29.253(3) \text{ \AA}$, $b = 16.9817(16) \text{ \AA}$, $c = 33.515(3) \text{ \AA}$, $\alpha = 90^\circ$, $\beta = 100.630(3)^\circ$, $\gamma = 90^\circ$, $V = 16363(3) \text{ \AA}^3$, $Z = 4$, $\rho = 1.360 \text{ mg}\cdot\text{M}^{-3}$, $\mu = 0.985 \text{ mm}^{-1}$, $\lambda = 0.71073 \text{ \AA}$, $T = 100(2) \text{ K}$, $F(000) = 7032$, crystal size = $0.20 \times 0.20 \times 0.05 \text{ mm}$, $\vartheta(\text{min}) = 1.42^\circ$, $\vartheta(\text{max}) = 26.82^\circ$, 128388 reflections collected, 34428 reflections unique ($R_{\text{int}} = 0.0453$), $\text{GoF} = 1.017$, $R_1 = 0.0435$ and $wR_2 = 0.1002$ [$I > 2\sigma(I)$], $R_1 = 0.0571$ and $wR_2 = 0.1064$ (all indices), min/max residual density = $-0.846/1.542 \text{ [e}\cdot\text{\AA}^{-3}]$. Completeness to $\vartheta(26.82^\circ) = 99.4\%$. The structure has been deposited at the CCDC with reference number 893439. This structure presents disorder in the various salphen units with occupancy ratios of 50:50 and 60:40. The structure is a DCM solvate.

Crystallographic details for assembly 1·(4)₂:

$C_{76}H_{100}N_7O_6PZn_2$, $M_r = 1369.34$, monoclinic, $P2(1)/c$, $a = 16.3497(13) \text{ \AA}$, $b = 15.1014(11) \text{ \AA}$, $c = 29.107(2) \text{ \AA}$, $\alpha = 90^\circ$, $\beta = 93.354(3)^\circ$, $\gamma = 90^\circ$, $V = 7174.3(9) \text{ \AA}^3$, $Z = 4$, $\rho = 1.268 \text{ mg}\cdot\text{M}^{-3}$, $\mu = 0.747 \text{ mm}^{-1}$, $\lambda = 0.71073 \text{ \AA}$, $T = 100(2) \text{ K}$, $F(000) = 2912$, crystal size = $0.30 \times 0.10 \times 0.02 \text{ mm}$, $\vartheta(\text{min}) = 1.52^\circ$, $\vartheta(\text{max}) = 25.91^\circ$, 71356 reflections collected, 13912 reflections unique ($R_{\text{int}} = 0.0846$), GoF = 1.017, $R_1 = 0.0547$ and $wR_2 = 0.1156$ [$I > 2\sigma(I)$], $R_1 = 0.0949$ and $wR_2 = 0.1313$ (all indices), min/max residual density = $-0.824/0.671$ [$e\cdot\text{\AA}^{-3}$]. Completeness to $\vartheta(25.91^\circ) = 99.6\%$. The structure has been deposited at the CCDC with reference number 893440. This structure shows disorder in both the adamantane backbone as well as in part of the tBu groups; the molecule contains two co-crystallized acetone solvent molecules disordered over two positions.

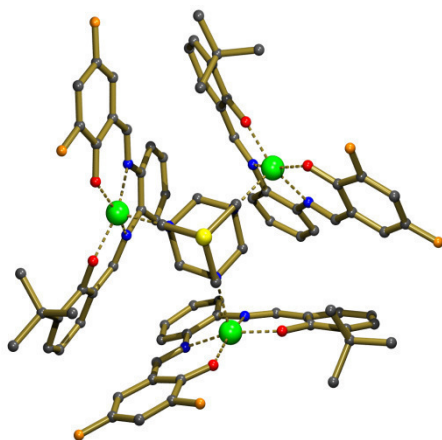
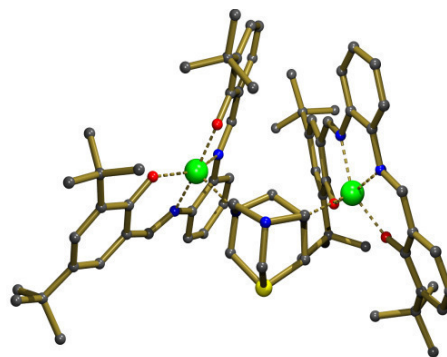
Crystallographic details for assembly 1·(5)₂:

$C_{64}H_{71}Cl_4N_8O_4PZn_2$, $M_r = 1319.80$, monoclinic, $C2/c$, $a = 30.798(2) \text{ \AA}$, $b = 13.5677(9) \text{ \AA}$, $c = 29.886(2) \text{ \AA}$, $\alpha = 90^\circ$, $\beta = 101.815(2)^\circ$, $\gamma = 90^\circ$, $V = 12223.7(14) \text{ \AA}^3$, $Z = 8$, $\rho = 1.434 \text{ mg}\cdot\text{M}^{-3}$, $\mu = 1.041 \text{ mm}^{-1}$, $\lambda = 0.71073 \text{ \AA}$, $T = 100(2) \text{ K}$, $F(000) = 5488$, crystal size = $0.20 \times 0.15 \times 0.15 \text{ mm}$, $\vartheta(\text{min}) = 1.35^\circ$, $\vartheta(\text{max}) = 28.20^\circ$, 211665 reflections collected, 15010 reflections unique ($R_{\text{int}} = 0.0466$), GoF = 1.060, $R_1 = 0.0310$ and $wR_2 = 0.0714$ [$I > 2\sigma(I)$], $R_1 = 0.0408$ and $wR_2 = 0.0753$ (all indices), min/max residual density = $-0.463/0.397$ [$e\cdot\text{\AA}^{-3}$]. Completeness to $\vartheta(28.20^\circ) = 99.7\%$. The structure has been deposited at the CCDC with reference number 893438. This structure is a CH_3CN solvate with disorder in both the adamantane structure as well as the co-crystallized CH_3CN molecules.



Crystal data for assembly 1·(6)₂:

$C_{70.50}H_{88}ClN_7O_4PZn_2$, $M_r = 1294.64$, monoclinic, $P2(1)/c$, $a = 14.3779(7) \text{ \AA}$, $b = 30.8290(15) \text{ \AA}$, $c = 17.5123(8) \text{ \AA}$, $\alpha = 90^\circ$, $\beta = 110.964(2)^\circ$, $\gamma = 90^\circ$, $V = 7248.6(6) \text{ \AA}^3$, $Z = 4$, $\rho = 1.186 \text{ mg}\cdot\text{M}^{-3}$, $\mu = 0.769 \text{ mm}^{-1}$, $\lambda = 0.71073 \text{ \AA}$, $T = 100(2) \text{ K}$, $F(000) = 2736$, crystal size = $0.35 \times 0.10 \times 0.10 \text{ mm}$, $\vartheta(\text{min}) = 1.41^\circ$, $\vartheta(\text{max}) = 26.80^\circ$, 73204 reflections collected, 15211 reflections unique ($R_{\text{int}} = 0.0410$), $\text{GoF} = 1.045$, $R_1 = 0.0588$ and $wR_2 = 0.1798$ [$I > 2\sigma(I)$], $R_1 = 0.0751$ and $wR_2 = 0.1907$ (all indices), min/max residual density = $-0.437/2.016 \text{ [e}\cdot\text{\AA}^{-3}]$. Completeness to $\vartheta(26.80^\circ) = 98.0\%$. The structure has been deposited at the CCDC with reference number 893441. This structure, a DCM solvate, was modelled using a disorder model for both the adamantane and part of the tBu groups. For resolving this structure the program SQUEEZE²⁵ was used.

Crystal data for assembly 1·(7)₃:

$C_{78}H_{72.5}N_9F_6O_{6.25}PZn_3$, $M_r = 1577.03$, monoclinic, $C2/c$, $a = 18.1552(4) \text{ \AA}$, $b = 31.5457(8) \text{ \AA}$, $c = 25.2433(7) \text{ \AA}$, $\alpha = 90^\circ$, $\beta = 105.4820(10)^\circ$, $\gamma = 90^\circ$, $V = 13932.7(6) \text{ \AA}^3$, $Z = 8$, $\rho = 1.504 \text{ mg}\cdot\text{M}^{-3}$, $\mu = 2.082 \text{ mm}^{-1}$, $\lambda = 0.71073 \text{ \AA}$, $T = 100(2) \text{ K}$, $F(000) = 6500$, crystal size = $0.10 \times 0.10 \times 0.05 \text{ mm}$, $\vartheta(\text{min}) = 2.80^\circ$, $\vartheta(\text{max}) = 66.71^\circ$, 15899 reflections collected, 16047 reflections unique ($R_{\text{int}} = 0.000$), $\text{GoF} = 1.147$, $R_1 = 0.0497$ and $wR_2 = 0.1436$ [$I > 2\sigma(I)$],

$R_1 = 0.0531$ and $wR_2 = 0.1487$ (all indices), min/max residual density = $-0.556/0.513 \text{ [e}\cdot\text{\AA}^{-3}]$. Completeness to $\vartheta(66.71^\circ) = 95.2\%$. The structure has been deposited at the CCDC with reference number 893437. This structure is a hemi-hydrate with the water molecules disordered over two positions. This sample was measured using Cu-radiation, and the sample turned out to be a combination of two crystals with a 71:29 occupancy ratio. For the absorption correction TWINABS was used.^[26]

Note that the structure for assembly **1**·(**8**)₂ was also determined; but since it constitutes a very similar structure compared to the other 2:1 assemblies, it was not completely refined.

5.5 Notes and references

- [1] *Supramolecular Catalysis*, ed. P. W. N. M. van Leeuwen, Wiley-VCH, Weinheim, Germany, 2008; (b) J. Meeuwissen and J. N. H. Reek, *Nature Chem.*, 2010, **2**, 615; (c) T. S. Koblenz, J. Wassenaar and J. N. H. Reek, *Chem. Soc. Rev.*, 2008, **37**, 247; (d) M. J. Wiester, P. A. Ulmann and C. A. Mirkin, *Angew. Chem. Int. Ed.*, 2011, **50**, 114; (e) B. Breit, *Pure Appl. Chem.*, 2008, **80**, 855; (f) D. Fiedler, D. H. Leung, R. G. Bergman and K. N. Raymond, *Acc. Chem. Res.*, 2005, **38**, 349; (g) A. W. Kleij, J. N. H. Reek, *Chem.–Eur. J.*, 2006, **12**, 4218.
- [2] (a) M. T. Reetz, *Angew. Chem. Int. Ed.*, 2008, **47**, 2556; (b) C. Gennari and U. Piarulli, *Chem. Rev.*, 2003, **103**, 3071; (c) A. J. Sandee and J. N. H. Reek, *Dalton Trans.*, 2006, 3385; (d) M. B. Francis, T. F. Jamison and E. N. Jacobsen, *Curr. Opin. Chem. Biol.*, 1998, **2**, 422; (e) B. Breit, *Angew. Chem. Int. Ed.*, 2005, **44**, 6816.
- [3] (a) P. W. N. M. van Leeuwen, D. Rivillo, M. Raynal and Z. Freixa, *J. Am. Chem. Soc.*, 2011, **133**, 18562; (b) D. M. Rivillo, H. Gulyas, J. Benet-Buchholz, E. C. Escudero-Adán, Z. Freixa and P. W. N. M. van Leeuwen, *Angew. Chem. Int. Ed.*, 2007, **46**, 7247.
- [4] (a) B. Breit and W. Seiche, *J. Am. Chem. Soc.*, 2003, **125**, 6608; for related aminopyridine derived P-ligands: (b) B. Breit and W. Seiche, *Angew. Chem. Int. Ed.*, 2005, **44**, 1640.
- [5] (a) V. F. Slagt, P. W. N. M. van Leeuwen and J. N. H. Reek, *Chem. Commun.*, 2003, 2474; (b) V. F. Slagt, M. Röder, P. C. J. Kamer, P. W. N. M. van Leeuwen and J. N. H. Reek, *J. Am. Chem. Soc.*, 2004, **126**, 4056; (c) A.M. Kluwer, R. Kapre, F. Hartl, M. Lutz, A. L. Spek, A. M. Brouwer, P. W. N. M van Leeuwen and J. N. H. Reek, *Proc. Nat. Ac. Sci. (USA)*, 2009, **26**, 10460.
- [6] (a) M. Kuil, P. E. Goudriaan, P. W. N. M. van Leeuwen and J. N. H. Reek, *Chem. Commun.*, 2006, 4679; (b) A. W. Kleij, M. Lutz, A. L. Spek, P. W. N. M. van Leeuwen and J. N. H. Reek, *Chem. Commun.*, 2005, 3661; (c) M. Kuil, P.E. Goudriaan, A. W. Kleij, D.M. Tooke, A. L. Spek, P. W. N. M. van Leeuwen and J. N. H. Reek, *Dalton. Trans.*, 2007, 2311; (d) J. Flapper and J. N. H. Reek, *Angew. Chem. Int. Ed.*, 2007, **46**, 8590.
- [7] (a) A. J. Sandee, A. M. van der Burg and J. N. H. Reek, *Chem. Commun.*, 2007, 864; (b) J. M. Takacs, D. S. Reddy, S. A. Moteki, D. Wu and H. Palencia, *J. Am. Chem. Soc.*, 2004, **126**, 4494; (c) N. C. Gianneschi, P. A. Bertin, S. T. Nguyen, C. A. Mirkin, L. N. Zakharov and A. L.

- Rheingold, *J. Am. Chem. Soc.*, 2003, **125**, 10508; (d) C. J. Brown, G. M. Miller, M. W. Johnson, R. G. Bergman and K. N. Raymond, *J. Am. Chem. Soc.*, 2011, **133**, 11964; (e) C. J. Hastings, M. D. Pluth, R. G. Bergman and K. N. Raymond, *J. Am. Chem. Soc.*, 2010, **132**, 6938; (f) V. Bocokić, M. Lutz, A. L. Spek and J. N. H. Reek, *Dalton Trans.*, 2012, **41**, 3740.
- [8] For some early examples: (a) V. F. Slagt, P. W. N. M. van Leeuwen and J. N. H. Reek, *Angew. Chem. Int. Ed.*, 2003, **42**, 5619; (b) V. F. Slagt, J. N. H. Reek, P. C. J. Kamer and P. W. N. M. van Leeuwen, *Angew. Chem. Int. Ed.*, 2001, **40**, 4271.
- [9] A. D. Phillips, L. Gonsalvi, A. Romerosa, F. Vizza and M. Peruzzini, *Coord. Chem. Rev.*, 2004, **248**, 955.
- [10] (a) A. M. Castilla, S. Curreli, M. Martínez Belmonte, E. C. Escudero-Adán, J. Benet-Buchholz and A. W. Kleij, *Org. Lett.*, 2009, **11**, 5218; (b) E. C. Escudero-Adán, M. Martínez Belmonte, J. Benet-Buchholz and A. W. Kleij, *Org. Lett.*, 2010, **12**, 4592; (c) E. C. Escudero-Adán, M. Martínez Belmonte, E. Martin, G. Salassa, J. Benet-Buchholz and A. W. Kleij, *J. Org. Chem.*, 2011, **76**, 5404; (d) A. W. Kleij, *Eur. J. Inorg. Chem.*, 2009, 193; (e) A. W. Kleij, D. M. Tooke, M. Lutz, A. L. Spek and J. N. H. Reek, *Eur. J. Inorg. Chem.*, 2005, 4626.
- [11] S. J. Wezenberg, G. Salassa, E. C. Escudero-Adán, J. Benet-Buchholz and A. W. Kleij, *Angew. Chem. Int. Ed.*, 2011, **50**, 713.
- [12] A. W. Kleij, D. M. Tooke, M. Kuil, M. Lutz, A. L. Spek and J. N. H. Reek, *Chem.–Eur. J.*, 2005, **11**, 4743.
- [13] M. Martínez Belmonte, S. J. Wezenberg, R. M. Haak, D. Anselmo, E. C. Escudero-Adán, J. Benet-Buchholz and A. W. Kleij, *Dalton Trans.*, 2010, **39**, 4541.
- [14] For some examples: (a) A. L. Singer and D. A. Atwood, *Inorg. Chim. Acta*, 1998, **277**, 157; (b) S. J. Wezenberg, E. C. Escudero-Adán, J. Benet-Buchholz and A. W. Kleij, *Inorg. Chem.*, 2008, **47**, 2925.
- [15] SPECFIT/32, version 3.0.40, Spectra Software Associates, R. A. Binstead, A. D. Zuberbühler, 1993-2007; original publication: H. Gampp, M. Maeder, C. J. Meyer and A. D. Zuberbühler, *Talanta*, 1985, **32**, 95.
- [16] K. Chichak, U. Jacquemard and N. R. Branda, *Eur. J. Inorg. Chem.*, 2002, 357.
- [17] A. W. Kleij, M. Kuil, D. M. Tooke, A. L. Spek and J. N. H. Reek, *Inorg. Chem.*, 2005, **44**, 7696.
- [18] R. Bellini, S. H. Chikkali, G. Berthon-Gelloz and J. N. H. Reek, *Angew. Chem. Int. Ed.*, 2011, **50**, 7342.
- [19] O. Niyomura, T. Iwasawa, N. Sawada, M. Tokunaga, Y. Obora and Y. Tsuji, *Organometallics*, 2005, **24**, 3468.

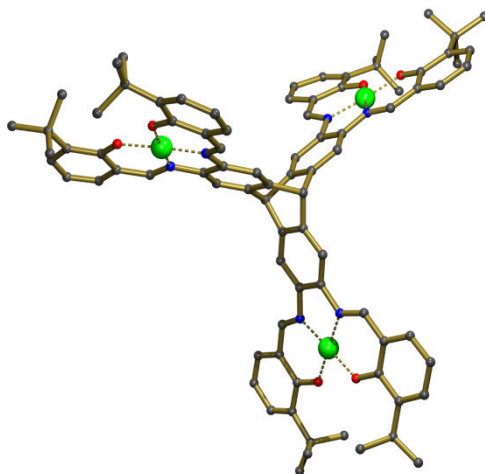
- [20] A. J. Naaktgeboren, R. J. M. Nolte and W. J. Drenth, *J. Am. Chem. Soc.*, 1980, **102**, 3350.
- [21] See for instance: A. S. C. Chan and J. Halpern, *J. Am. Chem. Soc.*, 1980, **102**, 838.
- [22] See for instance: C.-W. Huang, K. Y. Chiu and S.-H. Cheng, *Dalton Trans.*, 2005, 2417.
- [23] G. M. Sheldrick, SHELXTL Crystallographic System, version 6.10, Bruker AXS, Inc., Madison, Wisconsin, 2000.
- [24] M. C. Burla, R. Caliandro, M. Camalli, B. Carrozzini, G. L. Cascarano, C. Giacovazzo, M. Mallamo, A. Mazzone, G. Polidori and R. Spagna, *J. Appl. Cryst.*, 2012, **45**, 357.
- [25] SQUEEZE: P. van der Sluis and A.L. Spek, *Acta Cryst.*, 1990, **A46**, 194.
- [26] TWINABS Version 2008/4 Bruker AXS; R. Blessing, *Acta Cryst.*, 1995, **A51** 33.

Chapter VI

Merging Catalysis and Supramolecular Aggregation

Features of Triptycene based Zn(salphen)s

A series of trinuclear, triptycene based metallosalphen complexes ($M = \text{Zn}, \text{Ni}$) have been prepared incorporating various peripheral substituents. The introduction of Zn metal centres in these triptycene based salphen ligands gives rise to cross-linking between different triptycene molecules through μ -phenoxo bridges between the Zn metal centres, and variation in the peripheral groups allows controlling the self-assembling properties as shown by UV-Vis titration data. The strong association of these trinuclear Zn_3 complexes under relatively apolar conditions has been exploited to recover the complex after its application as a catalyst for the cycloaddition of carbon dioxide to 1,2-epoxyhexane. The catalysis results and recycling studies show that the co-catalyst structure is important for efficient recovery of the binary system, demonstrating that reversible supramolecular aggregation may become a useful tool for recycling homogeneous catalysts.



6.1 Introduction

Self-assembly constitutes a modern tool for the convenient construction of larger, complex molecules with minimal synthetic effort.^[1] Such non-covalent structures have shown to be useful in various areas of research such as nano-chemistry,^[2] supramolecular catalysis^[3] and the fabrication of functional polymers.^[4] The key factors adding to a successful self-assembly

approach are the type of molecular building block that is being used and the interactions involved, with H-bonding^[5] and metal-ligand coordination motifs^[6] being most frequently applied. Whereas metalloporphyrins, by virtue of their ability to bind pyridines,^[7] have conquered an important position in supramolecular chemistry, recently also other comparable building blocks such as metallosalens have emerged as powerful alternative supramolecular synthons.^[8] Specifically, the Zn(II) centered family of salphen derivatives (salphen = *N,N'*-phenylene-1,2-bis-salicylideneimine) have shown to be excellent and modular building blocks useful in the creation of artificial chirality^[9] and functional surfaces.^[10] These Zn(salphen)s can self-assemble in two distinct ways, viz. through Zn-pyridine coordination patterns or via dimerization mediated through μ -phenoxo bridges (Fig. 1); the latter type of self-assembly has become a popular way to construct functional materials with many appealing properties.^[11] We recently described that the salphen substitution pattern offers a way to fine-tune this self-assembly process,^[12] and especially the positions *ortho* with respect to the phenolic O-atoms give the opportunity to vary between predominant monomeric Zn(salphen) complexes (large *ortho* groups such as tBu) or dimeric complexes (no *ortho* or very small groups) under relative apolar conditions. At a later stage, multinuclear versions of these Zn(salphen)s have shown even higher tendency to form strongly aggregated species with very low solubility in many organic solvents.^[13] The aggregated state may be disrupted by addition of suitable donors such as THF, pyridines or even organic substrates.

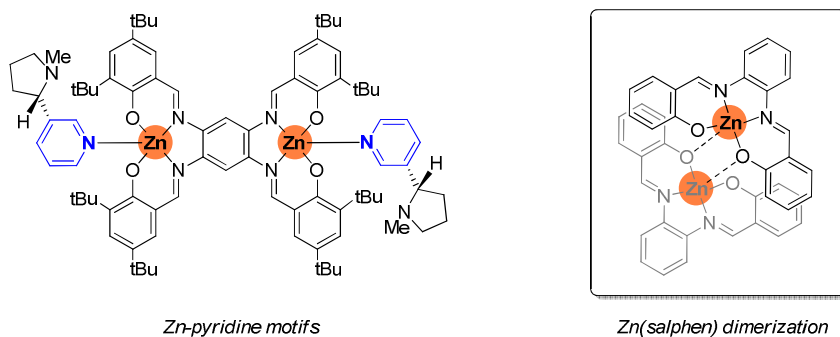


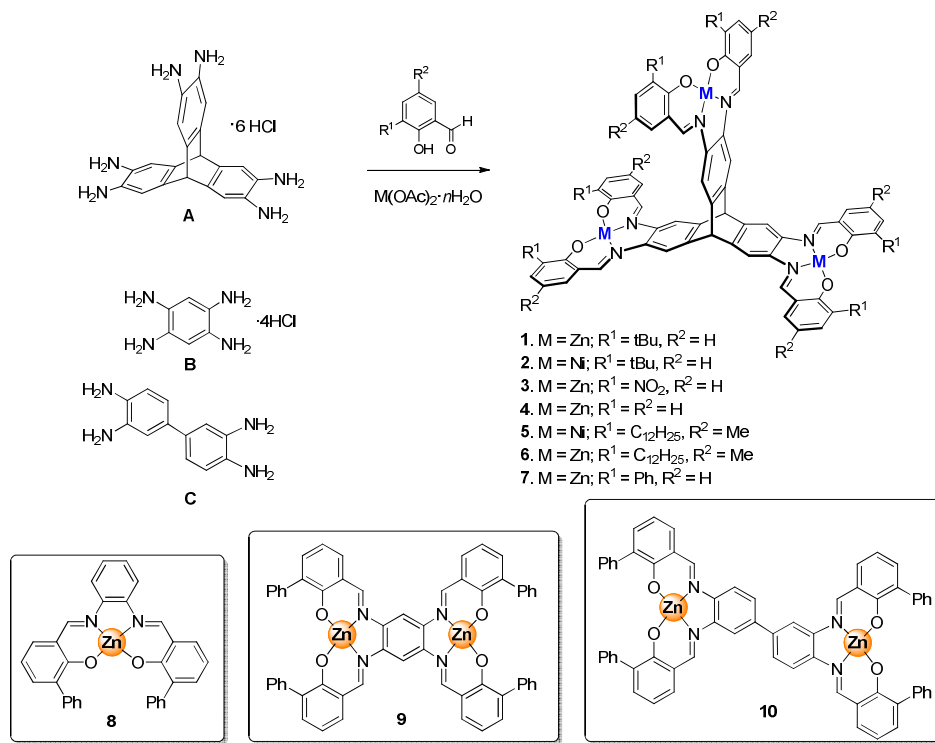
Figure 1. Possible self-assembly modes of Zn(salphen) complexes; pyridine-Zn coordination motifs (left) and Zn(salphen) dimerization (right).

This led us to believe that upon choosing a suitable multinuclear Zn(salphen) framework with appropriate *ortho* groups, a reversible switch between a highly aggregated, non-soluble state (apolar medium) and a soluble low-aggregated state in the presence of a coordinating substrate

can be realized. These smaller aggregates and/or monomers should be able to activate the substrate through binding to the Zn metal centres, after which extraction of the final product with a relative apolar solvent should render the multinuclear Zn(salphen) insoluble and thus give it efficient recycling potential. Triptycene (9,10-dihydro-9,10-[1,2]benzenoanthracene) offers a paddlewheel type structure with D_{3h} symmetry. Previously, triptycenes have been functionalized with metallosalphenes to give access to interesting porous materials with unusual properties.^[14] Motivated by these former results, we have now combined the triptycene scaffold with the self-assembling properties of Zn(salphen)s to create catalytic materials that can be applied in the cycloaddition reaction of carbon dioxide to epoxides giving cyclic carbonates as product. The self-assembly properties have been investigated in detail using UV-Vis spectroscopy, and recycling studies demonstrate that supramolecular aggregation of the catalyst after the reaction may be an attractive new way of creating separation potential.

6.2 Results and discussion

Synthesis: The synthesis of triptycene salphen complexes **1-7** (Scheme 1) was achieved using the previously reported reagent 2,3,6,7,14,15-hexaammoniumtrypticene hexachloride **A**,^[15] and combining this with an appropriate salicylaldehyde and $M(OAc)_2 \cdot nH_2O$ ($M = Zn, n = 2$; $M = Ni, n = 4$) under refluxing conditions (see Experimental section). In general this afforded, after work up, the trinuclear triptycene salphen complexes in isolated yields in the range 40–65% except for **6** (14%). The identity of **1-7** was easily deduced from the 1H NMR and MALDI(+) MS spectra. The D_{3h} symmetry pertaining to these complexes provides simple resonance patterns with a single peak for the CH=N and (Ar)CH_{trip} (*trip* = triptycene) groups. Whereas complexes **1, 2, 5** and **6** are reasonably soluble under relatively apolar conditions (acetone, chloroform), trinuclear derivatives **3, 4** and **7** required a much more polar solvent for NMR analysis (DMSO). Mononuclear Zn(salphen) complex **8** was prepared by combining *ortho*-phenylenediamine and 3-phenyl-salicylaldehyde^[16] in the presence of $Zn(OAc)_2 \cdot 2H_2O$ (92% yield); complex **8** was used as a model compound for the self-assembly studies which are discussed below. The dinuclear complexes **9** and **10** were obtained using similar procedures starting from commercially available polyamine precursors **B** and **C** (see Experimental section).



Scheme 1. Synthesis of trinuclear triptycene complexes **1-7** and schematic structure of mono- and dinuclear reference compounds **8-10**.

Solid state analyses: The X-ray structures for trinuclear complexes **1** and **2**, mononuclear **8** and dinuclear **9** were determined (see Figures 2–5). The molecular structure **2** (Fig. 2) confirms the proposed connectivity pattern with the three metallosalphenes connected through a pseudo “bicycle[2.2.2]octane” unit resulting in a paddlewheel structure. Bond lengths and distances fall within the range to be expected for Ni(II) and Zn(II) based salphen complexes.^[17] The structures determined for **8** (Figures 3 and 4) show that both dimeric as well as monomeric complexes can be obtained depending on the crystallization conditions. Under relative apolar conditions (i.e. a combination of CH₃N and CHCl₃), a dimeric structure is obtained (Fig. 3) that is the result of the well-known μ_2 -phenoxy-bridging capability of Zn(salens) if appropriately functionalized at the *ortho* positions with *small* substituents.^[10a+b,11-13] In the present example, both Zn(salphen) monomers are twisted such that a perpendicular mutual arrangement is obtained, and the structure is further stabilized by pi-stacking interactions between several aromatic groups of

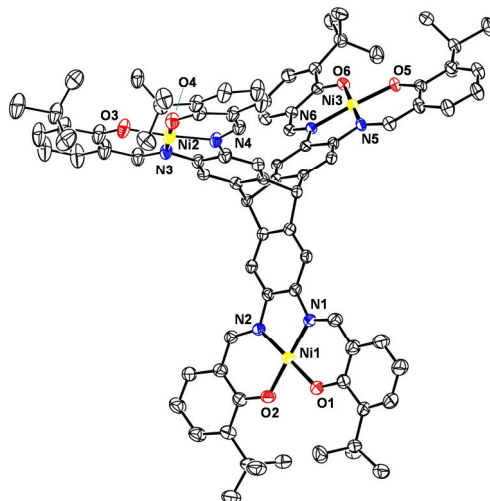


Figure 2. Molecular structure determined for Ni_3 triptycene complex **2**. H-atoms, co-crystallized solvent molecules, some disorder and most of the atom-numbering scheme are omitted for clarity. Selected bond lengths (\AA) and angles ($^\circ$): $Ni(1)-O(1) = 1.841(2)$, $Ni(1)-O(2) = 1.847(2)$, $Ni(1)-N(1) = 1.851(3)$, $Ni(1)-N(2) = 1.853(3)$; $O(1)-Ni(1)-O(2) = 85.64(10)$, $O(1)-Ni(1)-N(1) = 94.37(11)$, $O(1)-Ni(1)-N(2) = 178.12(12)$, $O(2)-Ni(1)-N(1) = 178.33(11)$, $O(2)-Ni(1)-N(2) = 94.35(11)$, $N(1)-Ni(1)-N(2) = 85.69(11)$.

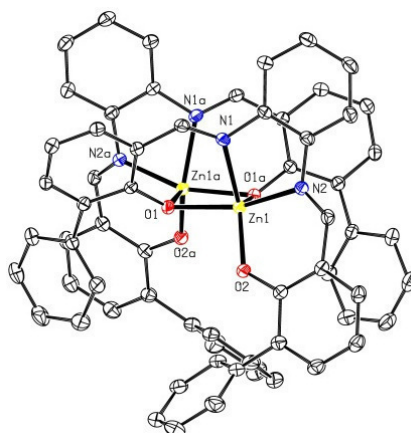


Figure 3. Molecular structure determined for dimeric **8**. H-atoms, co-crystallized solvent molecules, some disorder and most of the atom-numbering scheme are omitted for clarity. Selected bond lengths (\AA) and angles ($^\circ$): $Zn(1)-O(1) = 2.1044(11)$, $Zn(1)-O(2) = 1.9237(12)$, $Zn(1)-O(1a) = 2.0259(12)$, $Zn(1)-N(1) = 2.0887(14)$, $Zn(1)-N(2) = 2.0838(14)$; $O(1)-Zn(1)-O(2) = 99.65(5)$, $O(1)-Zn(1)-O(1a) = 83.73(5)$, $O(1a)-Zn(1)-O(2) = 119.03(5)$, $N(1)-Zn(1)-N(2) = 77.26(5)$, $N(1)-Zn(1)-O(1) = 84.46(5)$, $N(1)-Zn(1)-O(1a) = 104.08(5)$, $N(1)-Zn(1)-O(2) = 136.88(5)$, $N(2)-Zn(1)-O(1) = 161.10(5)$, $N(2)-Zn(1)-O(1a) = 105.18(5)$, $N(2)-Zn(1)-O(2) = 90.62(5)$; $O(1)-Zn(1a)-O(1a)-Zn(1) = -5.49(6)$.

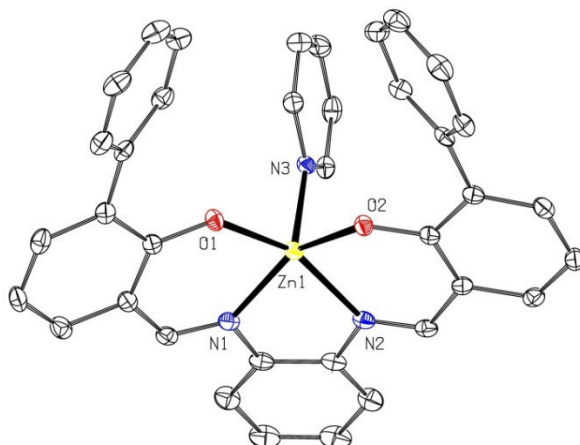


Figure 4. Molecular structure determined for mononuclear **8**-pyridine. H-atoms, co-crystallized solvent molecules, some disorder and most of the atom-numbering scheme are omitted for clarity. Selected bond lengths (Å) and angles (°): Zn(1)-O(1) = 1.9857(14), Zn(1)-O(2) = 1.9747(14), Zn(1)-N(1) = 2.0808(17), Zn(1)-N(2) = 2.1046(17), Zn(1)-N(3) = 2.0959(18); N(1)-Zn(1)-N(2) = 77.70(7), O(1)-Zn(1)-O(2) = 94.65(6), O(1)-Zn(1)-N(2) = 157.53(6), O(1)-Zn(1)-N(3) = 100.41(6), N(1)-Zn(1)-O(2) = 152.15(7), N(1)-Zn(1)-N(3) = 109.27(7).

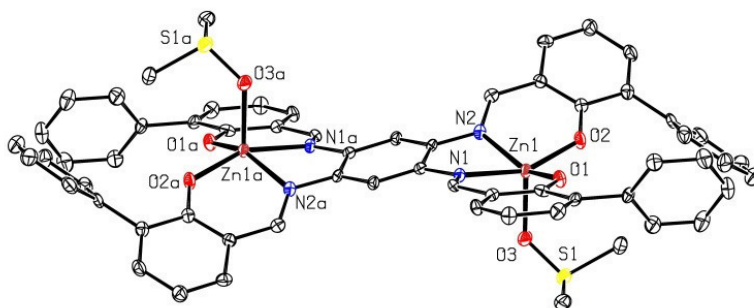


Figure 5. Molecular structure for dinuclear complex **9**. H-atoms, co-crystallized solvent molecules, some disorder and most of the atom-numbering scheme are omitted for clarity. Selected bond lengths (Å) and angles (°): Zn(1)-O(1) = 1.971(3), Zn(1)-O(2) = 1.975(3), Zn(1)-N(1) = 2.092(3), Zn(1)-N(2) = 2.103(3), Zn(1)-O(3) = 2.040(3); O(1)-Zn(1)-O(2) = 96.39(11), O(1)-Zn(1)-O(3) = 102.48(12), O(1)-Zn(1)-N(1) = 90.26(12), O(1)-Zn(1)-N(2) = 151.27(13), N(1)-Zn(1)-N(2) = 77.14, N(1)-Zn(1)-O(3) = 96.73(12).

both Zn(salphen) units. The dihedral angle O(1)-Zn(1a)-O(1a)-Zn(1) is -5.49° and closely resembles those found for similar Zn(salphen) dimeric assemblies.^[12] In the presence of pyridine, complex **8** crystallizes as a mononuclear complex as the expected pyridine adduct showing that both assembled and deaggregated forms of **8** can be easily accessed. Finally, the structure for **9**

shows (as can be expected) a monomeric dinuclear species with two molecules of the crystallization medium coordinating to the Zn(II) centers. The presence of strongly coordinating ligands is a prerequisite as apolar conditions favour aggregated species as observed in the solution phase (vide infra).

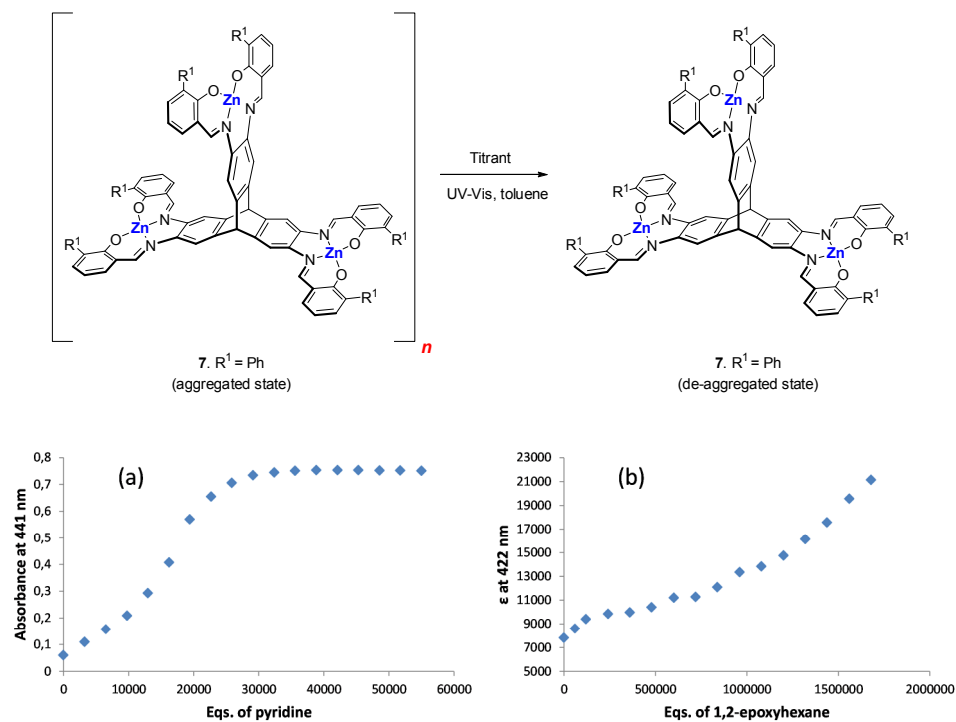


Figure 6. Representative examples of competitive UV-Vis titrations for complex **7** in dry toluene. (a) Titration with pyridine with $[7] = 0.96 \times 10^{-5} \text{ M}$; (b) Titration with 1,2-epoxyhexane with $[7] = 0.35 \times 10^{-5}$.

Self-assembly in solution: In order to assess the solution phase self-assembly, UV-Vis titrations of trinuclear complexes **1**, **6** and **7**, mononuclear **8** and dinuclear **9** and **10** with pyridine (a competitive ligand) in toluene were carried out.^[18] First, the titration of mononuclear complex **8** is considered: the titration curve for complex **8** shows similar behavior as previously observed when a Zn(salphen) complex with 5-*tert*-butyl groups was titrated under comparable conditions. In the present case, both the dimer (**8**)₂, the monomer **8** and the coordination complex **8**-pyridine were considered in the model describing the self-assembly process for complex **8** (see the Experimental Section). Fitting the titration curve for **8** using this assembly model based on three colored species (complex **8**, pyridine-ligated complex **8**-pyr, and dimeric species (**8**)₂) gave the dimerization constant (K_{dim}) $7.4 \times 10^8 \text{ M}^{-1}$. This very high stability for dimeric **8** shows that

multinuclear Zn(salphen)s equipped with *ortho* phenyl substituents should almost certainly result in strongly aggregated species. In order to investigate this hypothesis further, multinuclear complexes **1**, **6**, **7**, **9** and **10** were also titrated under comparable conditions with pyridine (see Table 1 and Fig. 6 for the results with complex **7**). The amount of pyridine needed to fully dissociate the aggregated species was extrapolated from the titration data giving a clear indication of the relative stability within the series of investigated compounds. As can be clearly seen, the highest amount of pyridine titrant needed (~ 30.000 equiv) was observed in the titration of triptycene Zn₃ complex **7**, with dinuclear Zn₂ complex **9** showing slightly lower but similar order-of-magnitude stability. The relatively high stability of assembled **9** is in line with our earlier observations for dinuclear Zn(salphen)s that were based on the same ligand skeleton but with different *ortho* substituents.^[10b] In these previous cases up to 500.000 equiv of pyridine titrant were required for complete dissociation to occur, and the current results for dinuclear **9** help to assess the influence of *ortho* phenyl groups on the strength of the assembled state.

Table 1. Titration studies performed with complexes **1** and **6-10** using pyridine or 1,2-epoxyhexane (1,2-EH) as titrant.^a

Entry	Complex	Titrant	Eq(min) ^b	Eq/Zn ^c
1	1	pyridine	20	7
2	8	pyridine	15	7.5
3	6	pyridine	120	40
4	10	pyridine	1.700	850
5	9	pyridine	18.000	9.000
6	7	pyridine	29.000	14.500
7	8	1,2-EH	800	800
8	10	1,2-EH	4.000	2.000
9	9	1,2-EH	300.000	150.000
10	7	1,2-EH	>1.000.000	>500.000

^a Conditions: dry toluene at an approximate 10⁻⁵ M in complex. ^b Eq(min) designates the extrapolated amount of titrant needed to fully disaggregate the assembled complex. ^c Normalized amount of pyridine needed per Zn(salphen) unit.

Although less titrant is needed to deaggregate **9** under apolar conditions, also for this dinuclear complex an appreciably high stability is still noted. After establishing that trinuclear complex **7** shows the highest tendency to form strongly aggregated species in solution, we were interested

in the effect of the addition of an epoxide (1,2-epoxyhexane) to a nonpolar solution of **7**. In order to be successful in catalysis, the aggregated state of **7** obviously needs to be reduced. UV-Vis titrations with 1,2-epoxyhexane were carried in toluene using complexes **7-10**. The titration curve for mononuclear **8** demonstrates that addition of around 800 eq (Table 1, entry 7) of the epoxide is sufficient to fully deaggregate dimeric **8** and catalysis carried out under neat conditions (*i.e.*, in the pure epoxide) should favour maximum reactivity. Under these conditions, it is likely that the epoxide substrate coordinates to the Zn metal centers as has recently been described as the onset of the catalytic conversion.^[19,20] The results obtained for multinuclear derivatives **7**, **9** and **10** (Table 1, entries 8-10) showed an increase in the amount of titrant to reach full disruption of the assembled species. For trinuclear **7** (which shows the strongest self-association) the indicated amount of 1,2-epoxyhexane requires potential catalysis operations to be carried out under neat conditions, *i.e.* using the epoxide both as solvent and reactant.

Catalysis studies: Complex **7** was thus carried out in neat epoxide and a nucleophile (NBu₄I) was further added to mediate ring-opening of the coordinated epoxide species. The catalytic performance of binary system **7**/ NBu₄I was compared against both mononuclear complex **8** and NBu₄I alone (see Table 2, entries 1 and 2). Although the use of complex **8** gives a higher yield compared with **7** (entry 1 versus 3), the mass recovery (64% versus 85%) was much lower indicating that recycling of mononuclear **8** is less favoured. In order to investigate the recycling potential of **7** in more detail six consecutive runs were carried out isolating after each run the binary catalyst system by precipitation from cold Et₂O (see Experimental Section), and using it as such in a subsequent run (entries 3-8). We noted that the catalyst mass recovery (85–91%) was more or less the same after each cycle; since the most soluble component (NBu₄I) is likely to be lost after each cycle, the mass difference after the second and fourth run (entries 4 and 6) was compensated with extra added NBu₄I to regain maximum activity. Interestingly, this addition indeed increased the yield in the subsequent cycle close to the value observed after the first cycle (isolated yield 72%). However, a closer inspection of the isolated catalyst after the sixth run by ¹H NMR showed that the mixture contained an excess of NBu₄-containing species. Further work-up of the isolated catalyst mixture by trituration with MeOH (in which **7** is insoluble) afforded only 50% of the original amount of complex **7**. This means that in each run an average of 8–9% of complex **7** is lost, and the recycling thereof under these conditions is far from ideal.^[21] The re-activation of the binary catalyst system is probably the result of the addition of more co-catalyst (NBu₄I) which itself shows reasonable activity under these conditions (entry 2).

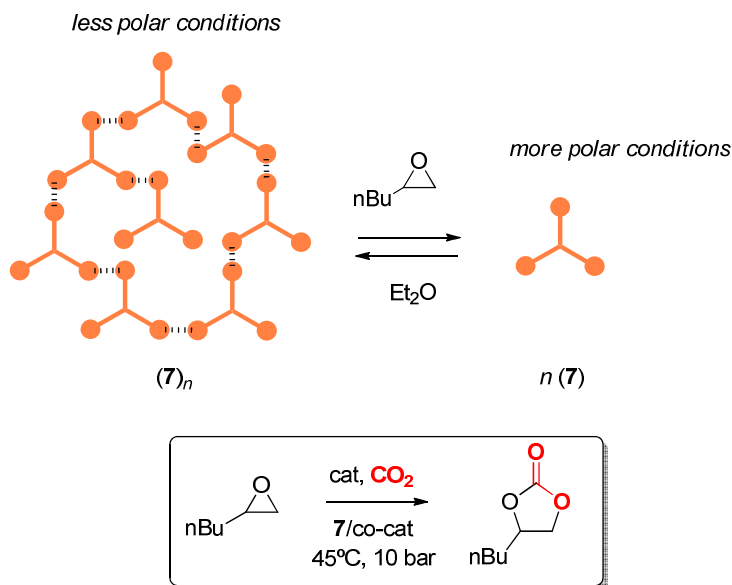


Table 2. Cycloaddition of CO_2 to 1,2-epoxyhexane catalyzed by trinuclear complex **7** and different nucleophiles.^a

Entry	Cat.	Run	Yield (%) ^b	Sel. (%) ^c	Rec. Mass (%) ^d
1	8	–	97	>99%	64
2	– ^e	–	32	>99%	–
3	7	1	72	>99%	85
4	7	2	52	>99%	91
5	7	3	71	>99%	90
6	7	4	63	>99%	84
7	7	5	72	>99%	89
8	7	6	62	>99%	85
9	– ^f	–	<1	–	–
10 ^g	7	1	54	>99%	98
11 ^g	7	2	48	>99%	91
12 ^g	7	3	45	>99%	99
13 ^g	7	4	43	>99%	99

^a Reaction conditions: no solvent, 1.0 g of 1,2-epoxyhexane, 1.25 mol% NBu_4I , 1.25 mol% $[\text{Zn}]$ in all cases, 45°C, 10 bar initial pressure, 18 h. ^b Isolated of the carbonate product. ^c Selectivity toward the carbonate product as determined by $^1\text{H NMR}$ (CDCl_3). ^d Percentage recovered mass after each reaction. ^e Only 1.25 mol% NBu_4I was used. ^f Only 1.25 mol% KI was used. ^g KI used as co-catalyst instead of NBu_4I .

The loss of catalyst mass may be rationalized by the interaction of the co-catalyst NBu_4I with Zn_3 complex **7** by reversible anion coordination to the Zn centers, a feature that was previously described by us.^[22] Thus, the co-catalyst apparently provides higher solubility of the Zn_3 triptycene complex **7** during the product extraction procedure after catalysis, and the structure of the cation (here NBu_4) could be crucial. Therefore, another co-catalyst was probed (KI, Table 2, entries 9–13) to increase the recycling potential of the catalyst couple **7**/KI. First the co-catalyst (KI) activity was determined (entry 9) showing only a trace amount of the product after work up. The combination of KI with **7** provided, however, a more efficient system giving 54% isolated yield of the carbonate product (entry 10). Although this yield is lower than the one reported for the binary system **7**/ NBu_4I (72%, entry 3)^[23] a much better catalyst recovery (99%) could be achieved. The subsequent cycles (entries 11–13) showed that the carbonate yield dropped slightly though catalyst recycling proved to be efficient. These latter results demonstrate that the co-catalyst is indeed a decisive parameter in the recycling procedure. Finally, the isolated catalyst after the fourth run (entry 13) was analysed by ^1H NMR and showed that no observable decomposition had taken place.

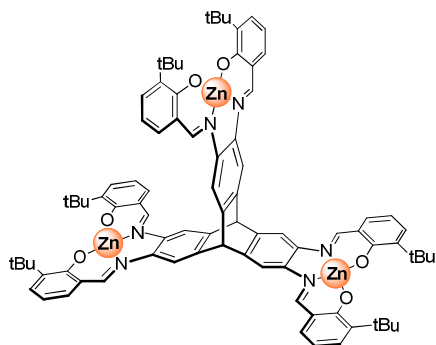
6.3 Conclusions

In summary, we have reported on a series of triptycene based trinuclear salphen derivatives with different peripheral groups that determine the self-assembly brought about by dimerization of the $\text{Zn}(\text{salphen})$ fragments. The spectroscopic studies have shown that phenyl-derived Zn_3 triptycenes show appreciable self-aggregation which can be reversed by the addition of a competitive ligand (pyridine) or a suitable substrate (1,2-epoxyhexane). Application of complex **7** in organic carbonate formation has revealed that reversible supramolecular aggregation can be made an efficient recycling strategy in homogeneous catalysis and the recycling properties also depend on the co-catalyst structure.

6.4 Experimental section

General comments: All salicylaldehyde reagents and 1,2-epoxyhexane were commercially purchased and were used as received. The hexamine reagent 2,3,6,7,14,15-hexammoniumtrypticene hexachloride was prepared according to a previously reported procedure.^[15] NMR spectra were recorded on a Bruker AV-400 or AV-500 spectrometer and referenced to the residual deuterated solvent signals. Elemental analysis was performed by the Unidad de Análisis Elemental at the University of Santiago de Compostela (Spain). Mass

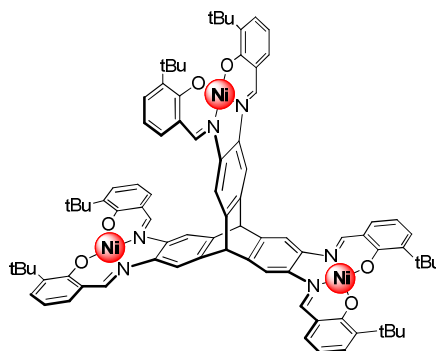
spectrometric analysis and X-ray diffraction studies were performed by the Research Support Area at the ICIQ.



Synthesis of trinuclear Zn₃ complex (1): In a round bottom flask 2,3,6,7,14,15-hexaammoniumtrypticene hexachloride (50 mg, 0.072 mmol), 3-*tert*-butyl-salicylaldehyde (98 mg, 0.55 mmol) and Zn(OAc)₂·2H₂O (46 mg, 0.21 mmol) were dissolved in a mixture of ethanol (6 mL) and DMSO (3 mL). The mixture was heated for 30 min at 90°C. After the mixture had cooled to rt, the yellow precipitate

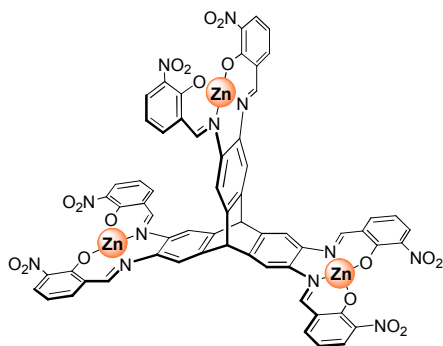
was collected on a sintered glass funnel and dried in vacuo stream to obtain trinuclear complex **1** as a yellow solid. Yield: 54.3 mg (41%). Crystals suitable for X-ray diffraction were obtained from MeOH. ¹H NMR (500 MHz, DMSO-*d*₆): δ = 9.01 (s, 6H, CH=N), 8.12 (s, 6H, ArH), 7.28 (d, ⁴*J* = 1.7 Hz, ³*J* = 8.1 Hz, 6H, ArH), 7.21 (d, ⁴*J* = 1.9 Hz, ³*J* = 7.3 Hz, 6H, ArH), 6.46 (t, ⁴*J* = 7.8 Hz, 6H, ArH), 5.86 (s, 2H, ArH), 1.45 (s, 54H, C(CH₃)₃); Compound too insoluble for a ¹³C NMR measurement; UV/vis (DMF): λ_{max} (log ε) = 305 nm (5.1), 426 nm (5.2); MS (MALDI+, DCTB): *m/z* = 1494.5 [M]⁺ (calcd. 1494.4); Anal. calcd. for C₈₆H₈₆N₆O₆Zn₃·3DMF·7H₂O: C 61.97, H 6.62, N 6.85; found: C 61.65, H 5.97, N 6.93. The presence of three molecules of DMF was supported by ¹H NMR analysis of the isolated and dried product.

Synthesis of trinuclear Ni₃ complex (2): In a round bottom flask 2,3,6,7,14,15-hexaammoniumtrypticene hexachloride (50 mg, 0.072 mmol), 3-*tert*-butyl-salicylaldehyde (98 mg, 0.55 mmol) and Ni(OAc)₂·4H₂O (70 mg, 0.28 mmol) were suspended in DMF (6 mL) and the mixture heated for 1 h at 90°C. After the mixture had cooled to rt a wine-red precipitate was collected by filtration and dried in vacuo.



Yield: 42 mg (40 %). Crystals suitable for X-ray diffraction were obtained from DMSO. ¹H NMR (500 MHz, CDCl₃): δ = 8.20 (s, 6H, CH=N), 7.80 (s, 6H, ArH), 7.34 (d, ⁴*J* = 1.4 Hz, ³*J* = 7.3 Hz, 6H,

ArH), 7.21 (d, $^4J = 1.5$ Hz, $^3J = 8.1$ Hz, 6H, ArH), 6.34 (t, $^3J = 7.6$ Hz, 6H, ArH), 5.54 (s, 2H, ArH), 1.46 (s, 54H, C(CH₃)₃); Compound too insoluble for a ^{13}C NMR measurement; UV-vis (DMF): λ_{max} (log ϵ) = 383 nm (4.5), 398 nm (sh, 4.4), 484 nm (4.1); MS (MALDI+, DCTB): $m/z = 1474.3$ [M]⁺ (calcd. 1474.4); HRMS (MALDI+): $m/z = 1472.4520$ [M]⁺ (calcd. 1472.4664).



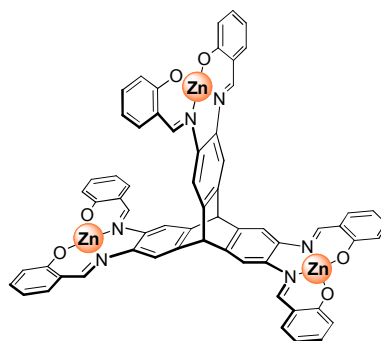
Synthesis of trinuclear Zn₃ complex (3):

2,3,6,7,14,15-Hexaammoniumtrypticene hexachloride (50 mg, 0.072 mmol), 3-nitrosalicylaldehyde (92 mg, 0.55 mmol) and Zn(OAc)₂·2H₂O (46 mg, 0.21 mmol) were dissolved in ethanol/DMSO (12 mL, 1:1 v/v). After 68 h, a wine-red precipitate was collected by filtration and dried in vacuo to

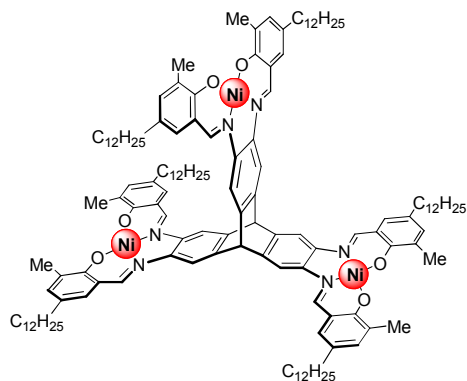
give **3** as an orange solid. Yield: 66 mg (52%). ^1H NMR (500 MHz, DMSO-*d*₆): $\delta = 9.04$ (s, 6H, CH=N), 8.13 (s, 6H, ArH), 7.84 (d, $^4J = 2.0$ Hz, $^3J = 7.8$ Hz, 6H, ArH), 7.72 (d, $^4J = 2.0$ Hz, $^3J = 8.1$ Hz, 6H, ArH), 6.63 (t, $^3J = 7.8$ Hz, 6H, ArH), 5.89 (s, 2H, ArH); $^{13}\text{C}\{^1\text{H}\}$ NMR (500 MHz, DMSO-*d*₆): $\delta = 163.60, 162.51, 143.90, 141.62, 137.52, 129.85, 123.72, 113.34, 111.78, 40.87$; UV-vis (DMF): λ_{max} (log ϵ) = 289 nm (4.8), 421 nm (4.9); MS (MALDI+, DCTB): $m/z = 1429.2$ [M]⁺ (calcd. 1429.1); HRMS (MALDI+): $m/z = 1425.0022$ [M+H]⁺ (calcd. 1424.9905).

Synthesis of trinuclear Zn₃ complex (4):

2,3,6,7,14,15-Hexaammoniumtrypticene hexachloride (50 mg, 0.072 mmol), salicylaldehyde (67 mg, 0.55 mmol) and Zn(OAc)₂·2H₂O (47 mg, 0.21 mmol) were dissolved in ethanol/DMSO (9 mL, 2:1 v/v) and some drops of NEt₃ were added. After stirring for 18 h stirring, a precipitate was collected by filtration and dried in vacuo to yield **4** as an



orange solid. Yield: 31 mg (48%). ^1H NMR (500 MHz, DMSO-*d*₆): $\delta = 8.99$ (s, 6H, CH=N), 8.10 (s, 6H, ArH), 7.40 (d, $^4J = 1.8$ Hz, $^3J = 8.1$ Hz, 6H, ArH), 7.22-7.25 (m, 6H, ArH), 6.69 (d, $^3J = 8.6$ Hz, 6H, ArH), 6.53 (t, $^3J = 7.3$ Hz, 6H, ArH), 5.87 (s, 2H, ArH); $^{13}\text{C}\{^1\text{H}\}$ NMR (125 MHz, DMSO-*d*₆): $\delta = 172.67, 162.65, 143.29, 137.42, 136.60, 134.78, 123.55, 119.97, 113.57, 112.62, 46.3$; UV-vis (DMF): λ_{max} (log ϵ) = 301 nm (4.9), 416 nm (5.0); MS (MALDI+, DCTB): $m/z = 1159.4$ [M]⁺ (calcd. 1158.1); HRMS (MALDI+): $m/z = 1154.0722$ [M]⁺ (calcd. 1154.0982).

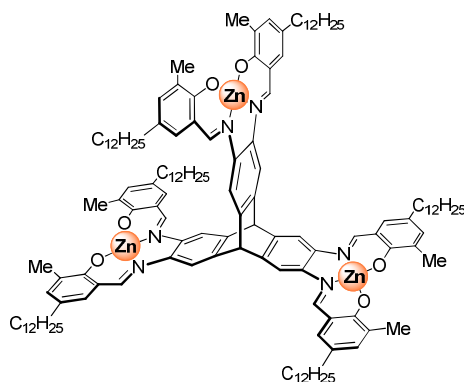
**Synthesis of trinuclear Ni₃ complex (5):**

2,3,6,7,14,15-Hexaammoniumtrypticene hexachloride (15 mg, 0.027 mmol), 5-dodecyl-3-methyl-salicylaldehyde (50 mg, 0.17 mmol) and Ni(OAc)₂·4H₂O (21 mg, 0.084 mmol) were suspended in chloroform/methanol (9 mL, 2:1 v/v) and some drops of NEt₃ were added to the mixture. The reaction mixture was kept at

reflux temperature for 18 h. After the mixture had cooled to rt, a wine-red precipitate was collected by filtration and dried in vacuo to give **5** as a wine-red solid. (8.5 mg, 14%). ¹H NMR (500 MHz, chloroform-d₁): δ = 8.16 (s, 6H, CH=N), 7.76 (s, 6H, ArH), 7.08 (s, 6H, ArH), 6.94 (s, 6H, ArH), 5.49 (s, 2H, ArH), 2.30 (s, 18H, ArCH₃), 1.57-1.60 (m, 12H, ArCH₂-), 1.29-1.34 (m, 120H, dodecyl-H), 0.88-0.91(m, 18H, dodecyl CH₃); Compound too insoluble for a ¹³C NMR measurement; UV-vis (DMF): λ_{max} (log ε) = 387 nm (4.9), 407 nm (sh, 4.8), 497 nm (4.5); MS (MALDI+, DCTB): m/z = 2233.2 [M]⁺ (calcd. 2233.3); HRMS (MALDI+): m/z = 2229.3115 [M]⁺ (calcd. 2229.2353).

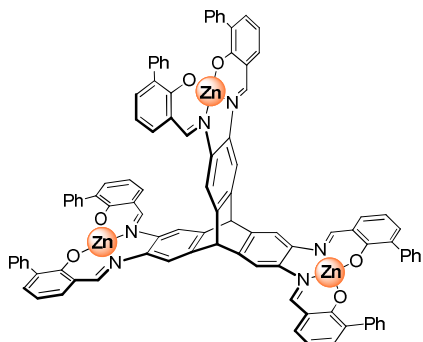
Synthesis of trinuclear Zn₃ complex (6):

2,3,6,7,14,15-Hexaammoniumtrypticene hexachloride (15 mg, 0.027 mmol), 5-dodecyl-3-methyl-salicylaldehyde (52 mg, 0.18 mmol) and Zn(OAc)₂·2H₂O (19 mg, 0.086 mmol) were suspended in chloroform/methanol (9 mL, 2:1 v/v) and some drops of NEt₃ were added to the mixture. The reaction mixture was kept at



reflux temperature for 18 h. After the mixture had cooled to rt, the orange precipitate was collected by filtration and dried in vacuo to give **6** as an orange solid. Yield: 36.9 mg (65%). ¹H NMR (500 MHz, acetone-d₆): δ = 8.85 (s, 6H, CH=N), 7.95 (s, 6H, ArH), 7.04 (s, 6H, ArH), 7.00 (s, 6H, ArH), 5.80 (s, 2H, ArH), 2.20 (s, 18H, ArCH₃), 1.59-1.64 (m, 12H, ArCH₂-), 1.30-1.36 (m, 120H, dodecyl-H), 0.87 (*pseudo t*, ³J = 6.7 Hz, 18H, dodecyl CH₃); Compound too insoluble for a ¹³C NMR measurement; UV-vis (DMF): λ_{max} (log ε) = 308 nm (4.8), 428 nm (4.8); MS (MALDI+, DCTB):

$m/z = 2252.4$ $[M]^+$ (calcd. 2252.9); Anal. calcd. for $C_{140}H_{194}N_6O_6Zn_3 \cdot 3H_2O$: C 72.88, H 8.74, N 3.64; found: C 72.50, H 8.37, N 3.63.

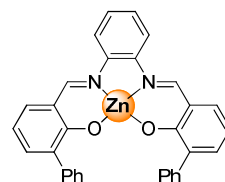


Synthesis of trinuclear Zn_3 complex (7):

2,3,6,7,14,15-Hexaammoniumtrypticene hexachloride (101 mg, 0.179 mmol), 3-phenylsalicylaldehyde (264 mg, 1.33 mmol) and $Zn(OAc)_2 \cdot 2H_2O$ (194 mg, 0.88 mmol) were suspended in ethanol/DMF (30 mL, 2:1 v/v) and the mixture was kept at reflux temperature for 18 h. After the mixture had cooled to rt an orange precipitate was collected by filtration and dried in vacuo to give **7** as a yellow solid. Yield: 151 mg (52%).

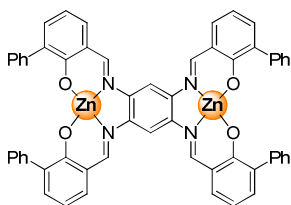
1H NMR (500 MHz, $DMSO-d_6$): $\delta = 9.03$ (s, 6H, CH=N), 8.10 (s, 6H, ArH), 7.67-7.69 (m, 12H, ArH), 7.43 (d, $^4J = 1.8$ Hz, $^3J = 8.21$ Hz, 6H, ArH), 7.38 (d, $^4J = 1.8$ Hz, $^3J = 7.0$ Hz, 6H, ArH), 7.21-7.25 (m, 18H, ArH), 6.63 (t, $^3J = 7.6$ Hz, 6H, ArH), 5.91 (s, 2H, ArH); $^{13}C\{^1H\}$ NMR (500 MHz, $DMSO-d_6$): $\delta = 169.90, 163.08, 143.39, 140.32, 137.64, 136.45, 134.98, 133.55, 129.59, 127.98, 126.12, 120.58, 113.69, 112.75, 46.21$; UV-vis (DMF): λ_{max} (log ϵ) = 305 nm (5.0), 427 nm (5.1); MS (MALDI+, DCTB): $m/z = 1614.4$ $[M]^+$ (calcd. 1614.3); Anal. calcd. for $C_{98}H_{62}N_6O_6Zn_3 \cdot DMF \cdot 7H_2O$: calcd. C 66.84, H 4.61, N 5.40; found C 66.75, H 4.00, N 5.56. The presence of about 1 eq of DMF was confirmed by 1H NMR analysis.

Synthesis of mononuclear Zn complex (8): To a solution of 3-phenylsalicylaldehyde (282.5 mg, 1.43 mmol) and *ortho*-phenylenediamine (70.4 mg, 0.651 mmol) in MeOH/THF (60 mL, 1:1 v/v) was added $Zn(OAc)_2 \cdot 2H_2O$ (272.7 mg, 1.24 mmol) dissolved in MeOH (10 mL). The resultant yellow solution was stirred for 18 h after which the reaction mixture was concentra-



ted, and triturated with MeOH to yield a yellow solid after filtration and drying. Yield: 318.5 mg (92%). Crystals suitable for X-ray diffraction were obtained from hot CH_3CN . 1H NMR (400 MHz, $DMSO-d_6$): $\delta = 9.03$ (s, 2H, CH=N), 8.10 (s, 6H, ArH), 7.87-7.91 (m, 2H, ArH), 7.70-7.73 (m, 4H, ArH), 7.38-7.46 (m, 6H, ArH), 7.25-7.28 (m, 6H, ArH), 6.61 (t, $^3J = 7.5$ Hz, 2H, ArH); $^{13}C\{^1H\}$ NMR (100 MHz, $DMSO-d_6$): $\delta = 169.98, 163.74, 140.37, 140.12, 136.59, 135.06, 133.55, 129.64, 128.01, 127.80, 126.14, 120.56, 117.06, 113.59$; MS (ESI+, MeOH): $m/z = 553.0$ $[M+Na]^+$ (calcd.

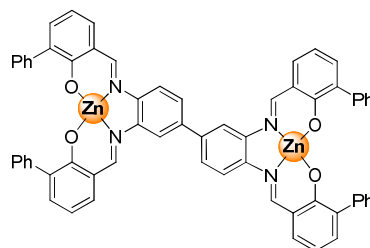
553.09); Anal. calcd. for $C_{32}H_{22}N_2O_2Zn \cdot 1\frac{1}{2} H_2O$: C 68.76, H 4.51, N 5.01; found: C 68.66, H 4.44, N 4.98.



Synthesis of dinuclear Zn complex (9): To a solution of 3-phenyl-salicylaldehyde (563.3 mg, 2.84 mmol) and 1,2,4,5-tetraaminobenzene tetra-hydrochloride (89.2 mg, 0.314 mmol) in DMSO (25 mL) was added a solution of $Zn(OAc_2) \cdot 2H_2O$ (326.1 mg, 1.49 mmol) dissolved in MeOH (8 mL). The resultant deep red

solution was stirred for 4 h after which the reaction mixture was diluted with MeOH (60 mL). After 18 h the mixture was gravity-filtered and the residue washed with MeOH (30 mL) to give a red solid. Yield: 151.9 mg (0.154 mmol, 49%). Crystals suitable for X-ray diffraction were obtained from DMSO. 1H NMR (400 MHz, DMSO- d_6): δ = 9.21 (s, 4H, CH=N), 8.35 (s, 2H, ArH), 7.73-7.75 (m, 8H, ArH), 7.50 (d, 3J = 7.9 Hz, 4J = 1.8 Hz, 4H, ArH), 7.43 (d, 3J = 7.2 Hz, 4J = 1.9 Hz, 4H, ArH), 7.26-7.29 (m, 12H, ArH), 6.68 (t, 3J = 7.5 Hz, 4H, ArH); The complex is too insoluble for a ^{13}C NMR analysis; UV-vis (toluene): λ_{max} (log ϵ) = 330 nm (4.4), 476 nm (4.5); MS (MALDI+, DCTB): m/z = 986.4 $[M]^+$ (calcd. 986.1); Anal. calcd. for $C_{58}H_{38}N_4O_4Zn_2 \cdot 2\frac{1}{2}H_2O \cdot \frac{1}{2}DMSO$: C 66.24, H 4.33, N 5.24, S 1.50; found: C 66.13, H 4.45, N 5.25, S 1.11. The presence of $\frac{1}{2}$ equiv of DMSO was supported by 1H NMR analysis of the dried sample.

Synthesis of dinuclear Zn complex (10): To a solution of 3-phenyl-salicylaldehyde (696.2 mg, 3.51 mmol) and 3,3'-diaminobenzidine (77.1 mg, 0.360 mmol) in DMSO (20 mL) was added a solution of $Zn(OAc_2) \cdot 2H_2O$ (382.2 mg, 1.74 mmol) dissolved in MeOH (8 mL).

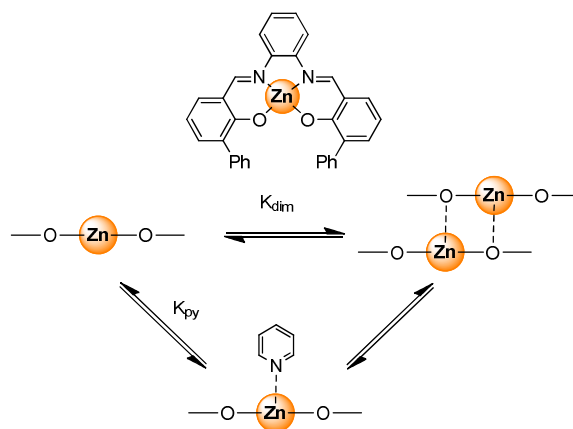


The resultant deep orange solution was stirred for 2 h after which the reaction mixture was diluted with MeOH (60 mL). Filtration of this mixture afforded an orange solid which was recrystallized from DMSO/MeOH. Yield: 355.1 mg (0.334 mmol, 93%). 1H NMR (400 MHz, DMSO- d_6): δ = 9.27 (s, 2H, CH=N), 9.12 (s, 2H, CH=N), 8.32 (s, 2H, ArH), 8.03 (d, 3J = 8.8 Hz, 2H, ArH), 7.91 (d, 3J = 8.5 Hz, 2H, ArH), 7.72-7.74 (m, 8H, ArH), 7.54 (d, 3J = 8.0 Hz, 4J = 1.9 Hz, 2H, ArH), 7.49 (d, 3J = 8.0 Hz, 4J = 1.8 Hz, 2H, ArH), 7.40-7.43 (m, 4H, ArH), 7.27-7.29 (m, 12H, ArH), 6.63-6.68 (m, 4H, ArH); $^{13}C\{^1H\}$ NMR (100 MHz, DMSO-

d_6): δ = 169.77, 169.75, 163.97, 163.06, 140.18, 140.01, 139.22, 138.46, 136.37, 136.24, 134.82, 133.25, 133.24, 129.28, 127.68, 125.86, 125.81, 120.31, 120.28, 117.11, 114.82, 113.35, 113.32; UV-vis (toluene): λ_{\max} (log ϵ) = 326 nm (4.73), 423 nm (4.70); MS (MALDI+, DCTB): m/z = 1062.2 $[M]^+$ (calcd. 1062.4), 2123.4 $(2M)^+$ (calcd. 2123.4); Anal. calcd. for $C_{64}H_{42}N_4O_4Zn_2 \cdot 2\frac{1}{2}DMSO \cdot 2H_2O$: C 64.09, H 4.75, N 4.33, S 6.20; found: C 63.97, H 4.59, N 4.58, S 6.09. The presence of DMSO was supported by 1H NMR analysis of the dried sample.

UV-Vis titrations: Typical procedure: a solution of the host (H) was prepared in dry toluene at an approximate concentration of 1×10^{-5} M. A solution of the guest (G) in the host was prepared to maintain a constant (H) concentration after each addition of the guest. Aliquots of the guest solution were added stepwise to 2.00 mL of the host solution in a 1.00 cm quartz cuvette. After each addition, a UV-Vis spectrum was acquired. The absorbance at the λ_{\max} of the characteristic band of the respective Zn(salphen) near 400 nm was plotted against the amount of guest added.

Determination of the K_{dim} for complex 8: The dimerization constant was determined for **8** by monitoring the disruption of the dimeric complex upon the addition of competitive pyridine using UV-Vis. Upon addition of pyridine, the absorption maximum at $\lambda = 409$ nm increased and a typical red-shift to $\lambda = 424$ nm occurred (see Fig. 7a below). The isosbestic point at $\lambda = 401$ nm suggested the presence of multiple species in solution.



Scheme 2. The involved equilibria; K_{dim} is the stability constant of the dimeric complex and K_{py} denotes the association constant for pyridine binding.

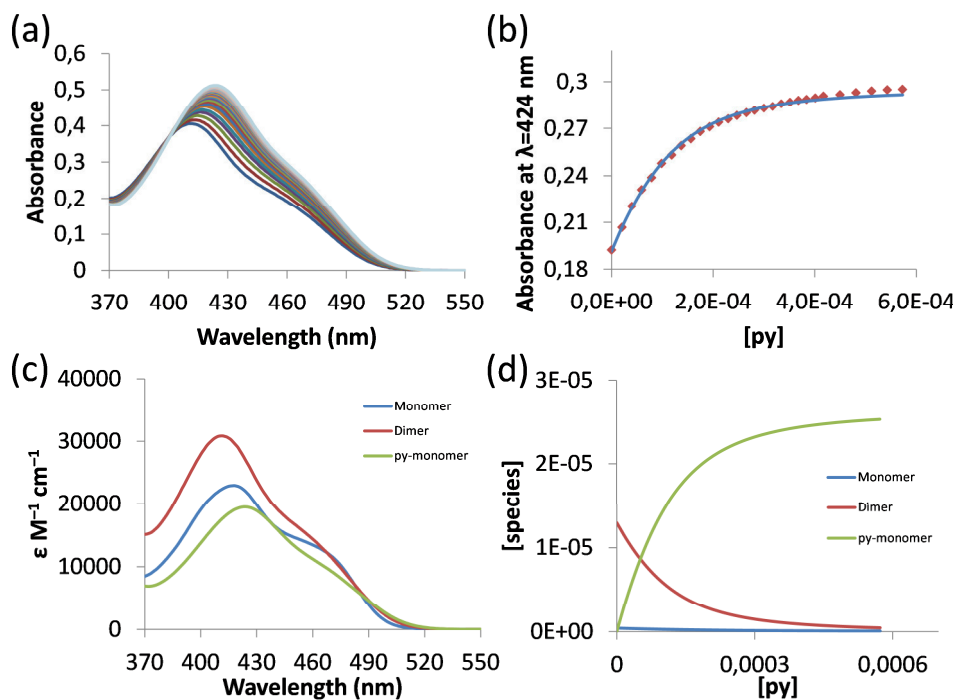


Figure 7: (a) Spectral changes of complex **8** upon the addition of pyridine carried out in toluene at $[\mathbf{8}] = 1 \times 10^{-5}$ M, and (b) the corresponding titration curves and data fits at $\lambda = 424$ nm. (c) Simulated spectra and (d) Simulated concentration profiles for this titration at the specified equilibrium constants.

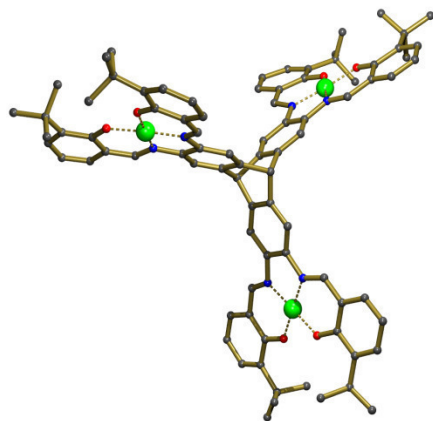
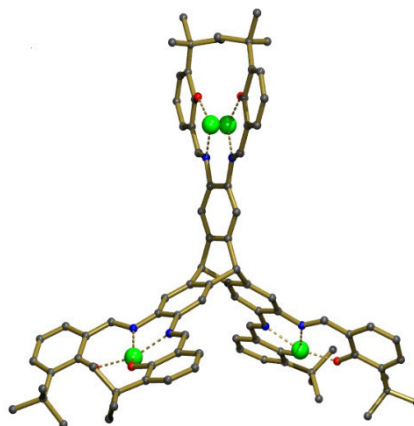
The pyridine titration data for complex **8** was analysed with Specfit/32^[29] considering the binding model shown in Scheme 2, which includes three coloured species (monomer, dimer and the pyridine-coordinated complex). If we assume the value of pyridine association is similar to a Zn(salphen) complex having two *tert*-butyl substituents in the 3-position ($K_{\text{py}} = 5.89 \times 10^5 \text{ M}^{-1}$)^[30] then the dimerization constant K_{dim} is determined at $7.31 (\pm 0.01) \times 10^8 \text{ M}^{-1}$.

X-ray crystallography: General: The measured crystals were stable under atmospheric conditions; nevertheless they were treated under inert conditions and immersed in perfluoropoly-ether as a protecting oil for manipulation. Data collection: Measurements were made on a Bruker-Nonius diffractometer equipped with an APPEX 2 4K CCD area detector, an FR591 rotating anode with MoK α radiation, Montel mirrors and a Kryoflex low temperature device ($T = -173$ °C). Full-sphere data collection was used with ω and ϕ scans. Programs used: Data collection Apex2 V2011.3 (Bruker-Nonius 2008), data reduction Saint + Version 7.60A

(Bruker AXS 2008) and absorption correction SADABS V. 2008-1 (2008). Structure solution: SHELXTL Version 6.10 (Sheldrick, 2000)^[24] was used. Structure refinement: SHELXTL-97-UNIX VERSION. For resolving the structures, SIR2011 was utilized.^[25]

Crystallographic data for Zn₃ complex 1:

C_{90.50}H₁₀₄N₆O_{10.50}Zn₃, $M_r = 1639.91$, orthorhombic, *Pnna*, $a = 27.692(7) \text{ \AA}$, $b = 23.442(6) \text{ \AA}$, $c = 14.633(3) \text{ \AA}$, $\alpha = 90^\circ$, $\beta = 90^\circ$, $\gamma = 90^\circ$, $V = 9499(4) \text{ \AA}^3$, $Z = 4$, $\rho = 1.147 \text{ mg}\cdot\text{M}^{-3}$, $\mu = 0.806 \text{ mm}^{-1}$, $\lambda = 0.71073 \text{ \AA}$, $T = 100(2) \text{ K}$, $F(000) = 3452$, crystal size = $0.20 \times 0.10 \times 0.10 \text{ mm}$, ϑ (min) = 1.57° , ϑ (max) = 25.44° , 7792 reflections collected, 7792 reflections unique ($R_{\text{int}} = 0.0000$), GoF = 0.987, $R_1 = 0.0993$ and $wR_2 = 0.2954$ [$I > 2\sigma(I)$], $R_1 = 0.1864$ and $wR_2 = 0.3151$ (all indices), min/max residual density = $-0.566/1.088 \text{ [e}\cdot\text{\AA}^{-3}]$. Completeness to ϑ (25.44°) = 58.5%. The structure has been deposited at the CCDC with reference number 910862. Notes: the structure shows disorder in one of the Zn atoms. Coordinating and co-crystallized molecules are omitted for clarity. Both PLATON^[26] and Squeeze^[27] were used to model the structure.



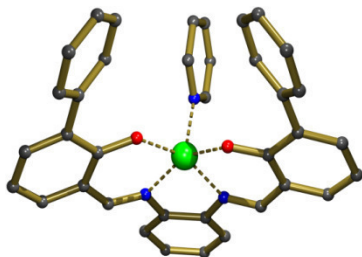
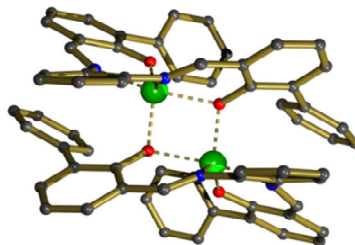
Crystallographic data for Ni₃ complex 2:

C_{92.5}H_{105.5}N₆O_{9.25}Ni₃S_{3.25}, $M_r = 1729.65$, triclinic, *P*-1, $a = 13.2122(4) \text{ \AA}$, $b = 22.0668(7) \text{ \AA}$, $c = 22.7321(8) \text{ \AA}$, $\alpha = 100.0770(10)^\circ$, $\beta = 96.7840(10)^\circ$, $\gamma = 105.8970(10)^\circ$, $V = 6178.5(3) \text{ \AA}^3$, $Z = 2$, $\rho = 0.930 \text{ mg}\cdot\text{M}^{-3}$, $\mu = 0.550 \text{ mm}^{-1}$, $\lambda = 0.71073 \text{ \AA}$, $T = 100(2) \text{ K}$, $F(000) = 1825$, crystal size = $0.25 \times 0.08 \times 0.05 \text{ mm}$, ϑ (min) = 0.92° , ϑ (max) = 25.86° , 72358 reflections collected, 23579 reflections unique ($R_{\text{int}} = 0.0351$), GoF = 1.104, $R_1 = 0.0548$ and $wR_2 = 0.1846$ [$I > 2\sigma(I)$], $R_1 = 0.0780$ and $wR_2 = 0.1951$ (all indices), min/max residual density = $-0.648/2.252 \text{ [e}\cdot\text{\AA}^{-3}]$. Completeness to ϑ (25.86°) = 98.5%. The structure has been deposited at the CCDC with reference number 910865. Notes: the structure

shows disorder in one of the salen units over two positions in a 70:30 occupancy ratio. Both PLATON^[26] and Squeeze^[27] were used to model the structure.

Crystallographic data for dimeric (8)₂:

$C_{67.8}H_{49.6}N_{5.8}O_4Cl_{0.6}Zn_2$, $M_r = 1161.54$,
monoclinic, $C2/c$, $a = 24.9324(18) \text{ \AA}$, $b = 11.9002(9) \text{ \AA}$, $c = 21.784(2) \text{ \AA}$, $\alpha = 90^\circ$, $\beta = 124.409(2)^\circ$, $\gamma = 90^\circ$, $V = 5332.3(8) \text{ \AA}^3$, $Z = 4$, $\rho = 1.447 \text{ mg}\cdot\text{M}^{-3}$, $\mu = 0.989 \text{ mm}^{-1}$, $\lambda = 0.71073 \text{ \AA}$, $T = 100(2) \text{ K}$, $F(000) = 2397$, crystal size = $0.10 \times 0.10 \times 0.04 \text{ mm}$, $\vartheta (\text{min}) = 1.98^\circ$, $\vartheta (\text{max}) = 29.40^\circ$, 52545 reflections collected, 7323 reflections unique ($R_{\text{int}} = 0.0491$), $\text{GoF} = 1.041$, $R_1 = 0.0349$ and $wR_2 = 0.0930$ [$I > 2\sigma(I)$], $R_1 = 0.0427$ and $wR_2 = 0.0972$ (all indices), min/max residual density = $-0.476/0.742$ [$e\cdot\text{\AA}^{-3}$]. Completeness to $\vartheta (29.40^\circ) = 99.7\%$. The structure has been deposited at the CCDC with reference number 910863.



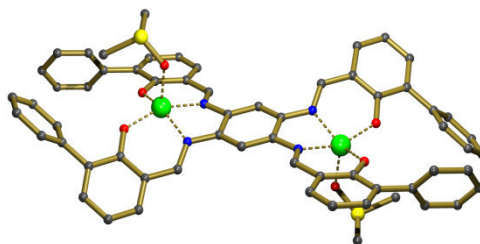
Crystallographic data for mononuclear 8-pyridine:

$C_{37}H_{27}N_3O_2Zn$, $M_r = 610.99$, monoclinic, $P2(1)/n$, $a = 14.0990(9) \text{ \AA}$, $b = 14.7495(9) \text{ \AA}$, $c = 14.5848(9) \text{ \AA}$, $\alpha = 90^\circ$, $\beta = 112.860(2)^\circ$, $\gamma = 90^\circ$, $V = 2794.7(3) \text{ \AA}^3$, $Z = 4$, $\rho = 1.452 \text{ mg}\cdot\text{M}^{-3}$, $\mu = 0.920 \text{ mm}^{-1}$, $\lambda = 0.71073 \text{ \AA}$, $T = 100(2) \text{ K}$, $F(000) = 1264$, crystal size = $0.10 \times 0.10 \times 0.03 \text{ mm}$, $\vartheta (\text{min}) = 2.05^\circ$, $\vartheta (\text{max}) = 30.02^\circ$, 14488

reflections collected, 14657 reflections unique, $\text{GoF} = 1.069$, $R_1 = 0.0502$ and $wR_2 = 0.1269$ [$I > 2\sigma(I)$], $R_1 = 0.0857$ and $wR_2 = 0.1507$ (all indices), min/max residual density = $-0.638/0.488$ [$e\cdot\text{\AA}^{-3}$]. Completeness to $\vartheta (30.02^\circ) = 91.2\%$. The structure has been deposited at the CCDC with reference number 910864. Notes: two crystalline domains (84:16 ratio) were observed and absorption correction was applied using TWINABS.^[28]

Crystallographic data for 9·(DMSO)₂:

C₆₆H₆₂N₄O₈S₄Zn, *M_r* = 1298.18, triclinic, *P*-1,
a = 9.1484(7) Å, *b* = 10.4688(8) Å, *c* =
17.6146(12) Å, α = 98.405(3)°, β =
97.457(4)°, γ = 114.971(3)°, *V* = 1477.98(19)
Å³, *Z* = 1, ρ = 1.459 mg·M⁻³, μ = 1.014 mm⁻¹,
λ = 0.71073 Å, *T* = 100(2) K, *F*(000) =



674, crystal size = 0.10 × 0.02 × 0.01 mm, ϑ (min) = 1.20°, ϑ (max) = 28.21°, 7022 reflections collected, 7022 reflections unique (*R*_{int} = 0.0719), GoF = 1.026, *R*₁ = 0.0589 and *wR*₂ = 0.1227 [*I* > 2σ(*I*)], *R*₁ = 0.1066 and *wR*₂ = 0.1476 (all indices), min/max residual density = -0.700/0.687 [e·Å⁻³]. Completeness to ϑ (28.21°) = 96.5%. The structure has been deposited at the CCDC with reference number 913293. Notes: for the absorption correction, TWINABS was used^[28] as the sample contained two crystalline domains (60:40 ratio).

Catalysis reactions: The catalytic reactions were carried out in neat 1,2-epoxyhexane (1.0 g, 9.98 mmol), NBu₄I (1.25 mol%, 46 mg), 1.25 mol% of complex **7** (61 mg) at 45°C and *p*CO₂⁰ = 10 bar for 18 h. After the reaction, diethyl ether was added (20 mL) and the mixture was cooled to -30°C. After 1 h, the precipitate was filtered off, dried and weighed and used in a subsequent run. The Et₂O extract was concentrated to dryness to afford the pure cyclic carbonate product.

6.5 Notes and references

- [1] For some recent general reviews on this topic: (a) M. J. Wiester, P. A. Ulmann and C. A. Mirkin, *Angew. Chem. Int. Ed.*, 2011, **50**, 114; (b) T. R. Cook, Y.-R. Zheng and P. J. Stang, *Chem. Rev.*, 2013, **113**, 734; (c) M. Yoshizawa, J. K. Klosterman and M. Fujita, *Angew. Chem. Int. Ed.*, 2009, **48**, 3418; (d) D. M. Vriezema, M. Comellas Aragonès, J. A. A. W. Elemans, J. J. L. M. Cornelissen, A. E. Rowan and R. J. M. Nolte, *Chem. Rev.*, 2005, **105**, 1445.
- [2] J. C. Love, L. A. Estroff, J. K. Kriebel, R. G. Nuzzo and G. M. Whitesides, *Chem. Rev.*, 2005, **105**, 1103.
- [3] *Supramolecular Catalysis*, P. W. N. M. van Leeuwen, Wiley-VCH, Weinheim, Germany, 2008.
- [4] F. J. M. Hoeben, P. Jonkheijm, E. W. Meijer and A. P. H. J. Schenning, *Chem. Rev.*, 2005, **105**, 1491.
- [5] (a) P. Park and S. C. Zimmerman, *J. Am. Chem. Soc.*, 2006, **128**, 14236; (b) W. Seiche, A. Schuschkowski and B. Breit, *Adv. Syn. Catal.*, 2005, **347**, 1488.

- [6] (a) M. Kawano and M. Fujita, *Coord. Chem. Rev.*, 2007, **151**, 2592; (b) A. W. Kleij and J. N. H. Reek, *Chem.–Eur. J.*, 2006, **12**, 4218; (c) D. Fiedler, D. H. Leung, R. G. Bergman and K. N. Raymond, *Acc. Chem. Res.*, 2005, **38**, 349.
- [7] (a) G. Sedghi, V. M. García-Suárez, L. J. Esdaile, H. L. Anderson, C. J. Lambert, S. Martín, D. Bethell, S. J. Higgins, M. Elliott, N. Bennett, J. E. Macdonald and R. J. Nichols, *Nat. Nanotech.*, 2011, **6**, 517; (b) M. C. O’Sullivan, J. K. Sprafke, D. V. Kondratuk, C. Rinfray, T. D. W. Claridge, A. Saywell, M. O. Blunt, J. N. O’Shea, P. H. Beton, M. Malfois and H. L. Anderson, *Nature*, 2011, **469**, 72.
- [8] (a) C. J. Whiteoak, G. Salassa and A. W. Kleij, *Chem. Soc. Rev.*, 2012, **41**, 622; (b) S. J. Wezenberg and A. W. Kleij, *Angew. Chem. Int. Ed.*, 2008, **47**, 2354.
- [9] (a) S. J. Wezenberg, G. Salassa, E. C. Escudero-Adán, J. Benet-Buchholz and A. W. Kleij, *Angew. Chem. Int. Ed.*, 2011, **50**, 713; (b) M. V. Escárcega-Bobadilla, G. Salassa, M. Martínez Belmonte, E. C. Escudero-Adán and A. W. Kleij, *Chem.–Eur. J.*, 2012, **18**, 6805.
- [10] (a) J. A. A. W. Elemans, S. J. Wezenberg, E. C. Escudero-Adán, J. Benet-Buchholz, D. den Boer, M. J. J. Coenen, S. Speller, A. W. Kleij and S. De Feyter, *Chem. Commun.*, 2010, **46**, 2548; (b) G. Salassa, M. J. J. Coenen, S. J. Wezenberg, B. L. M. Hendriksen, S. Speller, J. A. A. W. Elemans and A. W. Kleij, *J. Am. Chem. Soc.*, 2012, **134**, 7186; (c) M. Viciano-Chumillas, J. Hieulle, T. Mallah and F. Silly, *J. Phys. Chem. C.*, 2012, **116**, 23404; (d) J. Saiz-Poseu, A. Martínez-Otero, T. Roussel, J. K.-H. Hui, M. L. Montero, R. Urcuyo, M. J. MacLachlan, J. Farauto and D. Ruiz-Molina, *Phys. Chem. Chem. Phys.*, 2012, **14**, 11937.
- [11] For some examples: (a) C. T. L. Ma and M. J. MacLachlan, *Angew. Chem. Int. Ed.*, 2005, **44**, 4178; (b) J. K.-H. Hui, Z. Yu and M. J. MacLachlan, *Angew. Chem. Int. Ed.*, 2007, **46**, 7980; (c) E. C. Escudero-Adán, J. Benet-Buchholz and A. W. Kleij, *Inorg. Chem.*, 2008, **47**, 4256; (d) G. Consiglio, S. Failla, P. Finocchiaro, I. P. Oliveri, R. Purrello and S. Di Bella, *Inorg. Chem.*, 2010, **49**, 5134; (e) G. Consiglio, S. Failla, P. Finocchiaro, I. P. Oliveri and S. Di Bella, *Inorg. Chem.*, 2012, **51**, 8409.
- [12] M. Martínez Belmonte, S. J. Wezenberg, R. M. Haak, D. Anselmo, E. C. Escudero-Adán, J. Benet-Buchholz and A. W. Kleij, *Dalton Trans.*, 2010, **39**, 4541.
- [13] For some examples: (a) J. K.-H. Hui and M. J. MacLachlan, *Dalton Trans.*, 2010, **39**, 7310; (b) G. Salassa, A. M. Castilla and A. W. Kleij, *Dalton Trans.*, 2011, **40**, 5236. See also references 10a and 10b.

- [14] (a) J. H. Chong, S. J. Ardakani, K. J. Smith and M. J. MacLachlan, *Chem.–Eur. J.*, 2009, **15**, 11824; (b) M. Mastalerz, H.-J. S. Hauswald and R. Stoll, *Chem. Commun.*, 2012, **48**, 130; (c) M. Mastalerz and I. M. Oppel, *Eur. J. Org. Chem.*, 2011, 5971; See also: (d) J. H. Chong and M. J. MacLachlan, *J. Org. Chem.*, 2007, **72**, 8693; (e) M. Mastalerz and I. M. Oppel, *Angew. Chem. Int. Ed.*, 2012, **51**, 5252; (f) M. W. Schneider, H.-J. Siegfried Hauswald, R. Stoll and M. Mastalerz, *Chem. Commun.*, 2012, **48**, 9861.
- [15] M. Mastalerz, S. Sieste, M. Ceni and I. M. Oppel, *J. Org. Chem.*, 2011, **76**, 5873.
- [16] K. P. Bryliakov and E. P. Talsi, *Eur. J. Org. Chem.*, 2008, 3369.
- [17] (a) A. L. Singer and D. A. Atwood, *Inorg. Chim. Acta*, 1998, **277**, 157; (b) E. C. Escudero-Adán, J. Benet-Buchholz and A. W. Kleij, *Inorg. Chem.*, 2008, **46**, 7265; (c) S. Curreli, E. C. Escudero-Adán, J. Benet-Buchholz and A. W. Kleij, *Eur. J. Inorg. Chem.*, 2008, 2863.
- [18] Note that trinuclear complexes **3** and **4** proved to be too insoluble for the UV-vis titration experiments under apolar (toluene) conditions.
- [19] (a) A. Decortes, M. Martínez Belmonte, J. Benet-Buchholz and A. W. Kleij, *Chem. Commun.*, 2010, **46**, 4580; (b) A. Decortes and A. W. Kleij, *ChemCatChem*, 2011, **3**, 831; (c) M. Taherimehr, A. Decortes, S. M. Al-Amsyar, W. Lueangchaichaweng, C. Whiteoak, A. W. Kleij and P. P. Pescarmona, *Catal. Sci. Technol.*, 2012, **2**, 2231. For other representative recent examples see references 20.
- [20] (a) C. J. Whiteoak, E. Martin, M. Martínez Belmonte, J. Benet-Buchholz and A. W. Kleij, *Adv. Synth. Catal.*, 2012, **354**, 469; (b) T. Ohshima, J. Okudac and K. Mashima, *Catal. Sci. Technol.*, 2012, **2**, 509; (c) A. Castro, A. Lara-Sánchez, M. North, A. Otero and P. Villuendas, *Catal. Sci. Technol.*, 2012, **2**, 1021; (d) T. Ema, Y. Miyazaki, S. Koyama, Y. Yano and T. Sakai, *Chem. Commun.*, 2012, **48**, 4489.
- [21] We also attempted to recycle the binary catalyst systems based on NBU₄I and mononuclear **8** or dinuclear **9**; in both cases, during the Et₂O extraction procedure an inseparable mixture of two liquid phases was obtained.
- [22] S. J. Wezenberg, E. C. Escudero-Adán, J. Benet-Buchholz, A. W. Kleij, *Chem.–Eur. J.*, 2009, **15**, 5695.
- [23] Note that KI will represent a closer contact ion pair than NBU₄I considering the polarity of the medium during work up (Et₂O, cyclic carbonate and remaining epoxide) and therefore the iodide will be a less effective nucleophile resulting in lower conversion.
- [24] G. M. Sheldrick, SHELXTL Crystallographic System, Version 6.10, Bruker AXS, Inc., Madison (Wisconsin), 2000.

- [25] M. C. Burla, R. Caliandro, M. Camalli, B. Carrozzini, G. L. Cascarano, C. Giacovazzo, M. Mallamo, A. Mazzone, G. Polidori and R. Spagna, *J. Appl. Cryst.*, 2012, **45**, 357.
- [26] A. L. Spek, *PLATON – A Multipurpose Crystallographic Tool*, Utrecht University, Utrecht, The Netherlands 2010.
- [27] P. van der Sluis and A. L. Spek, *Acta Cryst.*, 1990, **A46**, 194.
- [28] TWINABS version 2008/4 Bruker AXS; R. H. Blessing, *Acta Cryst.*, 1995, **A51**, 33.
- [29] Specfit/32TM, version 3.0; Spectra Software Associates. Specfit/32 is a multivariate data analysis program for modeling and fitting multi-wavelength titration data sets giving more reliable parameters than single-wavelength fits. For software details and the related nonlinear algorithms see: a) H. Gampp, M. Maeder, C. J. Meyer and D. A. Zuberbühler, *Talanta*, 1985, **32**, 95; b) H. Gampp, M. Maeder, C. J. Meyer and D. A. Zuberbühler, *Talanta*, 1986, **33**, 943.
- [30] J. A. A. W. Elemans, S. J. Wezenberg, M. J. J. Coenen, E. C. Escudero-Adán, J. Benet-Buchholz, D. den Boer, S. Speller, A. W. Kleij and S. De Feyter, *Chem. Commun.*, 2010, **46**, 2548.

Summary

Schiff base ligands may be considered “privileged ligands”; they are easily prepared by the condensation between aldehydes and amines. These ligands are able to coordinate and stabilize metals in various oxidation states through the imine nitrogens and other donor atoms usually linked to the aldehyde enabling the use of Schiff base metal complexes for a large variety of useful catalytic transformations. When two equivalents of salicylaldehyde are combined with an *ortho*-phenyldiamine, a particular chelating Schiff base ligand is produced, known as “salphen” or “salophen” ligand. The salphen ligands pose a rigid geometry around the metal center that can be used to manipulate important properties such as the Lewis acidity. This Lewis acidity can be effectively used to increase the reactivity of coordinating ligands and/or substrates. Furthermore the steric properties of salphen complexes can be tuned with the introduction of different groups in their aldehyde or diamine precursors. When a Zn(II) cation is coordinated by a salphen ligand it is forced in an unusual (square) planar geometry that greatly enforces its Lewis acidity and makes it available for axial coordination, a feature that can be used in catalysis for substrate activation and stabilization. Despite this peculiar feature and the advantage that zinc is a cheap, abundant and relatively non-toxic metal, Zn(II) salphen complexes have received so far little attention in the field of catalysis. Therefore, the work reported in this thesis has focused on the development of new applications of Lewis acidic Zn(II) Schiff base complexes in homogeneous catalysis.

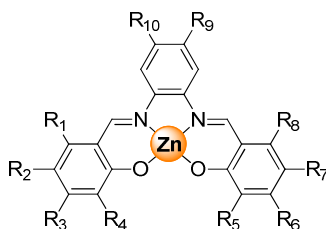
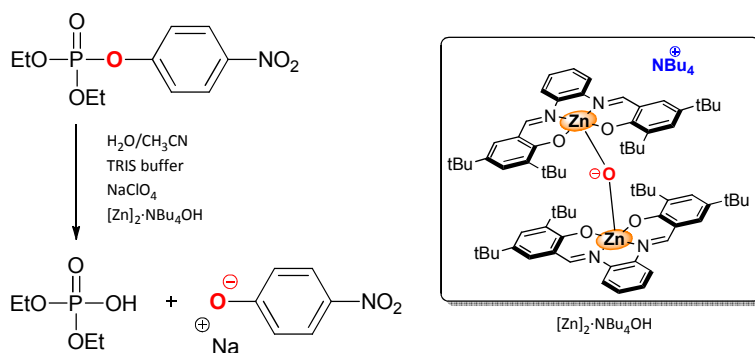


Figure 1. Schematic drawing of Zn(salphen) complexes with various possible substitutions.

In [Chapter 2](#) a new series of complexes comprising a binuclear, OH-bridging Zn₂ assembly based on a salphen scaffold has been presented. These structures are easily prepared in high yield and have been fully characterized by solution and solid state techniques. The stability properties of these assemblies under polar and non-polar conditions have been investigated and one typical example was applied as a potential catalyst for the phosphoester cleavage reaction involving paraoxon (Scheme 1). The low conversion rate observed is connected with an irreversible

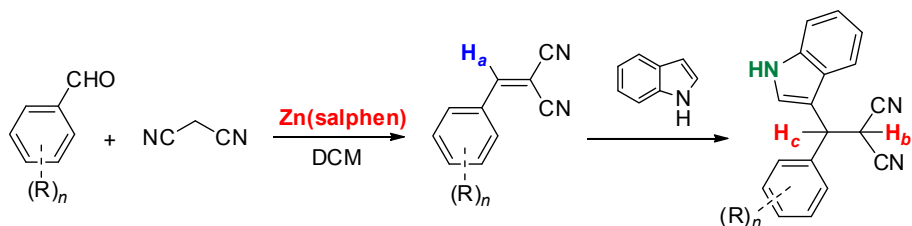
reaction that takes place between the assembly and the hydrolysis product *p*-nitro-phenolate derived from paraoxon. The fact that no further conversion takes place points at the formation of other type of mononuclear Zn(salphen) complexes under these conditions that can compete with the reformation of a hydrolysis active species. This has been illustrated by the ability of the *p*-nitro-phenolate anion to compete with the OH anion for coordination to the Zn(salphen) complex.



Scheme 1. Paraoxon hydrolysis catalyzed by hydroxo-bridged dinuclear Zn(salphen)

In [Chapter 4](#) the synthesis of 3-substituted indoles has been investigated through a multi-component reaction (MCR) approach using aldehydes, indole and malononitrile as reagents. The reaction is catalyzed by Lewis acidic Zn(salphen) complexes and their performance was compared against a number of other Zn(II) structures and M(salphen)s (M = Al, Cu) showing the Zn(salphen)s to be superior. However, the complex nature of this three-component reaction (3-CR) results in substantial by-product formation arising from the intermediate benzylidene malononitrile species (Scheme 2). The 3-CR has been studied in detail covering the influence of base, solvent, reagent stoichiometry and also involved stability studies. The results have led to a mechanistic proposal in which the benzylidene malononitrile intermediate plays a central role; it is one of the major species formed in most of the catalytic reactions studied, and furthermore provides also a prelude for in situ reaction with the malononitrile reagent to likely afford complex mixtures of N-containing heterocycles. The (irreversible) side-product formation depends on the type of benzaldehyde used, as larger amount of side-products seem to be evident when using electron-poor reagents. This work thus demonstrates that this MCR reaction is not as straightforward as previously communicated.

In *Chapter 5* the use of the commercially available, bifunctional phosphine 1,3,5-triaza-7-phosphaadamantane (abbreviated as PN_3) is described; this PN_3 scaffold in conjunction with a



Scheme 2. 3-CR catalyzed by a $\text{Zn}(\text{salphen})$ complex affording the benzylidene malononitrile intermediate and 3-substituted indoles.

series of $\text{Zn}(\text{salphen})$ complexes that leads to sterically encumbered phosphine ligands as a result of (reversible) coordinative Zn-N interactions (Figure 2). The solid state and solution phase behaviour of these supramolecular ligand systems have been investigated in detail and revealed their stoichiometries in the solid state observed by X-ray crystallography, and those determined in solution by NMR and UV-Vis spectroscopy. Also, upon application of these supramolecular bulky phosphines in hydrosilylation catalysis employing 1-hexene as substrate, the catalysis data infer the presence of an active Rh species with two coordinated, bulky $\text{PN}_3/\text{Zn}(\text{salphen})$ assemblies unit having a maximum of three $\text{Zn}(\text{salphen})$ s associated per PN_3 scaffold, with an excess of bulky phosphine hardly affecting the overall activity.

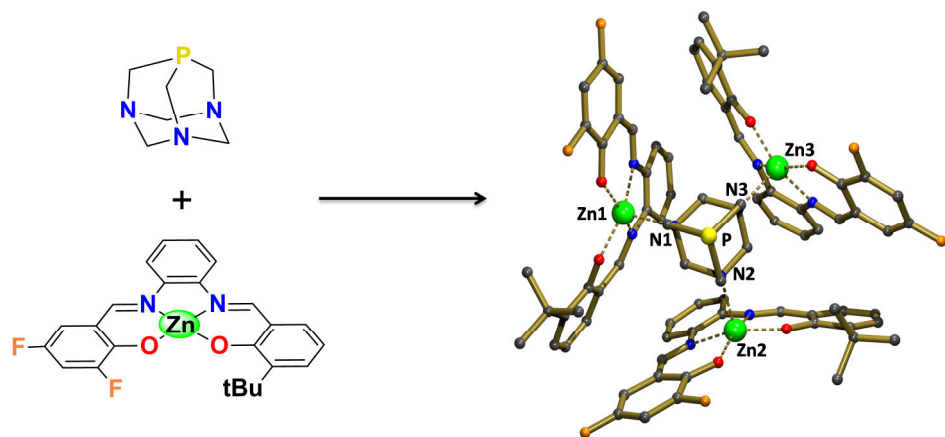
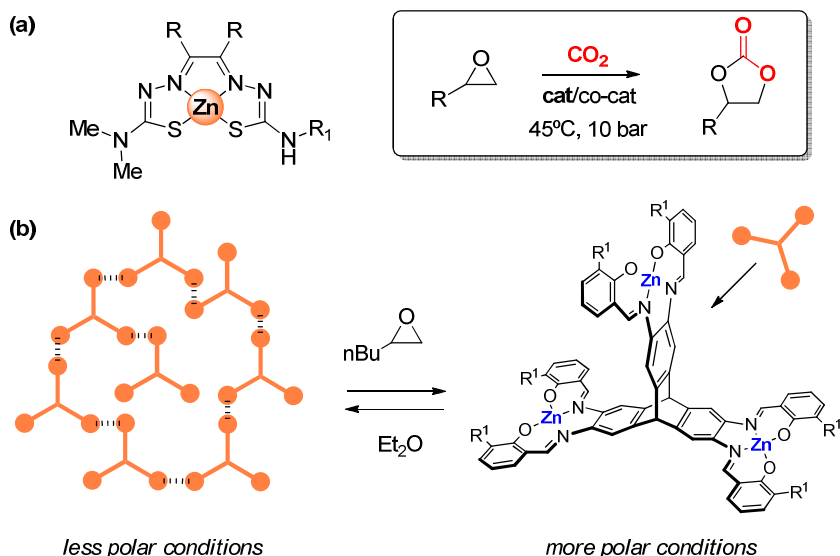


Figure 2. Molecular structure of a supramolecular bulky phosphine described in *Chapter 5*.

The supramolecular formation of these bulky phosphines with little synthetic effort may be a useful alternative for *covalent*, bulky phosphines as the hydrosilylation catalysis data for 1-

hexene has shown comparable effects and catalytic efficiencies obtained with covalent and supramolecular phosphine ligands.

Chapters 3 and 6 focus in particular on the catalyzed cycloaddition of CO_2 to terminal epoxides. A series of Zn(II) complexes based on a versatile N_2S_2 -chelating ligand abbreviated as btsc [btsc = bis(thiosemicarbazonato)] derived from simple and accessible building blocks have been presented in **Chapter 3** (Scheme 3a). These complexes which comprise a Lewis acidic Zn(II) centre useful for substrate activation proved to be effective catalysts for the cycloaddition of CO_2 to various terminal epoxides under relatively mild reaction conditions. The use of a cheap and abundant metal in combination with an environmentally tolerable solvent such as MEK and mild reaction conditions further mark this catalytic process as a potentially sustainable way for cyclic carbonate synthesis.



Scheme 3. Cycloaddition of CO_2 to 1,2-epoxyhexane catalyzed by (a) Zn(II) complexes based on bis(thiosemicarbazonato) ligands, and (b) a trinuclear triptycene complex.

In **Chapter 6** a series of trinuclear, triptycene based metallosalphen complexes ($\text{M} = \text{Zn}, \text{Ni}$) prepared incorporating various peripheral substituents has been presented. The introduction of Zn metal centres in these triptycene based salphen ligands gives rise to cross-linking between different triptycene molecules through μ -phenoxo bridges between the Zn metal centres, and variation in the peripheral groups allows controlling the self-assembling properties as shown by

UV-Vis titration data. These spectroscopic studies have shown that phenyl-derived Zn₃ triptycenes show appreciable self-aggregation which can be reversed by the addition of a competitive ligand (pyridine) or a suitable substrate (1,2-epoxyhexane, Scheme 3b). Application of this kind of complexes in organic carbonate formation has revealed that reversible supramolecular aggregation can be made an efficient recycling strategy in homogeneous catalysis and that the recycling properties also depend on the co-catalyst structure.

The work described in this thesis demonstrates that Zn(II) Schiff base complexes and in particular salphen complexes have great potential in homogeneous catalysis. Their ease of access, the versatility of their precursors and thus the facile fine-tuning of their electronic and steric properties, and the enhanced Lewis acidity of the metal centre are amongst the most interesting features than can be exploited in catalysis operations. We have demonstrated that these complexes are very versatile and able to catalyse several organic transformations: from multi-component reactions to the cycloaddition of CO₂ to various terminal epoxides. Efforts have also been made in the recycling of the catalysts by means of reversible supramolecular aggregation, a new conceptual approach towards homogeneous catalyst recycling. We also have reported that Zn(II) salphens can play the (spectator) role of steric mediators in hydrosilylation catalysis, where they are ligated by a templating, bifunctional aza-phosphine. Further studies may explore the potential of these Zn(II) Schiff base complexes in asymmetric catalysis by introduction of stereogenic centres or other elements of chirality in the salphen backbone. Alternatively, the exploitation of the high Lewis acidity of the Zn(salphen) family of complexes could be of great use in other types of catalytic transformations where O- or N-containing substrates/intermediates are involved.

UNIVERSITAT ROVIRA I VIRGILI

LEWIS ACIDIC ZN(II) SCHIFF BASE COMPLEXES IN HOMOGENEOUS CATALYSIS

Daniele Anselmo

Dipòsit Legal: T. 1564-2013

Acknowledgements

Now that this thesis is complete I would like to acknowledge all the people that have helped me, one way or the other, to achieve this goal. First of all I wish to thank my supervisor, Prof. Arjan Kleij, for offering me the opportunity to develop a research project, for the constructive discussions and for supervising my work with attention and professionalism. I thank all the present and past members of the Kleij group for the nice time spent together in our lab, in particular Giovanni and Martha for their scientific contributions to this thesis. Thanks to Ingrid Mateu, our secretary, and before her Elena Masdeu, Marta Moya and Aurora Cáceres, for all the precious help they offered me through these years. I kindly thank Prof. Pau Ballester for the helpful discussions regarding the titration studies described throughout the thesis. Chapters 3 and 5 are the fruit of a collaboration with the group of Prof. Joost Reek from the University of Amsterdam (The Netherlands), in particular with Dr. Rafael Gramage-Doria, Dr. Tatiana Besset and Dr. Vladica Bocokic; I would like to thank them all for the nice contribution to this thesis and the papers that we published together. I especially thank all the members of the research support units of ICIQ, in particular Dr. Jordi Benet Buchholz and Eduardo Escudero Adán from the X-Ray Diffraction unit, Dr. Noemí Cabello from the High Resolution Mass Spectrometry unit, Dr. Gabriel González, Kerman Gómez and Israel Macho from the Nuclear Magnetic Resonance unit, Dr. Yvette Mata Campaña from the Chemical Reaction Technologies unit and Simona Curreli from the Chromatography, Thermal Analysis and Electrochemistry unit. Thanks to Maria Fernandez, for the first smile of every working day. I am grateful to the ICIQ Foundation and the Spanish Ministry of Education for providing me with pre-doctoral fellowships (ICIQ and F.P.U. grants).

Living in another country changes you forever, you will never be the same and will look at things the same way again but one of the hardest things of living abroad is the feeling of belonging nowhere. You get to understand that you don't belong anymore to the place you left and struggle to feel at home in a new country with different uses and culture. You idealize what you left and try to adapt it to the new setting. You end up wanting to live in a place that is a collage of memories, experiences and people...but that place doesn't exist. Across two banks of the Mediterranean Sea, stranded in a jungle of trains, planes and airports as an eternal traveler I spent these years pondering what I should consider home and what not. Eventually I found out that there are a couple of things or a few chosen ones that were "home" to me, regardless of

where I was. Home was not a single place anymore; it got diluted into a number of places and people who crossed my path: home was a beach and a good book on a summer sunset, home was a small town in the countryside, home was a house where the friends of a lifetime are, home is my family wherever I am. The following thanking words are dedicated to the people that made me feel home no matter where I was.

To Carlo, friend and companion of this experience, to these years of ice and fire, to the adventures that we've been through together, ai momenti improbabili. To Toni and Claudio, best friends and guides in the Kingdom of Spain, for showing me all the good that there is in this country. To Antonello, to the great times and to our jokes on "distorted realities" which made me laugh like with none else during these years. To my best friends, Silvia and Enrico, a harbor where I'm forever home, because, each in his own way, was with me when I needed them most. To Dario, who joined our team of drifters off to see the world, to Claudio, memory alpha, to Davide that will never stop surprising me and to Serena and Marzia, beloved friends and goddesses. To Núria Sugranyes for her caring friendship, to Caterina, first friend at ICIQ and reference postdoc, to Moira, for our wars and peaces and to Ana, who I knew too late.

To my family, who looks after me from afar and silently pushes me forward in this race which is life.

And now that this chapter of my life is coming to an end, bearing in my heart all the wonderful memories and experiences I collected in these years, I look forward to the new worlds and to the new days to see.

- Daniele -

Curriculum Vitae

Daniele Anselmo was born on the 14th of September, 1981 in Palermo, Italy. He started studying chemistry at the Università degli Studi di Palermo in October 1999 and obtained his MSci degree in July 2007 with a major in Inorganic Chemistry with a dissertation on experimental work performed under the direction of Prof. Dr. Arturo Silvestri. From March 2008 until February 2013 he carried out the work described in this thesis in the group of Prof. Dr. A. W. Kleij at the Institute of Chemical Research of Catalonia (ICIQ). During his PhD studies he obtained an MSc in Nanoscience and Nanotechnology from the Universitat Rovira i Virgili in Tarragona (Spain). Part of his research was communicated at the 239th American Chemical Society National Meeting in San Francisco, CA, USA, (2010), at the XIIth Netherlands Catalysis and Chemistry Conference in Noordwijkerhout, The Netherlands, (2011) and at the Zing Conference on Coordination Chemistry in Xcaret, Mexico (2011). His PhD research was financially supported with pre-doctoral fellowships from the ICIQ Foundation and the Spanish Ministry of Education and Science (FPU grant).

UNIVERSITAT ROVIRA I VIRGILI

LEWIS ACIDIC ZN(II) SCHIFF BASE COMPLEXES IN HOMOGENEOUS CATALYSIS

Daniele Anselmo

Dipòsit Legal: T. 1564-2013

List of Publications

- D. Anselmo, G. Salassa, E. C. Escudero-Adán, E. Martin, A. W. Kleij, "Merging Catalysis and Supramolecular Aggregation Features of Triptycene based Zn(salphen)s", *Dalton Trans.*, 2013, *advance article*, DOI: 10.1039/C3DT00067B.
- D. Anselmo, R. Gramage-Doria, T. Besset, M. V. Escárcega-Bobadilla, G. Salassa, E. C. Escudero-Adán, M. M. Belmonte, E. Martin, J. N. H. Reek, A. W. Kleij, "Supramolecular Bulky Phosphines Comprising of 1,3,5-triaza-7-phosphaadamantane and Zn(salphen)s: Structural Features and Application in Hydrosilylation Catalysis", *Dalton Trans.*, 2013, *advance article*, DOI: 10.1039/C3DT00078H.
- M. V. Escárcega-Bobadilla, D. Anselmo, S. J. Wezenberg, E. C. Escudero-Adán, M. Martínez Belmonte, E. Martin, A. W. Kleij, "Metal-directed assembly of chiral bis-Zn(II) Schiff base structures", *Dalton Trans.*, 2012, **41**, 9766-9772.
- D. Anselmo, V. Bocokić, A. Decortes, E. C. Escudero-Adán, J. Benet-Buchholz, J. N. H. Reek, A. W. Kleij, "Mild Formation of Cyclic Carbonates using Zn(II) Complexes based on N₂S₂-Chelating Ligands", *Polyhedron*, 2012, **32**, 49-53.
- D. Anselmo, E. C. Escudero-Adán, M. Martínez Belmonte, A. W. Kleij, "Zn-Mediated Synthesis of 3-Substituted Indoles using a Three-Component Reaction Approach", *Eur. J. Inorg. Chem.*, 2012, **29**, 4694-4700
- S. J. Wezenberg, D. Anselmo, E. C. Escudero-Adán, J. Benet-Buchholz, A. W. Kleij, "Dimetallic activation of dihydrogen phosphate by Zn(salphen) chromophores", *Eur. J. Inorg. Chem.*, 2010, **29**, 4611-4616.

- M. Martínez Belmonte, S. J. Wezenberg, R. M. Haak, D. Anselmo, E. C. Escudero-Adán, J. Benet-Buchholz, A. W. Kleij, "Self-assembly of Zn(salphen) complexes: steric regulation, stability studies and crystallographic analysis", *Dalton Trans.*, 2010, **39**, 4541-4550.
- D. Anselmo, E. C. Escudero-Adán, J. Benet-Buchholz, A. W. Kleij, "Isolation and Characterization of a New Type of μ -Hydroxo-bis-Zn(salphen) Assembly", *Dalton Trans.*, 2010, **39**, 8733-8740.
- D. Anselmo, E. C. Escudero-Adán, J. Benet-Buchholz, A. W. Kleij, "Assembly of unusual Zn-cluster compounds based on pyridinealcohol platforms", *Dalton Trans.*, 2009, **36**, 7368-7373.
- A. Silvestri, G. Barone, G. Ruisi, D. Anselmo, S. Riela, V. Turco Liveri, "The interaction of native DNA with Zn(II) and Cu(II) complexes of 5-triethyl ammonium methyl salicylidene ortho-phenylenediamine", *J. Inorg. Biochem.*, 2007, **101**, 841-848.